RESEARCH INTO THE DEVELOPMENT AND FABRICATION OF STEELS FOR USE IN THE CONSTRUCTION OF OFFSHORE STRUCTURES AND ARCTIC VESSELS

by

J. D. Ray, R. J. Ackert, M. K. McLean
Research Department
The Algoma Steel Corporation Limited

Work on this Project was conducted under the auspices of the Canada Centre for Mineral and Energy Technology; Energy, Mines and Resources, Canada.

DDS FILE NUMBER: 23SQ.23440-2-9027-2
DDS CONTRACT SERIAL NUMBER: OSQ82-00230
CANMET PROJECT NUMBER: 425254
CANMET SCIENTIFIC AUTHORITY: J.D. Boyd

FEB 27 1985
MICROMEDIA

RESEARCH INTO THE DEVELOPMENT AND FABRICATION OF STEELS FOR USE IN THE CONSTRUCTION OF OFFSHORE STRUCTURES AND ARCTIC VESSELS

by

J. D. Ray, R. J. Ackert, M. K. McLean
Research Department
The Algoma Steel Corporation Limited

EXECUTIVE SUMMARY

The discovery of off-shore oil and gas reserves in Canadian east coast and Beaufort Sea regions has created a challenging market potential for Canadian industry to supply materials and equipment. However, the material property requirements for service in these regions are very severe, surpassing those encountered in the North Sea. In recognition of the need for further research, the Federal Government, through Energy Mines and Resources Canada, solicited research proposals relating to a "Research Program on Steels for Offshore and Arctic Use".

Algoma's proposal was one of five projects supported by the resulting E.M.R. - CANMET 50/50 program. Half of the total cost (including subcontracts) was covered by contract with the Federal Government under DDS file number 23SQ.23440-2-9027-2.

Algoma's project entailed the manufacture, testing and welding evaluation of plates up to 75 mm in thickness which met all the requirements of the Lloyd's LT60 specification. The Lloyd's LT60 grade, which is only applicable to plate thicknesses above 30 mm by agreement, has been identified as meeting the most stringent materials requirements envisioned for use in the hulls of Arctic class liquified natural gas tankers and off-shore structures.

This experimental heat of ingot steel was successfully produced to Lloyd's LT60 requirements. All plates exhibited good cleanness (ASTM Level B1 to B1-1/2) and mechanical properties of the parent plate were excellent. This material exceeded the Lloyd's specification at the 355 MPa yield strength level while Charpy impact energies were far in excess of

the Lloyd's specifications, averaging 200 Joules and 125 Joules at -60°C in the longitudinal and transverse directions respectively. Navy drop weight nil ductility and CTOD test results on the parent plate were also favorable.

The main emphasis of the welding evaluation was to develop procedures for this heat of LT60 steel which would retain adequate heat-affected zone properties. Lloyd's specifications deal primarily with parent plate and weld metal with no mention being made of heat affected zone (HAZ) Charpy or CTOD fracture toughness testing.

In addition to a literature review, the welding evaluation, conducted under subcontract to Welding Institute of Canada, included three testing methods: Bead on Plate, K-Preparation and Butt. Bead on Plate welds were used in the evaluation of heat-affected zone hardness and toughness. K-Preparation welds were prepared for full thickness CTOD testing. Weld procedure qualification testing (tensile and Charpy impact) was done using the butt weld configuration. The Welding Institute of Canada, in their report, compared the results of the procedure testing of the butt weld assemblies with criteria found in testing guidelines drafted by Lloyd's for LNG carriers operating in the Canadian Arctic.

The welding literature review highlighted the importance of fine grain size, the use of precipitates to restrict grain growth in the coarse-grained HAZ, the significance of interstitials, and the effect of overall microstructure on the HAZ.

Butt welds made from the 25 mm plate were shown to be acceptable in terms of tensile and impact results. The 75 mm butt welds produced acceptable tensile results, but impact values in the HAZ were subject to large variations. The region of minimum toughness was situated just outside of the visible HAZ. It is argued that strain-induced embrittlement is the most probable cause for the observed behaviour.

Microstructural examinations showed that optimum HAZ properties were obtained for heat inputs between 3 and 4 kJ/mm, typical of current fabricating practices. However, the CTOD results at these heat inputs for the Bead on Plate welds were below 0.10 mm at -60°C. The CTOD of full thickness welds (K-preparation) completed using the same nominal heat input produced similar toughness. However, the problems associated with measuring and interpreting low heat affected zone toughness at very low service temperatures are far from unique to this heat, and may well be universal.

Although this intensive testing has been limited to one heat, the information has provided a level of confidence concerning Algoma's ability to participate in these demanding applications; In addition, the work has defined areas of continuing concern with respect to the evaluation of weld heat-affected zone toughness.

TABLE OF CONTENTS

		Page
1.0	Introduction	1
2.0	Program Objectives	2
3.0	Summary	4
4.0	Conclusions	5
5.0	Recommendations	8
6.0	Fracture Design Criteria	10
	6.1 Steel Requirements and Fracture Criteria	10
	6.2 Fracture Behavior and Testing	12
7.0	Specifications	14
	7.1 Chemistry	14
	7.2 Mechanical Properties	14
	7.3 Welding	15
8.0	Parent Plate Test Program	16
	8.1 Manufacture	16
	8.2 Tensile Testing	17
	8.3 Charpy Impact Testing	17
	8.4 Nil Ductility	18
	8.5 CTOD Testing	18
	8.6 Metallographic Evaluation	19
	8.7 Discussion	19
9.0	Welding Test Program	21
	9.1 Background and Experimental Design	21
	9.1.1 Factors Influencing Heat Affected Zone Toughness	21
	9.1.2 Heat Affected Zone Characteristics	22
	9.1.3 Experimental Approach	24
	9.1.4 Bead on Plate Test Welds	25
	9.1.5 K-Preparation Welds	26
	9.1.6 Weld Procedure Qualification of Butt Welds	27

TABLE OF CONTENTS (Cont)

		Page
9.0	Welding Test Program (Cont.)	
9.2	Results	27
9.2.1	Hardening Curves and Metallographic Inspection	27
9.2.2	Fracture Toughness Testing of Bead on Plate Welds	28
9.2.3	Fracture Toughness Testing of K-Preparation Welds	29
9.2.4	Procedure Testing of Butt Weld Assemblies	30
9.3	Discussion	31
9.3.1	Hardening Curves and Metallographic Inspection	32
9.3.2	Fracture Toughness Testing of Bead on Plate and K-Preparation Welds	33
9.3.3	Application of CTOD Results	34
9.3.4	Procedure Testing of Butt Weld Assemblies	36

LIST OF TABLES

1) Chemistries: Lloyd's Specification, Algoma Specification and Ladle Analysis

2) Tensile Results (Mean Values)

3) CVNL Impact Results (Mean Values)

4) CVNT Impact Results (Mean Values)

5) CVNL Minimum Values

6) CVNT Minimum Values

7) CVNL Standard Deviations

8) CVNT Standard Deviations

9) CVNL Percent Shear

10) CVNT Percent Shear

11) Metallographic Examination

12) CTOD Testing of Parent Plate Material

13) Summary of Hardening Curve Results

14) CTOD Testing of Bead on Plate Welds

15) Butt Weld Procedure Testing (25 mm plate)

16) Butt Weld Procedure Testing (75 mm plate)

LIST OF FIGURES

1 Parent Plate Yield Strength vs Plate Thickness and Test Location

2 CVNL Impact Energy vs Temperature for 25 mm Plate

3 CVNL Impact Energy vs Temperature for 50 mm Plate

4 CVNL Impact Energy vs Temperature for 63 mm Plate

5 CVNL Impact Energy vs Temperature for 75 mm Plate

6 CVNT Impact Energy vs Temperature for 25 mm Plate

7 CVNT Impact Energy vs Temperature for 50 mm Plate

8 CVNT Impact Energy vs Temperature for 63 mm Plate

9 CVNT Impact Energy vs Temperature for 75 mm Plate

10 Frequency Histogram of CVNL Impact Energy at -60°C

11 Percent Shear vs Temperature for CVNL and CVNT Impact Tests

12 Photo micrographs of 25, 50, 63 and 75 mm Plate Thicknesses

13 Cleanliness Rating Photo micrographs

14 Schematic Microstructure of a 0.2%C Steel Weld

15 Hardening Curve Results for Bead-On-Plate Welds

16 CTOD versus Heat Input for Bead-On-Plate Welds

17 CTOD Transition Curve for Bead-On-Plate Weld

18 CTOD versus Temperature for Base Plate, Fine and Coarse Grained HAZ

19 Hardening Curve Results for A710 Gr A Cl 3, BS4360 Gr50E, and Algoma's LT60 Steels

20 Hot Strain Embrittlement in a Multipass Weld

21 Comparison of CTOD Results for Algoma's LT60 Steel and a 0.15C-1.35Mn-0.07Nb Steel

LIST OF APPENDICES

1) Welding Institute of Canada Report to Algoma Steel

2) Ontario Research Foundation Report on Nil Ductility Testing

1.0 INTRODUCTION

The discovery of off-shore oil and gas reserves in Canadian east coast and Beaufort Sea regions has created a challenging market potential for Canadian industry to supply materials and equipment. However, the material property requirements for service in these regions are very severe, surpassing those encountered in the North Sea. To ensure that Canadian Industry was in a position to support the development of the Canadian Artic, the Federal Government, through Energy, Mines and Resources Canada, solicited research proposals with an offer to fund 50% of the costs. Proposals were to relate to a "Research Program on Steels for Offshore and Arctic Use". Algoma Steel was among the successful candidates.

Algoma's proposal entailed the manufacture, testing and welding evaluation of a candidate steel meeting all the requirements of Lloyd's LT60. The Lloyd's LT60 grade has been identified as meeting the most stringent material requirements envisioned for use in hulls of Arctic class, liquified natural gas tankers and off-shore structures.

This project was supported by the E.M.R. - CANMET 50/50 Research Program on Steels for Offshore and Arctic Use. Half of the total cost (including subcontracts) is covered by contract with the Federal Government under DSS file number 23SQ.23440-2-9027-2. A package of 5 projects relating to materials and fabrication for northern transportation and development received funding in 1983: one each from Algoma, Stelco, and AMCA and two from NOVA, An Alberta Corporation.

2.0 PROGRAM OBJECTIVES

This project was intended to assist in the development of a steel suitable for Arctic offshore structures and for the hull construction of Arctic service natural gas tankers. The development of welding procedures for this steel, that would be practical in Canadian shipyards, was also included in the program. The information would also apply to a wide range of offshore construction applications.

The objectives of the proposal submitted by Algoma were:

i) To design and manufacture a steel that meets grade requirements described in Lloyd's Rules and Regulations for the Classification of Ships, Grade LT60. This includes testing to determine chemistry, longitudinal and transverse tensiles, longitudinal and transverse Charpy impact transition curves, and longitudinal and transverse nil ductility transition temperatures.

ii) To develop and qualify welding procedures for the steel in order to retain adequate heat-affected zone toughness and which would be practical for Canadian shipyards.

The objectives of the welding and fabrication studies conducted at the Welding Institute of Canada were:

(a) A literature review of welding results for heavy section plates used specifically for shipbuilding and offshore structures, with emphasis on the fracture behaviour.

(b) To conduct (1) basic weldability tests and metallurgical examinations to ascertain the changes in the heat-affected zone.

(2) fracture mechanics testing of selected regions of the welds to determine the resistance of the completed weld to fracture initiation.

(3) welding procedure qualification tests to evaluate the suitability of the LT60 for Arctic use.

3.0 SUMMARY

One ingot cast heat of approximately 200 product tonnes was produced in Algoma Steel's #2 Basic Oxygen Steel Plant. This heat was controlled rolled to plate thickness of 25, 50, 63 and 75 mm. All plates were subsequently normalized as required by the Lloyd's LT60 specification. Samples from front, middle and back locations of the normalized plate were taken to determine tensile and charpy impact properties. Samples of each size were also evaluated in the longitudinal and transverse directions using the Navy drop weight nil ductility test. CTOD testing was also completed on the parent plate. Samples of these plates were also sent to CANMET, NOVA, An Alberta Corporation, AMCA, Gulf Research, Chinook Fuel Innovations Ltd., and the Association of American Railroads.

Testing, using bead on plate welds was conducted on the 25, 50 and 75 mm plates over a range of heat inputs at the Welding Institute of Canada. K-Preparation welds for full size CTOD fracture toughness tests were made on 25 and 75 mm material. Butt weld procedure qualification testing was done on 25 and 75 mm plates. Metallographic and toughness data were interpreted and compared on the basis of a literature survey of similar steels.

Although this intensive testing has been limited to one heat, the information has provided a level of confidence concerning Algoma's potential ability to participate in these demanding applications, and defined areas of continuing concern with respect to evaluation of weld heat-affected zone toughness.

4.0 CONCLUSIONS

4.1 Parent Plate

An experimental heat of ingot steel was successfully produced to meet Lloyd's LT60 requirements for the parent plate. Specifically:

1) This material exceeded the Lloyd's LT60 specification at the 355 MPa yield strength level. Yield strength averaging 380 MPa was achieved with an ultimate tensile strength near 520 MPa and an elongation of approximately 30%.
2) An average CVNL energy of 200 Joules at -60°C was realized with a minus 2 sigma value of approximately 95 Joules (Lloyd's specification: 41 Joules).
3) An average CVNT energy of 125 Joules at -60°C was realized with a minus 2 sigma value of approximately 50 Joules (Lloyd's specification: 27 Joules).
4) The Navy drop weight nil ductility test temperature ranged from -43°C to -54°C.
5) Parent plate CTOD tests demonstrated some ductility at -60°C with the samples failing in an elastic plastic or fully ductile manner.

4.2 Welding

The main emphasis of the welding evaluation has been to develop procedures for this heat of LT60 steel which would retain adequate heat-affected zone properties.

On the basis of the literature review, the best HAZ characteristics were expected for a steel with fine grain size, stable precipitates to prevent grain growth, a minimal content of interstitial elements, and a balanced HAZ microstructure of martensite

and bainite. The laboratory examination included a study to ascertain the overall welding characteristics and procedure qualification butt weld trials. The main points which were determined in the course of the work are summarized below. More detail is found in Appendix 1.

1) Although this material has met the Lloyd's specification, it must be noted that the written specifications deal primarily with parent plate and weld metal. No mention, for example, is made of heat affected zone Charpy or CTOD fracture toughness testing. Lloyd's appears to have adopted a policy of approving a specific material under defined welding conditions using a procedure test which it reviews and accepts on a case by case basis.

2) The change in microstructure and hardness of the LT60 HAZ with different heat inputs can be used to determine welding procedures for optimum mechanical properties. For this steel, a heat input of 3 to 4 kJ/mm resulted in the optimum microstructure of a 50/50 mixture of martensite and bainite.

3) CTOD results for the HAZ regions have confirmed that the regions of low toughness may be a concern with C-Mn microalloyed steels at very low service temperatures.

4) The results of impact testing at -60°C in the HAZ of the 25 mm butt weld exceeded the minimum requirements of the Lloyd's LT60 parent plate specification. However, low toughness was found in the HAZ of the 75 mm butt weld which has been attributed to strain-induced hardening.

HAZ toughness might well prove to be the most serious concern affecting design and construction of offshore structures for several more years. The problems associated with measuring and interpreting low heat affected zone toughness at very low service

temperatures are far from unique to this heat, and may well be universal. The broadly based support for the recently initiated group sponsored research on heat affected zone toughness at the Welding Institute (UK) is a clear indication of widespread interest.

5.0 RECOMMENDATIONS

The weld evaluations have raised a number of points which require further study. In the shorter term, subjects requiring further study include:

1) Although the LT60 specification generally applies to plates under 30 mm in thickness, re-examination of the critical areas of the 75 mm procedure butt weld through further testing is required. This should include adequate consideration of the influence of restraint and strain hardening, thermal cycling of multipass welds, and interpass temperature.

2) An improved understanding of the relative performance of the heat affected zone toughness of Algoma's LT60 is necessary. This could include an examination of the heat-affected zone toughness of other candidate steels (such as the Ni-Cu A710 GrA Cl 3 or Lloyds 1/2% Ni steels) which also have acceptable baseplate properties at -60°C.

3) The loss of toughness which occurs during the stress relief of C-Mn microalloyed steels should be better understood in order to recommend chemistries for the optimization of multipass or stress-relieved weldment properties.

Some aspects of longer term and more general interest should also be given consideration:

1) Toughness requirements which have been proposed for Arctic structures and vessels should be reviewed in order to develop realistic requirements for structures fabricated with very heavy plates. The relevance of design criteria based on a minimum CTOD value at very low service temperatures should be better understood.

2) A more general understanding of the influence of chemistry and parent plate properties on the heat affected zone microstructures and toughness of microalloyed steels is necessary in determining the direction of future research.

3) The corrosion resistance of weld metal, heat affected zone and parent plate should be studied under conditions relevant to Arctic marine environments.

Work has already been initiated in a number of these areas. Additional procedure butt weld testing of 75 mm plate has been authorized at the Welding Institute of Canada. AMCA International has received approval to begin work on heat affected zone toughness of ASTM A710 Grade A Class 3, Lloyd's LT60, and BS4360 Grade 50E steels. Algoma is participating in the Welding Institute (UK) group sponsored work on heat affected zone toughness evaluations of a number of commercial steels. Algoma in conjunction with AMCA and Paprican has recently submitted an unsolicitated proposal on Weld Zone Corrosion to the Canadian Government.

6.0 FRACTURE DESIGN CRITERIA

The structural integrity of Arctic ships and structures is of extreme importance with regard to human life and environmental concerns. Acknowledging the importance of structural safety, one must consider whether there is any evidence that future ships will be subject to the risk of fracture. For this reason, it is necessary to understand the fracture behaviour of steel at low temperatures, and review the effect of fatigue and its interrelation with brittle fracture.

Brittle fractures involve a cleavage type of failure of the metal, characterized by a square break with relatively low amounts of deformation and energy absorption. These cracks generally propagate at high speed.

6.1 STEEL REQUIREMENTS AND FRACTURE CRITERIA

The steel requirements for welded ship and offshore construction adopted by regulatory bodies (ie Lloyd's, ABS, DnV) are based on theoretical design criteria which include fatigue and fracture mechanics and also give consideration to production techniques. Areas of a structure which are subject to impact and abrasion, or experience partial or periodic immersion require higher quality steels. Higher impact energies at lower test temperatures are required as the applications become more demanding.

Steels in the LT60 class are specified for structural parts which are subject to periodic immersion. The actual grades are determined on the basis of design air temperatures. The design air temperature of Arctic applications is expected to be at least -40°C, and some arguments have been presented for the use of a design temperature as low as -60°C. The properties of LT60 represent a

satisfactory choice for the most stringent requirements currently envisioned.

Several factors determine the selection of structural fracture criteria and the degree of structural reliability required for Arctic use, including environmental conditions, service temperature, and practical difficulties associated with repair of fractured members. Pellini* notes that a separate analysis of structural reliability may be required for various parts of a structure, and suggests that the concept of redundancy be incorporated into design philosophy. Regions where fracture can cause total failure or seriously affect the residual life of a structure should be designed on the basis of fracture-arrest safe steels. Regions which are not fracture critical may be designed on the basis of fracture initiation prevention.

The concept of structural reliability outlined by Pellini is not the same as that adopted by the Welding Institute (UK).* Their approach to fracture philosophy considers the locally brittle HAZ, assuming that fracture initiation is favoured for defects in this region. Once initiated, a crack will either stop or continue to propagate, depending on the arrest properties of the steel and the energy available for fracture. Since the arrest toughness is significantly lower than the initiation toughness for most structural steels, arrest is unlikely unless the driving force decreases rapidly as the crack extends. These factors, combined with difficulties in designing to arrest criteria and difficulties in achieving steels with the necessary toughness, have led The Welding Institute (UK) to adopt the methodology of designing to prevent fracture initiation.

* References in the W.I.C. Report, attached as Appendix 1.

The design against brittle fracture in fixed structures adopted by governmental bodies and classification societies has been to specify minimum Charpy impact requirements; the aim being to prevent initiation of unstable fracture. This behaviour is ensured by either specifying high upper shelf energy for arrest performance or by requiring a low transition temperature. This design procedure requires correlations between toughness requirements and practical experience. Extrapolation of Charpy requirements to the thicknesses found in critical parts of deep water platforms has been considered insufficient and doubtful due to lack of relevant service data. To overcome this problem, fracture mechanics is now being used to assess the risk of brittle fracture.

6.2 FRACTURE BEHAVIOR AND TESTING

When fracture mechanics testing is deemed necessary, the testing methods and strain rates are chosen to conform to those of the actual structure. The crack tip opening displacement (CTOD) technique is normally specified since the subsequent analysis is relatively straightforward and can account for residual stresses. This in turn requires a realistic test assembly to be prepared using thicknesses, consumables, and welding procedures representative of the actual structure. Tests are normally conducted on both the weld metal and the heat-affected zone at the lowest anticipated service temperature.

The initiation approach to fracture control aims at ensuring that the toughness of the most brittle microstructure present in the fabrication is high enough to tolerate the maximum stresses to be imposed, in the presence of any defects that might remain after inspection. This philosophy has been extensively used for ferritic steels, which show a transition behavior with temperature. This transition temperature is heavily influenced by thickness and strain rate, and hence the initiation approach must take these effects

into account. In order to do this the fracture toughness of all of the microstructures within the weld region must be measured.

The CTOD test provides a measure of elastic-plastic fracture toughness, i.e. the resistance to crack extension, which is unique to the specimen design and material sampled at the tip of the notch in a test at the temperature and strain rate specified.

This test has been under development for many years and has culminated in a British Standard, BS5762:1979, which defines a standard testing technique. However, the results can be influenced by many factors, the most important being geometry. It was realized from the start that the tests in the elastic-plastic regime would be thickness dependent. For this reason, BS5762: 1979 requires that full thickness specimens should be used.

In evaluating the fracture behaviour of welds, another important factor in CTOD testing is the notch tip location. This is because the CTOD test measures initiation toughness. Measurements of HAZ toughness can be of value only if it can be envisaged that defects exist or can form in these regions. The transformed heat affected zone, particularly the grain-coarsened region, is a potential site for hydrogen-induced cracks, liquation cracks and reheat cracks. Sub-critical HAZ embrittlement (i.e. in regions heated to below the ferrite/austenite transition temperature) has been found to be significant only if welding is done in the presence of a strain concentrator. Since, all regions of the weldment should be assessed to determine the lowest toughness region, it therefore becomes important to determine the exact notch tip location in the HAZ after testing.

7.0 SPECIFICATIONS

Chemical, mechanical and welding requirements for Lloyd's LT60 are summarized below.

7.1 CHEMISTRY

Carbon	0.16% maximum
Silicon	0.1 - 0.5%
Manganese	1.00 - 1.6% (1.65% maximum if C $\leq$ 0.14%)
Phosphorus	0.025% maximum
Sulphur	0.020% maximum
Chromium*	0.25% maximum
Copper*	0.35% maximum
Molybdenum*	0.08% maximum
Nickel*	0.30% maximum
Aluminum	minimum 0.015% soluble or 0.020% total
Niobium	0.015 - 0.05% (optional grain refiner)
Vanadium	0.03 - 0.10% (optional grain refiner)

* Cr + Cu + Mo + Ni $\leq$ 0.70%

7.2 MECHANICAL PROPERTIES

Three strength levels are permitted in the specification:

YIELD STRENGTH MPa	ULTIMATE STRENGTH MPa	ELONGATION (%)
245	360 - 480	24
285	410 - 530	24
355	490 - 610	22

CVNL minimum average energy 41 Joules @ -60°C

CVNT minimum average energy 27 Joules @ -60°C
(transverse requirement for LNG tanker only)

These requirements are applicable to products not exceeding 30 mm thickness. The requirements for thicker products are subject to agreement.

In designing the chemistry and processing of this steel, Algoma's first objective was the realization of the impact properties. Yield strength was to meet the highest level possible subject to meeting the toughness requirements.

7.3 WELDING

There is no reference to HAZ testing in the Lloyd's LT60 specification. As a result, the Welding Institute of Canada designed a test program incorporating elements of the limited number of published guidelines available for butt weld procedure tests. Those guidelines, taken mainly from a draft Lloyd's document on LNG tankers operating in the Canadian Arctic, are summarized in the following chart.

Thickness	Transverse Test	Charpy V-Notch			
		Weld Metal *		Fusion Line & HAZ	
mm	MPa	Test Temp °C	Average Energy Joules	Test Temp °C	Average Energy Joules
≤ 35	490	-60	27	-60	31
>35 <55	490	-80	27	-60	31

* No individual result to be lower than 18J

8.0 PARENT PLATE TEST PROGRAM

8.1 MANUFACTURE

One 250 tonne B.O.S.P. heat was produced to LT60 specifications and rolled using the normal ingot processing route to plates of 25, 50, 63 and 75 mm in thickness. All plates were normalized and ultrasonically inspected. Samples from front, middle and back locations of the normalized plate were taken to determine tensile and Charpy impact properties. Samples of each size were also evaluated in the longitudinal and transverse directions using the Navy drop weight nil ductility test. Material for CTOD testing was taken from the 25 mm and 75 mm plates. Ladle and LT60 specification chemistries are compared in Table 1.

In addition to being normalized, as required by the Lloyd's LT60 specification, the 25 mm plate was thermo-mechanically controlled rolled on Algoma's computer controlled 4,220 mm wide plate mill. Plates over 25 mm were subjected to a partial "controlled rolling" schedule with the aim being to finish below the grain-coarsening temperature of this steel.

Essentially, Algoma's patented thermo-mechanical controlled rolling may be defined as a specific pass and reduction schedule to a finish temperature below the grain growth region. An important feature of this controlled rolling is continuous reduction through the grain growth region with a specific reduction in plate cross-sectional area. The plate mill computer automatically determines and controls every phase of the reduction schedule to assure adherence to, and reproduceability of the controlled rolling schedule. The practice of controlled rolling at Algoma was presented by R.J. Ackert and M. Bowie at the International Conference on Steel Rolling sponsored by the Iron and Steel Institute of Japan in 1980.

8.2 TENSILE TESTING

Tensile results are summarized in Table 2 and in Figure 1. The performance was excellent. Yield and ultimate strengths (averaging 387 and 513 MPa respectively) exceeded the most stringent of the three specifications in all four thicknesses. Elongation averaged 31% which is well in excess of the specified minimum of 22%.

Figure 1 shows a small decrease in yield strength (from 407 to 370 MPa) with increasing thicknesses. This may be indicative of the diminishing effectiveness of controlled rolling with heavier thicknesses. A trend towards a slightly lower yield strength at the mid-plate position is also indicated, with the highest strengths being measured in front location. It should be noted that in all cases the range of variation is very small. Although these trends may be of some metallurgical interest, they are well within the normal distribution anticipated in commercial production.

8.3 CHARPY IMPACT TESTING

Impact toughness on all thicknesses averaged 200 Joules longitudinal and 125 Joules transverse at -60°C. Details of impact testing mean values, minimums, standard deviations and per cent shear are summarized in Tables 3 through 10 inclusive. CVNL and CVNT impact energies are also summarized as a function of temperature in Figures 2 through 9 inclusive. The standard deviations and minima are calculated on the basis of the 3 point averages for each test. Impact energy decreases with temperature but no rapid change characteristic of a ductile to brittle transition temperature is observed. This is not unusual since high strength steels frequently fail to exhibit a distinct transition temperature. The impact energies are similar for all plate thicknesses, although marginally better for the 25mm material at the very low temperatures. Minus 2 sigma is a statistically predicted line above which 95.5% of all test results

should lie if the data is normally distributed. The histogram in Figure 10 shows the distribution of CVNL energy at -60°C.

Per cent shear is shown as a function of temperature in Figure 11. Shear values are essentially independent of plate thickness with the exception of the slightly higher values for the 25 mm material in the transverse direction.

8.4 NIL DUCTILITY TEMPERATURE (NDT)

Nil ductility testing (ASTM E208) was contracted to Ontario Research Foundation. Their report is attached as Appendix 2. Nil ductility temperatures ranged from -54°C for the 25 mm material to -43°C for the 75 mm material. Although there is no Lloyd's specification for nil ductility temperature, none of the NDT temperatures were less than the LT60 design temperature of -60°C. This may be of concern since nil ductility temperature is the temperature at which fully brittle fracture behavior is observed, and is thought to be indicative of an optimistic lower performance limit for the material.

8.5 CTOD TESTING

CTOD testing of the parent plate materials was conducted at the Welding Institute of Canada. The 25 and 75 mm plates had full-thickness CTOD samples (t x 2t and t x t, respectively) machined such that their principal axes were transverse to the principal rolling direction, and the fatigue crack was therefore along the rolling direction. All testing was done in accordance to BS5762:1979 at -60°C, and the results are given in Table 12. Minimum CTOD values for both plate thicknesses was approximately 0.6 mm (Su). The first 25 mm sample exhibited fully ductile behavior while all of the remaining tests failed in an elastic-plastic manner.

8.6 METALLOGRAPHIC EVALUATION

Data for cleanness and grain size are summarized in Table 11. Cleanness ratings generally indicated alumina type inclusions with severity B1 to B1-1/2, however one 50 mm plate had a severity rating of B2-1/2 to B3-1/2. The ferrite grains were uniform and equiaxed, with ASTM grain size in the range of 8 to 9. There appeared to be a slight tendency towards a larger grain size in the thicker material.

Photo micrographs representative of the grain size found in the four plate thicknesses are shown in Figure 12. Typical cleanness photo micrographs are presented in Figure 13.

8.7 DISCUSSION

The production of this experimental heat has demonstrated Algoma's ability to produce normalized plate with toughness and ductility which exceed Lloyd's LT60 requirements.

Ultrasonic and Metallographic inspection have confirmed relatively good cleanness in this rare earth treated steel. All of the mechanical properties were consistent and reproducible. There was no significant trend with ingot number, plate thickness, or test location . Yield strength was successfully controlled within a range of 365 to 415 MPa with a marginal decrease seen with increasing plate thickness. Ultimate strength and elongation were also acceptable.

Parent plate impact toughness was excellent. No trend dependent on plate or test location was noted. No distinct ductile to brittle transition was apparent from the transition curves, typical of microalloyed steels. A ductile to brittle transition temperature can be estimated by taking the temperature for one half the upper shelf energy. For these plates a ductile to brittle transition could be

estimated as -70°C. It must be noted that extreme caution is necessary when drawing practical conclusions from this estimate. The ductile to brittle transition temperature is very dependent on sample size and constraint. Because of its very small size, a Charpy test will show much lower transition temperatures than would be anticipated in full sized structures. Concern regarding the applicability of Charpy testing is supported by the drop weight nil ductility temperatures which were reported in the range of -43 to -54°C on this parent plate material. However, CTOD fracture testing on the parent plate material showed that some ductility was evident at the test temperature of -60°C, with most of the samples failing in an elastic plastic manner.

9.0 WELDING TEST PROGRAM

9.1 BACKGROUND AND EXPERIMENTAL DESIGN (WELDING)

This section summarizes portions of the Welding Institute of Canada submission to the Algoma Steel Corporation. Their final report, including an extensive literature review, is attached as Appendix 1.

9.1.1 FACTORS INFLUENCING HEAT-AFFECTED ZONE TOUGHNESS

Many factors influence the fracture behavior of heat affected zones, including thermal cycling and heat input, microstructures, alloys, microalloys, precipitates and inclusions.

The development of high strength steels with minimum property requirements at temperatures as low as -60°C has been realized through the use of carefully controlled rolling procedures and alloying with Nb, V, and rare earths. Heavier sections (>40 mm) require normalizing or quenching and tempering to achieve uniformity through the thickness. The HSLA steels exhibited the improved properties compared to C-Mn steels because of the fine grain size after rolling, dispersion strengthening by microalloy based precipitates and inclusion size and shape control when modified by alloys such as Ce, Te or Ca.

Although the HSLA steels demonstrate obvious benefits over the C-Mn steels in terms of strength and toughness, the microalloy additions have a strong and sometimes deleterious influence on weldability.

Therefore, it is necessary to study the effect of the thermal cycles induced by welding on grain size, precipitates, etc. in

order to understand the resulting heat-affected zones and its properties.

9.1.2 HEAT AFFECTED ZONE CHARACTERISTICS AND THE INFLUENCE OF MICROSTRUCTURE PRECIPITATES, STRAIN AGING AND HEAT INPUT

The width of the heat-affected zone and the nature of microstructures depend on the heat input and cooling as shown schematically in Figure 14. Between T_2 and T_3 (upper austenite region), grain boundary migration and coalescence causes rapid grain growth leading to a grain-coarsened HAZ. In the lower austenite range (T_1 to T_2), a fine-grained structure is produced. The upper limit T_2 is controlled largely by grain refining elements such as Al, Ti, Nb, V, and N. These form carbides and nitrides which prevent grain boundary migration but their usefulness reduces as the temperature is increased, since they go into solution. High yield strengths can be obtained by a uniform dispersion of precipitates throughout the matrix. Some of the strengthening may be lost if the precipitates are taken into solution in the high temperature HAZ near the fusion line (just below T_3). In addition, they may be overaged, in lower temperature regions, in which case the precipitates coarsen, and the strength is reduced. In such cases, the original properties can only be restored by reheat treatment. In the remaining portion of the HAZ between T_0 and T_1, pearlite in the original parent material begins to transform to austenite. If subsequent cooling is fast enough, and the material is high in carbon and microalloying elements, martensite may also be formed in this region.

Thus, a composite picture can be constructed as in Figure 14 of microstructure which varies continuously from the unaffected parent material at T_0, through fine-and coarse-grained phases to the fusion line, and finally to the cast structure of the weld metal.

Many factors are important in assessing the toughness of the HAZ toughness. It must be stressed that all these factors are interrelated and their combined effect on the HAZ toughness may not be simply cumulative. The effects of gross microstructures (i.e. ferrite, bainite, and martensite), precipitates, inclusions, and grain size on toughness should be considered. The compositions of the HSLA steels are such that they produce ferrite-pearlite microstructures under normal steel finishing procedures. However, after welding, a variety of microstructures can result in the HAZ of the base plate due to the rapid thermal cycles experienced in the various regions of the HAZ. Mixtures of lath structures (ferrite or bainite) and martensite are commonly believed to represent the best compromise between hardness and toughness.

The importance of precipitates in assessing the HAZ toughness increases in the presence of elements such as niobium, vanadium, and titanium as these alloy elements readily form carbide or nitride precipitates. These microalloy elements are used for strength and grain refinement in low-alloy structural steels. In normalized or controlled rolled plate the precipitates seem not to be detrimental. This is partly due to their size and distribution, and partly due to the fact that their beneficial grain refining action outweighs their detrimental aspects. However, after the thermal cycle associated with welding, the grain refinement effect is lost in the coarse-grained region of the HAZ. During the heating cycle, some of the precipitates will dissolve back into the austenitic matrix due to high solubilities at high temperatures. The extent of dissolution and the temperature at which this occurs depend on the solubilities of these carbide/nitride particles in the steel at a given temperature. When these precipitates are dissolved they cannot retard grain growth and regions of coarse grains are formed. Their reappearance on cooling depends on the composition of the steel, the type of precipitates concerned, and the cooling rate. If precipitates reappear in a continuous row-like

manner, or as fine dispersions, low toughness and high hardness will result.

The effects of heat input are very important in determining the HAZ toughness. Excessive heat input will always degrade toughness in the HAZ, especially in steels that contain microalloy elements where precipitation hardening is detrimental. From an economic point of view, particularly when thicker and thicker sections are being welded, research will continue to develop steel compositions which can be welded with high heat input without loss of HAZ toughness.

In summary, HAZ toughness is a function of microstructure, composition and heat input. The problem is further complicated by the fact that there is always a gradient of microstructures across the HAZ. The quantity and location of microstructures are also important. For example, the alignment of martensite-austenite particles along prior austenite grain boundaries may be significant. The effect of alloy elements, both in solid solution and as precipitates, is not totally clear. The possible interactions amongst alloys have been even less studied. The ideal base material would be one that possesses a fine grain size, has stable precipitates to prevent grain growth during welding, contains a minimal of interstitial elements and would transform to microstructures having the desired properties after the welding cycle.

9.1.3 EXPERIMENTAL APPROACH

Three types of weld tests were conducted on the LT60 material: bead on plate, K-prep for fracture toughness, and butt weld procedure testing. Bead on plate welding was conducted in order to determine the optimum heat input conditions for the larger weld tests.

9.1.4 BEAD ON PLATE TEST WELDS

Bead on plate welds were used in order to develop hardening curves, examine microstructural changes in the heat affected zone, and determine fracture toughness in the heat affected zone. The heat affected zone hardness of weldments is determined by both the chemical composition of the plate and the thermal history. The thermal histories of the welds as they cooled to room temperature were recorded using thermocouples which were mechanically plunged into the molten weld pool. The time to cool between 800°C, and 500°C, t_{8-5}, was obtained for each weld.

The nominal welding conditions for the five welds are listed below.

Weld Number	Initial Plate Temperature °C	Voltage volts	Current amperes	Travel Speed mm/s	Nominal Heat Input kJ/mm
1	20	32	425	14.8	0.86
2	20	30	550	8.3	2.0
3	30	32	576	6.8	3.19
4	20	32	700	5.3	4.23
5	200	32	700	5.3	4.23

The cooling cycle for the lowest heat input is comparable to manual welding with a 4 mm diameter electrode on thick plates without preheat while the highest heat input represents realistic welding conditions for actual construction projects.

In order to examine the changes in the heat-affected zone, a metallographic study was conducted on the welds deposited for the hardening curve. The results of this detailed examination gave an understanding of the microstructural transformations in the heat-affected zone. This information was used in support of the hardening curve results, in determining the procedures for K-prep and butt welding.

The effect of welding procedure variables on the fracture toughness was examined by CTOD testing of the hardening curve welds. This work was intended to investigate the toughness of various regions of the heat-affected zone. Two t x t specimens were tested for each of the hardening curve welds. The notch was extended by fatigue pre-cracking into the coarse-grained heat-affected zone. All of the notches were made in the base plate and then grown towards the weld. Most testing for the CTOD evaluation was done at -60°C, although a transition curve over the temperature range of -90°C to 0°C was also determined for the 3 kJ/mm weld.

9.1.5 K-PREP WELDS FOR FULL THICKNESS FRACTURE TOUGHNESS TESTING

A series of K-preparation welds were made from each plate. This joint configuration was chosen so that the fatigue crack notch tip could be accurately grown into the region of interest for subsequent testing. The specimen type and notch locations tested are summarized below. The surface notched specimens were required because of limitations in the capacity of the testing machine. Three specimens were to be tested for each case.

Specimen Type	Notch Location	Region to be Tested		
		25 mm	50 mm	75 mm
t x 2t	through-thickness	Coarse HAZ	-	-
t x 2t	through-thickness	Fine HAZ	-	-
t x t	surface	Coarse HAZ	Coarse HAZ	Coarse HAZ
t x t	surface	Fine HAZ	Fine HAZ	Fine HAZ

9.1.6 WELD PROCEDURE QUALIFICATION OF BUTT WELD TEST ASSEMBLIES

Butt weld assemblies were prepared in the downhand position, using Lloyd's approved consumables and welding equipment. Test plates were made by welding two plates together in two thicknesses, 25 mm and 75 mm. Butt weld tensile test specimens were machined through the weld metal and HAZ. Charpy V notch testing was done on each weld. Notches were located at:

(a) centre of weld
(b) on fusion line
(c) in HAZ, 1 mm from fusion line
(d) in HAZ, 3 mm from fusion line
(e) in HAZ, 5 mm from fusion line

Specimens were polished, etched and hardness tests conducted. The specimen was examined to insure fusion at the root, full penetration and freedom from cracks and other defects.

9.2 RESULTS

9.2.1 HARDENING CURVES AND METALLOGRAPHIC INSPECTION OF BEAD ON PLATE WELDS

Four sections from each weld were removed for hardness measurements. The maximum hardness of the coarse-grained HAZ was recorded for each weld and the average values for each heat input are plotted against cooling cycle in Figure 15. All of the results can be represented by the same curve, which is expected, since the plates were all rolled from the same heat of steel.

The heat-affected zones of these welds were examined to assess what microstructural changes could be attributed to various heat inputs. The prior austenitic grain size was determined by counting the number of grain boundaries intercepted over a distance of 120 mm at a magnification of 500X. At the same time, a qualitative

assessment was made of the relative proportions of various microconstituents.

The results of the semi-quantitative metallographic examination of the hardening curve welds are presented in Table 13. Although there are many subtleties in the appearance of the microstructures, three categories were chosen to quantify the results. These categories are proeutectoid ferrite (PF),lath structure (LS), and martensite (M).

All of the welds at 1 kJ/mm had 80% martensite and 20% lath structure, a 50% martensite and 50% lath structure at 2 kJ/mm and 3 kJ/mm, and at the highest heat inputs the heat-affected zones were essentially lath structure with some limited areas of proeutectoid ferrite. From a metallurgical viewpoint, the optimum balance in structures is obtained for the intermediate heat inputs, 2 to 3 kJ/mm, in which the HAZ is comprised of 50% martensite and 50% lath structure. At lower heat inputs, the risk of hydrogen cracking is increased because of the higher martensite content and hardness, whereas at higher heat inputs the formation of coarse lath structures is detrimental to toughness.

9.2.2 FRACTURE TOUGHNESS (CTOD) TESTING OF BEAD ON PLATE WELDS

The effect of welding heat input on fracture behavior was examined using CTOD test methods as outlined in BS5762:1979. The location of the fatigue pre-crack tip relative to the coarse grained HAZ is of critical importance in insuring that the proper area is tested. The steps taken at the Welding Institute of Canada to confirm this tip location are detailed in their reports, (Appendix 1 section 3.2.2).

At least two CTOD samples were tested at -60°C from each hardening curve weld. The results are summarized in Table 14.

The CTOD toughness from the hardening curve welds are plotted against cooling rate in Figure 16. Full data is presented in Appendix 1, Figure 14. The lines in the figure represent the lower bound toughness for the 25, 50, and 75 mm plates based on the limited number of tests.

Although additional testing would be required, the lower bound toughness results from the hardening curve welds seem to indicate that the largest CTOD values in the coarse-grained HAZ were obtained at intermediate heat inputs. This toughness was measured for microstructures which contained a 50% martensite-50% lath structure mixture which, as mentioned previously, was the optimum combination. The limited hardening curve CTOD values seems to confirm the decision to use a nominal heat input of 3 kJ/mm for the full thickness welds.

The CTOD evaluations of the effects of heat input on the hardening curve welds involved testing only at -60°C. This temperature was expected to lie within the lower shelf regime and thus the results would represent the worst case. A transition curve was subsequently determined for weld 3A (25 mm, 3 kJ/mm) to examine the variation of toughness with temperature. The details of testing are given in Appendix B of Appendix 1, while the CTOD values are plotted against temperature in Figure 17. The lower shelf CTOD of approximately 0.05 mm was maintained up to -50°C, above which temperature there is a trend to increased CTOD values.

9.2.3 FRACTURE TOUGHNESS TESTING OF K-PREPARATION WELDS

The attainment of a planar zone on the vertical side of the K-prep was difficult to obtain using methods representative of good welding practice. When the capping passes were deposited, the depth of penetration and the necessary bead placement resulted in a weld looking as if it had been prepared using a butt weld joint. It was therefore not possible to place a through-thickness notch such that

testing was in a single region, either coarse-grained or fine-grained. The actual testing was a combination of the two and is referred to as a 'mixed zone'. However, the surface notches were located such that the fatigue crack tips were in the region of interest, either the coarse-grained or fine-grained zones.

The CTOD specimens were tested in the as-welded condition. The 25 mm weld was tested at -60°C, -35°C, and -10°C, while the 50 mm and 75 mm welds were tested only at -60°C. The complete results are given in Appendix B of the WIC report, which includes the specimen measurements and loading curves. The interpretation of the CTOD values for these K-prep welds showed that a distinction could be made between the coarse-grained and fine-grained regions, as shown in Figure 18. The values in this figure also include the results from the bead on plate weld transition curve to complement the lower bound values. Since most of the points refer to lower shelf CTOD values where specimen size and geometry effects are less significant than in the transition zone, comparing all of the results without correction is not expected to influence the outcome. The low toughness of the coarse-grained zone is evident through most of the temperature range, although there is a slight improvement at +10°C (Bead on Plate result). The fine-grained region exhibits improved toughness at -60°C compared to the coarse zone and the lone result at -10°C suggests that the toughness improves rapidly between -60 and -10°C. A final point worth noting from Figure 18 is the large difference between the baseplate toughness and that of the weld zones at -60°C.

9.2.4 PROCEDURE TESTING OF BUTT WELD ASSEMBLIES

Butt welds were made using 25 and 75 mm plates to examine the weldability of the LT60 steel at 3 kJ/mm.

When welding had been completed, the 25 mm plate was radiographically inspected to ASME Section IX and the 75 mm plate was

examined ultrasonically. The radiograph met the specification and no reflectors were apparent for the ultrasonic test.

Full thickness cross-weld tensile specimens were removed from each weld. The tensile specimens failed in the baseplate, above the minimum specified yield showing the soundness of the weld.

Standard Charpy impact specimens were machined transverse to the welding direction with the notches perpendicular to the plate surface and located at several positions across the weld as shown in Table 15 and 16. Accurate positioning of the Charpy notches required etching of the finished blanks to reveal the fusion boundary, locating the notch, and then cutting the specimens to length. The fusion line position conforms to the Lloyd's Registry of Shipping Rules for Welding and Inspection. One set of 15 specimens was prepared from the 25 mm plate while two sets were prepared from the 75 mm plate. The weld metal specimens for the 75 mm weld were tested at -80°C while all other testing was done at -60°C.

The hardnesses across the heat-affected zones of the butt welds were measured using a Vickers diamond point indenter with a 5 kg load (Tables 15 and 16). The hardnesses at 5 mm from the fusion line, for both the 25 mm and 75 mm butt welds were only slightly different than the unaffected baseplate.

9.3 DISCUSSION

The weldability of the steel is discussed by referring to each phase of the experimental program. This involved examination of the basic response of the steel to welding thermal cycles using hardening curves and mechanical testing of procedure qualification welds.

9.3.1 HARDENING CURVES AND METALLOGRAPHIC INSPECTION OF BEAD ON PLATE WELDS

The maximum hardness in the heat-affected zone is one of the most important parameters in estimating the resistance of a steel to hydrogen cracking. The value of this parameter reflects a necessary selection of materials and welding conditions to prevent cracking, and is often referred to when describing the weldability.

The hardness, in turn, gives a rough indication of the susceptibility of the HAZ to hydrogen cracking since the microstructures produced at rapid cooling rates are more susceptible to cold cracking as a result of hydrogen embrittlement. The response of the heat-affected zones of these steels to changes in cooling rates can be represented by "hardening curves". The shape of the hardening curve, and the maximum hardness at fast cooling rates are indicative of the degree to which HAZ crack susceptibility can be controlled by the welding procedures. Generally if the hardness is above 350 HV, cold cracking may become a problem.

A part of this current EMR-sponsored project has been involved with examining this LT60 steel and two others (an A710 GrA, Class 3 and a BS4360 Gr50E steel) using a hardening curve approach at AMCA. The curves in Figure 19 shows the comparative hardening behavior of the three steels. The A710 steel is less hardenable than the LT60 steel while the BS4360 50E steel is more hardenable, although all are acceptable in that they would pose no problems with current welding procedures.

The precise metallurgical conditions which control toughness are difficult to identify. Austenite grain size, which is certainly of paramount importance, will be controlled by effective net heat input, alloying additions, and precipitation effects. Long cooling times may permit the microstructure to become 100% Bainite and exhibit

low toughness as in its presence, cracks can propagate readily across ferrite-ferrite boundaries within a bainitic colony.

Consideration must also be given to the changes in the dispersion of fine carbides, either niobium or vanadium. Such changes could be brought about by interactions between the niobium and vanadium or any other carbide formers, or could simply result from the fall in transformation temperature with increasing alloying. The interaction between these factors has yet to be resolved.

9.3.2 FRACTURE TOUGHNESS (CTOD) TESTING OF BEAD ON PLATE AND K-PREPARATION WELDS

Measurements of CTOD have become increasingly important in recent years with the introduction of fracture mechanics methods which evaluate allowable defect sizes. Past experience has indicated that the HAZ CTOD is generally lower than that of the weld metal. When measuring toughness in the HAZ, the crack tip location is crucial to obtain the minimum CTOD, particularly in multipass welds.

The concensus developed over the years for CTOD testing has been that numerous repetitions must be made to obtain the minimum CTOD value of any region being tested. The scatter in the results of this study and published work is evident, and this confirms the requirement of testing many specimens. It would be necessary to perform in the range of 12 to 20 CTOD tests at a single point in order to obtain a reliable -2 sigma lower bound estimate. This difficulty is well illustrated for bead on plate data in Figure 17. Although there is a trend to higher CTOD values at temperatures in excess of -40^{o}C, there is one very low value at -10^{o}C. Much more testing would be required in order to properly define the lower bound transition curve for this material.

In a multipass weld assembly such as a K-preparation, the initial HAZ regions subjected to reheating from subsequent passes undergo additional microstructural changes which result in the following structures (Figure 20): a coarse-grained region (A), fine-grained (B), granular pearlite (C), and coarse structures (regions D and E). This accounts for the principal difference expected between a single pass bead on plate weld, and a multipass weld. The potential effect of this reheating on toughness is unclear. Although toughness may be improved in the refined region, it may also deteriorate due to precipitate growth.

Reheating from subsequent passes also results in the plastic deformation due to the rotational distortion of the joint. This promotes dynamic strain aging, or hot strain embrittlement, which can lead to loss in toughness.

The measured CTOD values on this LT60 material were generally very low at the anticipated service temperatures of -60°C when compared with the North Sea design criteria at -10°C. This should be of concern to the extent that the problem be studied in further detail. However, the difficulties experienced in CTOD testing of this material are far from unique. In Figure 21 this LT60 steel compares favourably with the CTOD results from a steel evaluated at the Welding Institute (UK). These and other published results show that the heat-affected zones of single pass and multipass welds can produce extremely low CTOD results at testing temperatures below 0°C. It is unclear at this time what CTOD values can be reasonably expected at temperatures below -40°C in commercially produced and welded steels.

9.3.3 APPLICATION OF CTOD RESULTS

The CTOD test has been developed to determine a fracture toughness measure of the significance of a particular defect in a known stress field. However, to apply CTOD to a structure it is

necessary to complement it with other test results since it is relevant to only one part of the structure. Failure of part of the overall fabrication may or may not lead to catastrophic failure. All of these factors must then be considered when determining the structural integrity of a welded structure.

The difficulties associated with the interpretation of HAZ CTOD test results are considerable. In measuring toughness for fracture initiation, the CTOD measures the lowest toughness region within the very small plastic zone that envelops the fatigue crack tip. In the heat affected zone there is a steep microstructural gradient so that the crack tip location must be very accurately positioned. Since the test samples a very small region, the reproducibility of the test is relatively poor in these complex microstructures and the scatter of data necessitates testing many samples.

The lowest result from CTOD testing has been used to determine the minimum toughness of the region being tested and additional testing would generally lead to a decreasing minimum CTOD value. This use of CTOD values did not take into account the distribution of CTOD values about a mean. the Welding Institute (UK) has stated that based on its experience and a sufficient number of samples (minimum 6), they would be able to statistically determine the ability of the tested material to meet any stated CTOD requirements. In other words, an extremely low or high CTOD value would not be considered as solely indicative of the material's fracture toughness.

As discussed, the scatter in the results of this study and published work is evident. Although there is a trend to higher CTOD values at temperatures above -40°C for the bead on plate samples, there is one very low value at -10°C, and one very high value at -30°C. Although more tests at temperature would be required, it would follow, using the Welding Institute (UK) procedures that those two

values would not be counted too heavily in determining a HAZ fracture toughness transition curve of this LT60 steel.

9.3.4 PROCEDURE TESTING OF BUTT WELD ASSEMBLIES

The mechanical testing of butt-welded joints was done to determine the acceptability of LT60 steel for welded construction, particularly for the fabrication of Arctic icebreakers. The requirements were based on the W.I.C. survey of procedure testing guidelines and were used in our testing as the acceptance criteria. These requirements were outlined in Section 7.3 (27 Joules at -60°C for weld metal and 31 Joules at -60°C for fusion line and HAZ). It should again be noted that the LT60 grade is limited to a maximum thickness of 30 mm except by agreement.

The impact energies at -60°C for the 25 mm plate (Table 15) gave good results averaging 80 Joules in the weld metal with a low of 50 Joules in the coarse-grained HAZ, and an improvement in the baseplate away from the weld. Referrring to the acceptance criteria, the 25 mm butt weld exceeded the minimum requirements.

The Charpy values for the 75 mm plate are listed in Table 16. At the testing locations for the butt weld procedures, our requirements specified that the weld metal must attain a minimum 27 ft-lbs at -80°C and 31 Joules for the fusion line at -60°C. The weld metal toughness at -80°C was only 14 Joules but improved to 43 Joules average at -60°C for the testing position 2 mm below the surface of the plate. The corresponding HAZ impact results were 40-50 Joules within 5 mm of the fusion line but the 5 mm position showed a distinct reduction in toughness (28 Joules). This variation in Charpy results was repeated for the root position of the 75 mm plates. The weld centreline gave very poor results, 8 Joules at -80°C. There was an improvement in the coarse-grained HAZ (70 Joules average at -60°C) and then a marked reduction at the 3 mm position (17 Joules at -60°C). In

interpreting the requirements of Section 7.3, the butt weld for the 75 mm plate did not satisfy the requirements, if the limit of 55 mm was extended to include the 75 mm plates. The results for the 75 mm plate do give a cause for concern and the possible causes for the poor toughness must be addressed.

The poor weld metal toughness may be due to the dilution of the Tibor weld deposit into the 2% Ni capping pass. Tibor metal is known to experience toughness degradation during the reheating from subsequent passes. Of more concern to Algoma is the poor toughness of the HAZ of the 75 mm plate, especially for the notches located 5 mm from the fusion line at the surface (29 Joules) and 3 mm from the fusion line at the root (17 Joules). Examination of the microstructures at these locations showed that the root of the notch was located just outside of the spheroidized region and thus the maximum temperature was below 400°C. Reduction of toughness in this region has been attributed in the literature to strain aging, provided that sufficient interstitial solute is present, either carbon or nitrogen. Strain aging due to nitrogen is prevented if the ASA:N $\geq$ 2:1. In the present material, the ASA:N ratio is greater than 3:1 and thus one would not expect strain aging due to nitrogen. With embrittlement due to solute interaction being unlikely, the possibility of toughness degradation due to local stain-induced hardening was deemed the most likely cause since restraint had been lost during welding.

The main effect of plastic straining, which can be caused by forming or thermally-induced strains, is to increase the strength with a concurrent loss of toughness. The detrimental effect on impact properties is noted for most pressure vessel steels, and the maximum allowable strain before heat treatment is necessary ranges from 2.5 to 10%.

In some grades a normalizing treatment may be necessary to restore properties. In most C-Mn steels, stress relief at normal temperatures (625°C) can recover a substantial part of the toughness lost to strain-induced effects. For C-Mn microalloyed steels, however, stress relief may reprecipitate microalloy carbides and carbonitrides which can lead to significant toughness losses. At the present time, there is no clear indication on what type of treatment is the best way to proceed to recover toughness. Additional testing is being completed at W.I.C. by Algoma to determine the influence of the loss of restraint on toughness outside the visible HAZ.

TABLE 1

Chemical Anaylsis and Specification

	A.S.C. Specification	Ladle Analysis	Lloyd's LT60 Specification
Carbon	0.12 - 0.14	0.12	0.16% maximum
Silicon	0.25 - 0.30	0.28	0.1 - 0.5%
Manganese	1.30 - 1.40	1.39	1.00 - 1.6% (1.65% max. if C $\leq$ 0.14%)
Phosphorus	0.00 - 0.020	0.017	0.025% maximum
Sulphur	0.00 - 0.012	0.011	0.020% maximum
Chromium*	0.14 - 0.16	0.17	0.25% maximum
Copper*	0.16 - 0.20	0.15	0.35% maximum
Molybdenum*	-	0.001	0.08% maximum
Nickel*	0.14 - 0.18	0.15	0.30% maximum
Aluminum	0.025 - 0.055	0.027	minimum 0.015% soluble or 0.020% total
Niobium	0.025 - 0.035	0.041	0.015 - 0.05% (optional grain refiner)
Vanadium	0.040 - 0.060	0.052	0.03 - 0.10% (optional grain refiner)

*Cr + Cu + Mo + Ni < 0.70%

TABLE 2
TENSILE RESULTS
(Mean Values)

PLATE THICKNESS (mm)	YIELD (MPa)	ULTIMATE (MPa)	ELONGATION (%)*
25	407	515	29
50	387	517	32
63	386	516	32
75	370	506	32

* 400 mm gauge length for 25 mm plate, 50 mm gauge length for other thicknesses

TABLE 3
CVNL IMPACT RESULTS (Mean Values)
(Joules)

PLATE THICKNESS (mm)	-90°C	-80°C	-60°C	-50°C	-40°C	-30°C	0°C
25	146	170	195	225	248	315	344
50	106	151	202	283	285	320	340
63	83	148	182	232	309	313	361
75	-	134	206	252	-	-	-

TABLE 4
CVNT IMPACT RESULTS (Mean Values)
(Joules)

PLATE THICKNESS (mm)	-90°C	-80°C	-60°C	-50°C	-40°C	-30°C	0°C
25	80	106	129	159	149	161	209
50	69	95	123	137	146	163	199
63	58	85	104	134	144	182	224
75	-	94	140	135	-	-	-

TABLE 5
CVNL MINIMUM VALUES
(Joules)

PLATE THICKNESS (mm)	-90°C	-80°C	-60°C	-50°C	-40°C	-30°C	0°C
25	110	127	113	114	201	228	321
50	53	113	151	205	222	311	324
63	53	118	168	195	297	286	325
75	-	89	96	134	-	-	-

TABLE 6
CVNT MINIMUM VALUES
(Joules)

PLATE THICKESSS (mm)	-90°C	-80°C	-60°C	-50°C	-40°C	-30°C	0°C
25	61	62	76	73	88	153	176
50	35	56	84	104	130	151	176
63	24	42	68	115	121	163	221
75	-	43	96	106	-	-	-

TABLE 7
CVNL STANDARD DEVIATIONS

PLATE THICKNESS (mm)	-90°C	-80°C	-60°C	-50°C	-40°C	-30°C	0°C
25	34.6	18.0	43.7	60.1	49.0	79.1	38.0
50	42.0	21.8	37.7	41.5	44.7	6.6	27.1
63	41.8	27.0	16.7	55.2	13.7	38.0	49.9
75	-	23.5	64.3	49.1	-	-	-

TABLE 8
CVNT STANDARD DEVIATIONS

PLATE THICKNESS (mm)	-90°C	-80°C	-60°C	-50°C	-40°C	-30°C	0°C
25	21.6	38.0	40.1	78.0	53.7	10.6	45.4
50	22.5	17.8	16.7	17.9	14.2	25.9	30.4
63	46.6	29.0	33.0	25.9	18.7	27.8	3.8
75	-	21.8	23.1	31.9	-	-	-

TABLE 9
CVNL PERCENT SHEAR

PLATE THICKNESS (mm)	-90°C	-80°C	-60°C	-50°C	-40°C	-30°C	0°C
25	34	46	55	82	84	100	100
50	30	31	54	81	88	100	100
63	31	30	46	64	94	97	100
75	-	25	55	76	-	-	-

TABLE 10
CVNT PERCENT SHEAR

PLATE THICKNESS (mm)	-90°C	-80°C	-60°C	-50°C	-40°C	-30°C	0°C
25	17	25	37	65	73	100	100
50	17	19	25	28	29	35	79
63	15	16	22	21	28	48	100
75	-	13	24	28	-	-	-

TABLE 11
METALLOGRAPHIC EXAMINATION

SIZE	PLATE NUMBER	CLEANNESS		GRAIN SIZE (ASTM No.)	
		Surface	Core	Surface	Core
25	32345	B1	B1	9	9
	32347	B1-1/2	B1-1/2	8	8
50	32339	B3-1/2	B2-1/2	8-1/2	8
	32340	B1-1/2	B1-1/2	8	8
63	32322F	B1-1/2	B1-1/2	8	8
	32322B	-	B1	-	8
75	32873	-	B1	-	7-1/2
	32875	-	B1	-	8

TABLE 12
CTOD TESTING OF PARENT PLATE MATERIAL

Plate Thickness	25mm	75mm
Testing Temp °C	-60	-60
Specimen Type	tx2t	txt
Sample 1 (mm)	δ_m=1.12	δ_u=0.75
Sample 2 (mm)	δ_u=0.62	δ_u=0.59

TABLE 13

SUMMARY OF HARDENING CURVE RESULTS

WELD CODE	THICKNESS mm	t_{8-5},s	R540(a), °C/s	HAZ HARDNESS	Grain Size ASTM No (b)	MICROSTRUCTURAL CATEGORY PF	LS	M (c)
1A	25	4.50	48.2	329	5.6	0	20	80
2A		11.55	18.8	282	4.7	0	50	50
3A		17.0	12.8	260	3.9	0	50	50
4A		29.5	7.4	239	3.3	0	90	10
5A		61.0	3.6	224	2.8	6	95	0
1B	50	4.35	49.9	326	5.7	0	20	80
2B		9.39	23.1	293	4.5	0	50	50
3B		16.2	13.4	264	3.9	0	50	50
4B		20.4	10.6	254	3.3	0	100	0
5B		46.6	4.7	231	2.5	3	97	0
1C	75	4.35	49.9	324	5.5	0	20	80
2C		8.88	24.4	287	4.2	0	50	50
3C		15.9	13.7	263	3.8	0	50	50
4C		21.0	10.3	251	3.5	2	80	15
5C		44.4	4.9	228	2.8	3	97	0

(a) $R_{540} = \frac{217}{t_{8-5}}$ for 3D cooling (Graville)

(b) calculated from grains/mm

(c) PF - proeutectoid ferrite
LS - lath structure
M - martensite

TABLE 14

RESULTS OF CTOD TESTING OF COARSE-GRAINED HAZ OF BEAD ON PLATE WELDS

Weld	Test Temperature °C	CTOD Values (mm) Average	Minimum
1A	-60	0.041 (1)*	0.041
2A	-60	0.048 (1)	0.048
3A	-90	0.034 (2)	0.023
	-70	0.042 (2)	0.041
	-60	0.074 (2)	0.066
	-50	0.055 (3)	0.041
	-30	0.163 (3)	0.091
	-10	0.128 (3)	0.041
	+ 5	0.177 (2)	0.119
4A	-60	0.130 (2)	0.099
5A	-60	0.051 (2)	0.026
1B	-60	0.038 (2)	0.025
2B	-60	0.072 (2)	0.071
3B	-60	0.127 (2)	0.104
4B	-60	0.077 (2)	0.069
5B	-60	0.060 (2)	0.028
1C	-60	0.048 (1)	0.048
2C	-60	0.079 (2)	0.064
3C	-60	0.091 (1)	0.091
4C	-60	0.105 (2)	0.073
5C	-60	0.061 (2)	0.058

* Indicates number of specimens tested.

TABLE 15

PROPERTIES OBTAINED FROM BUTT WELD PROCEDURE ON 25 MM PLATE

Tensile Properties	
Yield Strength, MPa	440
Tensile Strength, MPa	612
% Elongation	38
Location of Fracture	Base metal

Impact Properties						
Test Temp. °C	Notch Location	Sample 1	2	3	Avg (Joules)	Hardness DPH_5
-60	A	98	64	77	80	
-60	B	78	40	53	57	229
-60	C	40	73	41	51	214
-60	D	90	90	92	91	190
-60	E	85	67	110	87	171
baseplate						165

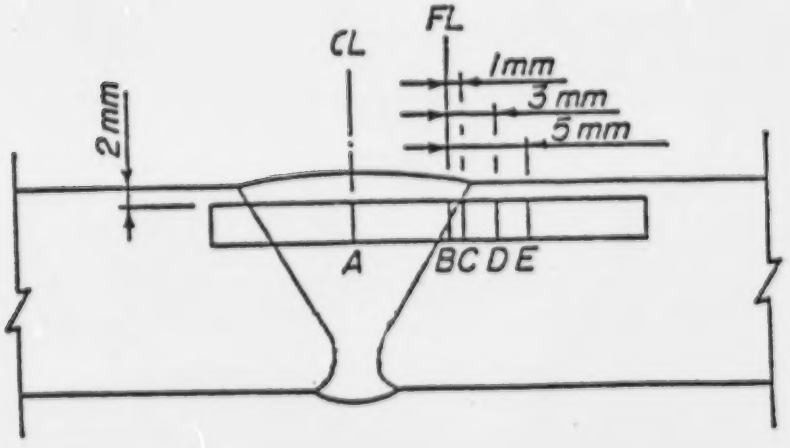

TABLE 16

PROPERTIES OBTAINED FROM BUTT WELD PROCEDURE ON 75 MM PLATE

Tensile Properties	
Yield Strength, MPa	356
Tensile Strength, MPa	521
% Elongation	29
Location of Fracture	Base metal

Impact Properties						
Test Temp. °C	Notch Location	Sample 1	2	3	Avg (Joules)	Hardness DPH_5
-80	A	13	22	8	14	200
-60	A	39	46	44	43	
-60	B	48	46	27	40	202
-60	C	35	77	42	51	224
-60	D	42	50	57	50	196
-60	E	30	28	28	29	176
-80	F	6	7	10	8	212
-60	G	15	23	17	18	244
-60	H	64	35	111	70	254
-60	J	8	32	10	17	199
-60	K	80	88	76	81	193
baseplate						183

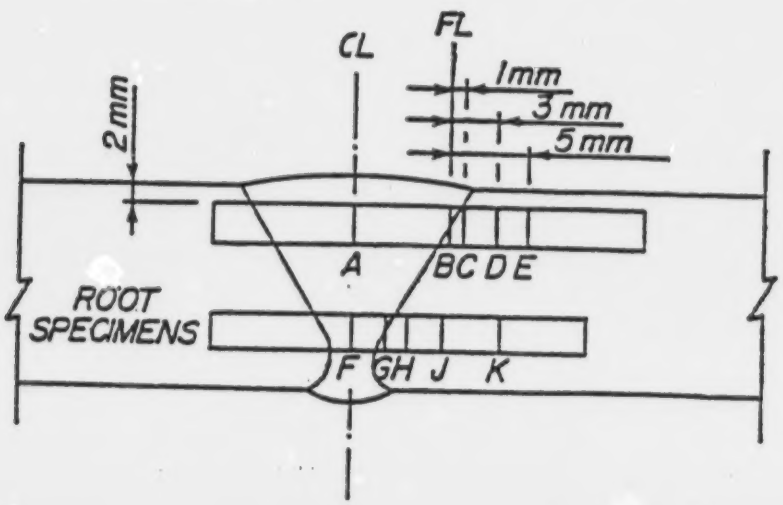

Figure 1: Parent Plate Yield Strength vs Plate Thickness and Test Location

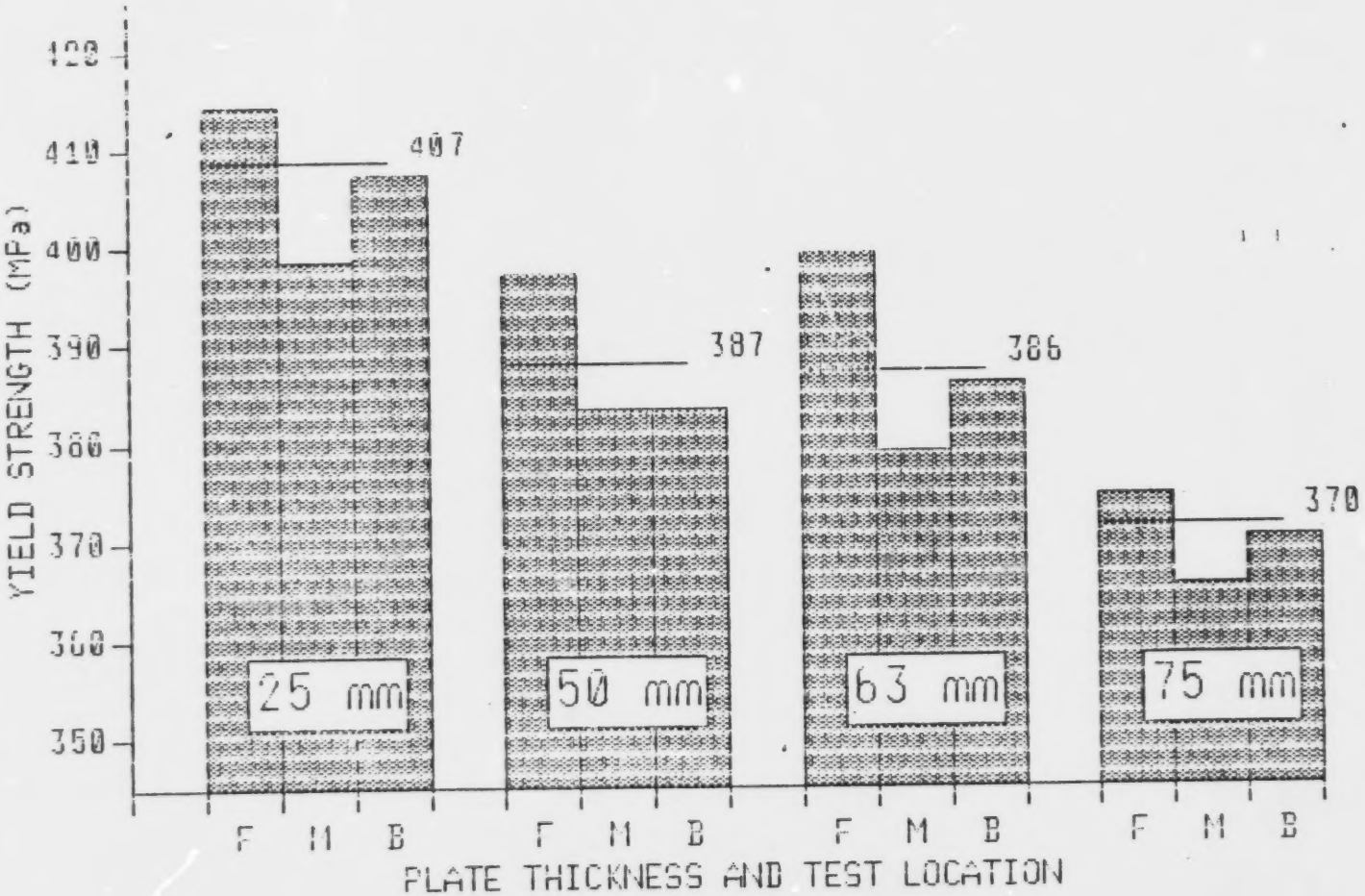

Figure 2: CVNL Impact Energy vs Temperature for 25 mm Plate

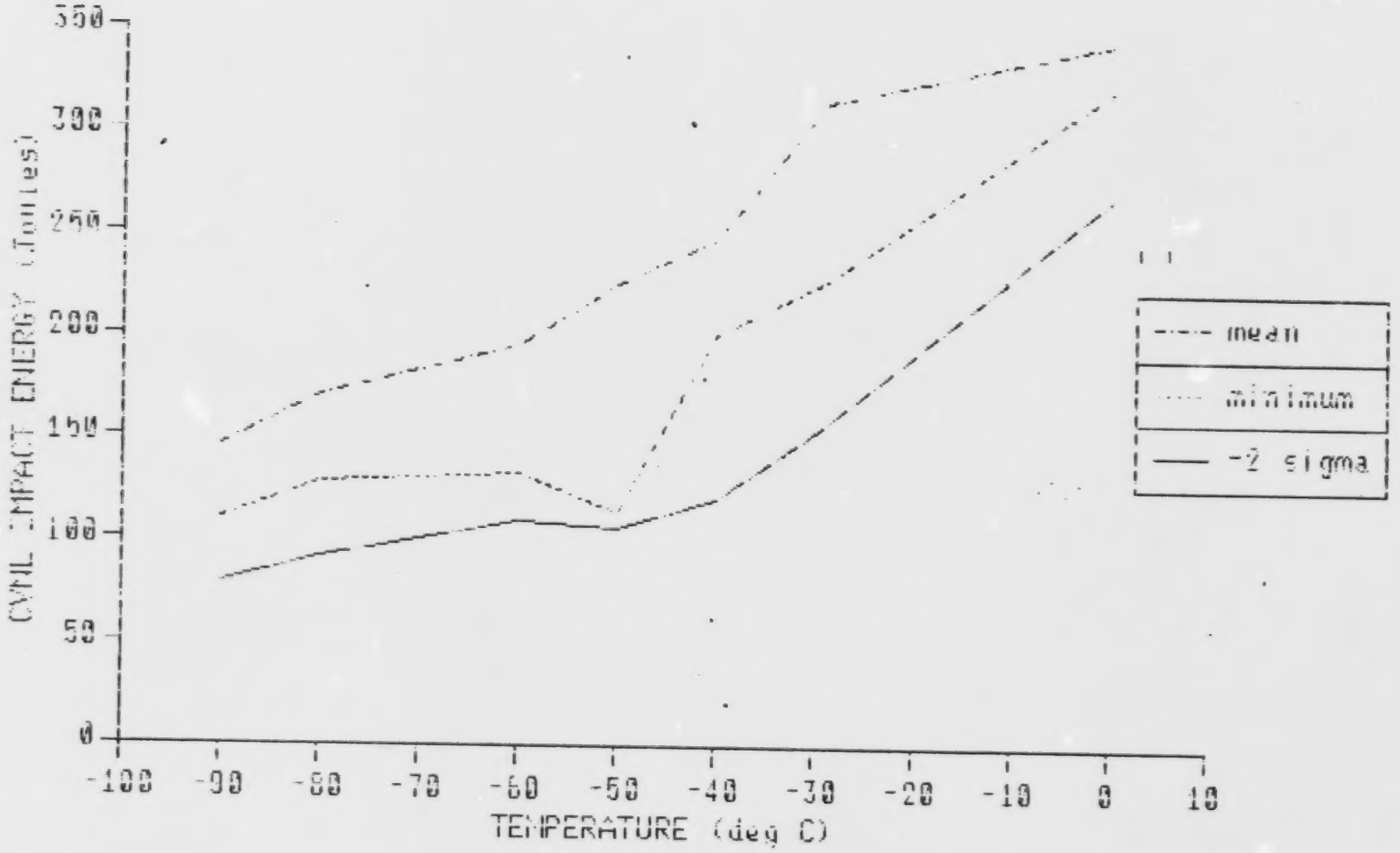

Figure 3: **CVNL Impact Energy vs Temperature for 50 mm Plate**

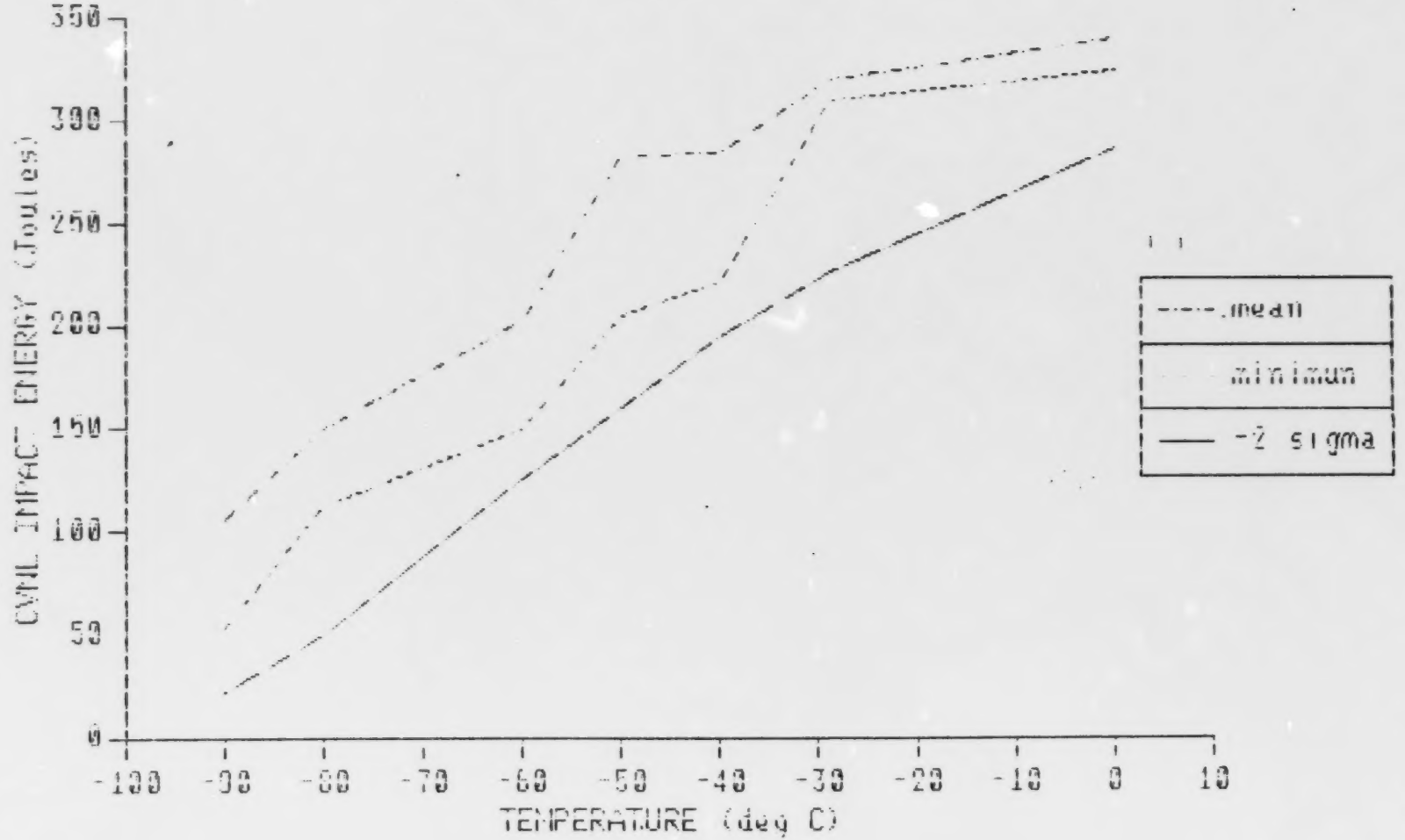

Figure 4: CVNL Impact Energy vs Temperature for 63 mm Plate

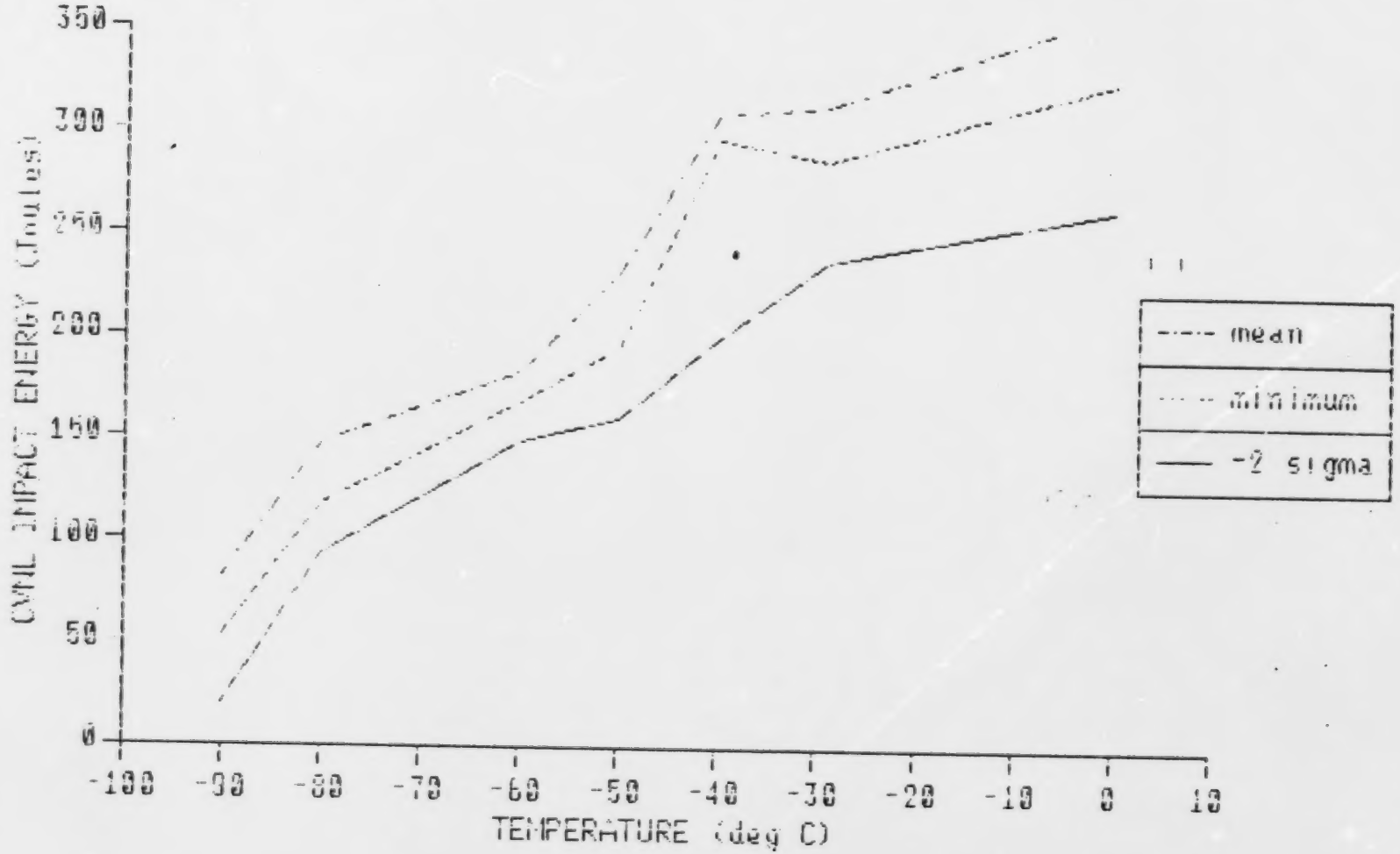

Figure 5: CVNL Impact Energy vs Temperature for 75 mm Plate

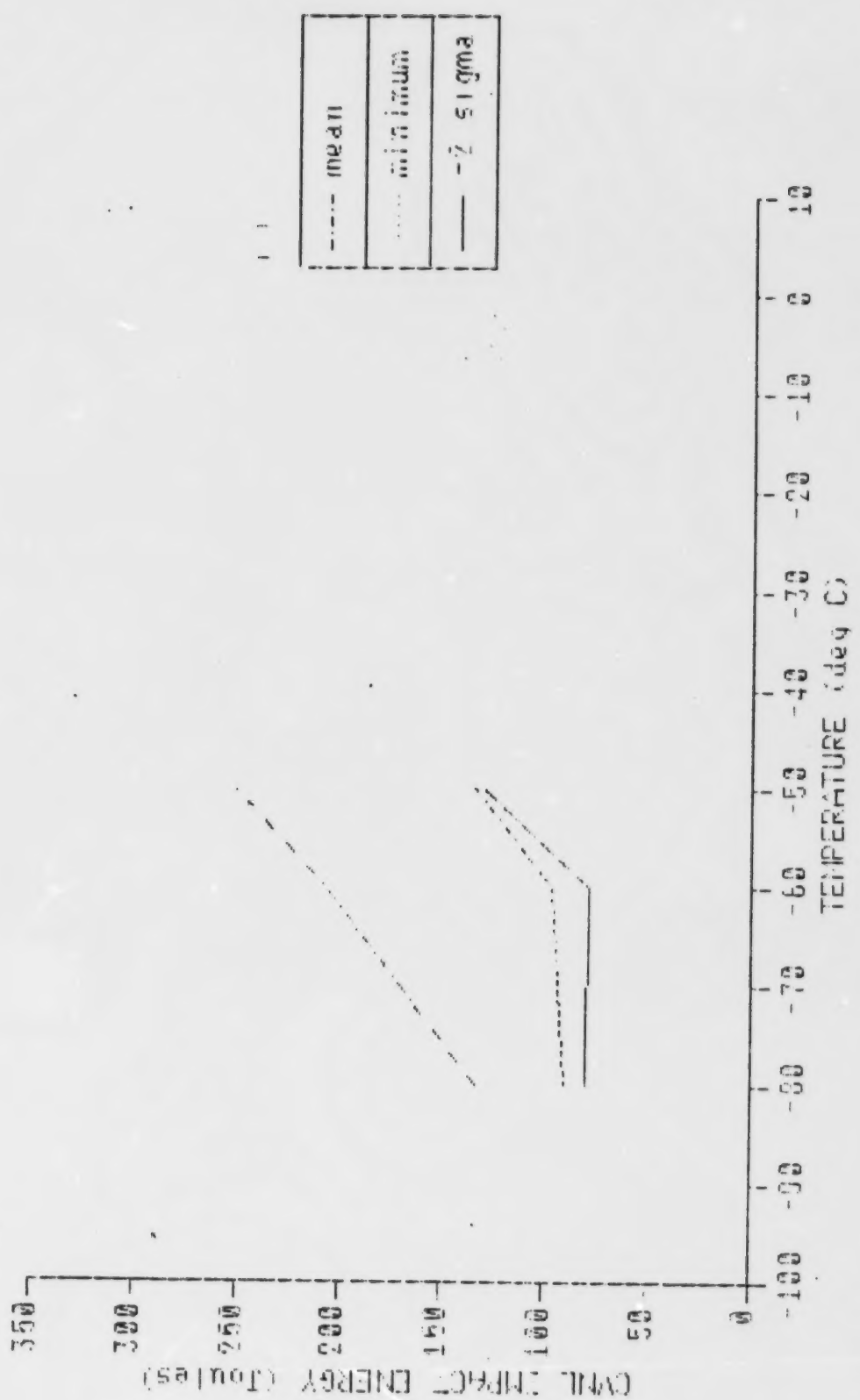

Figure 6: CVNT Impact Energy vs Temperature for 25 mm Plate

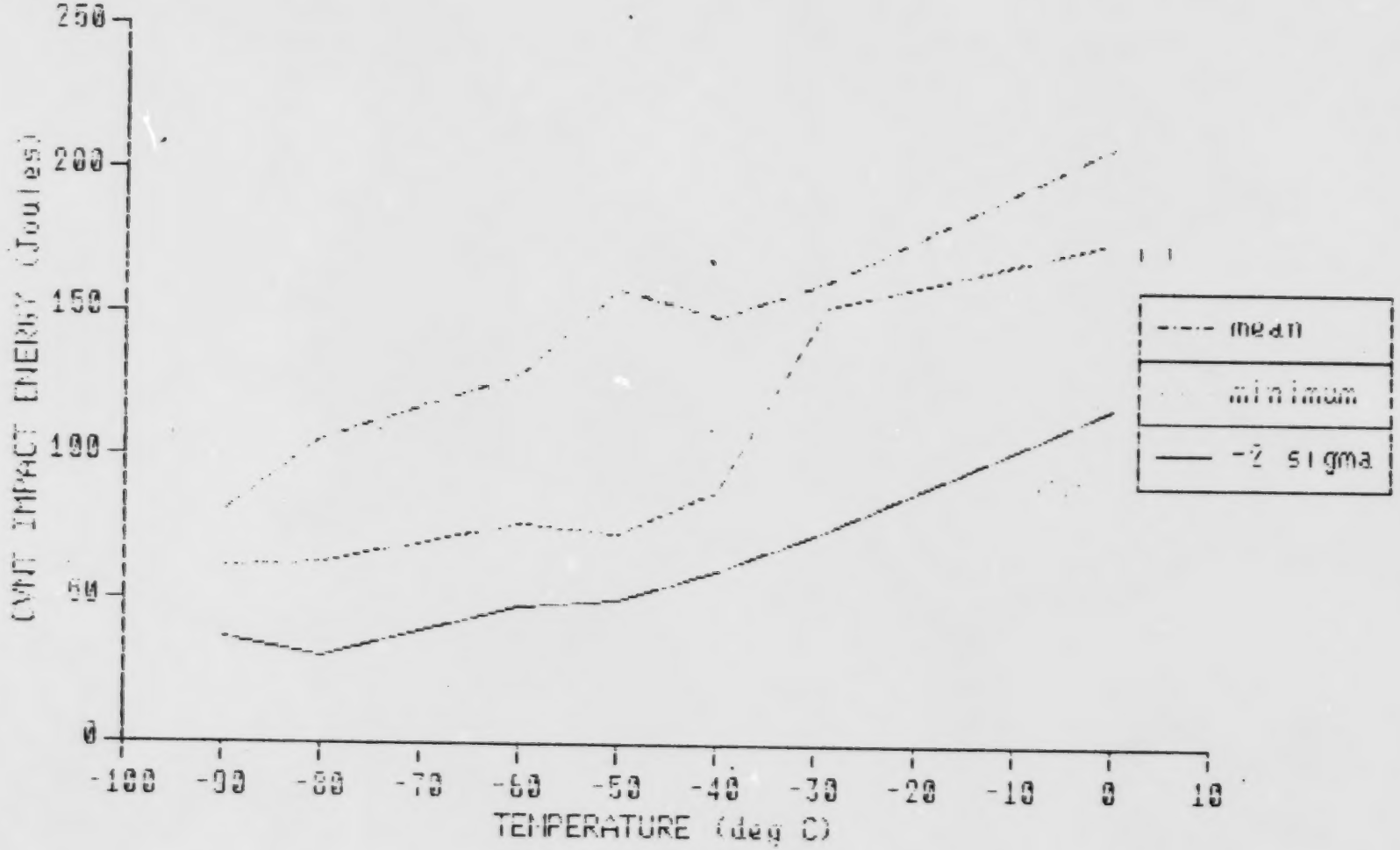

Figure 7: CVNT Impact Energy vs Temperature for 50 mm Plate

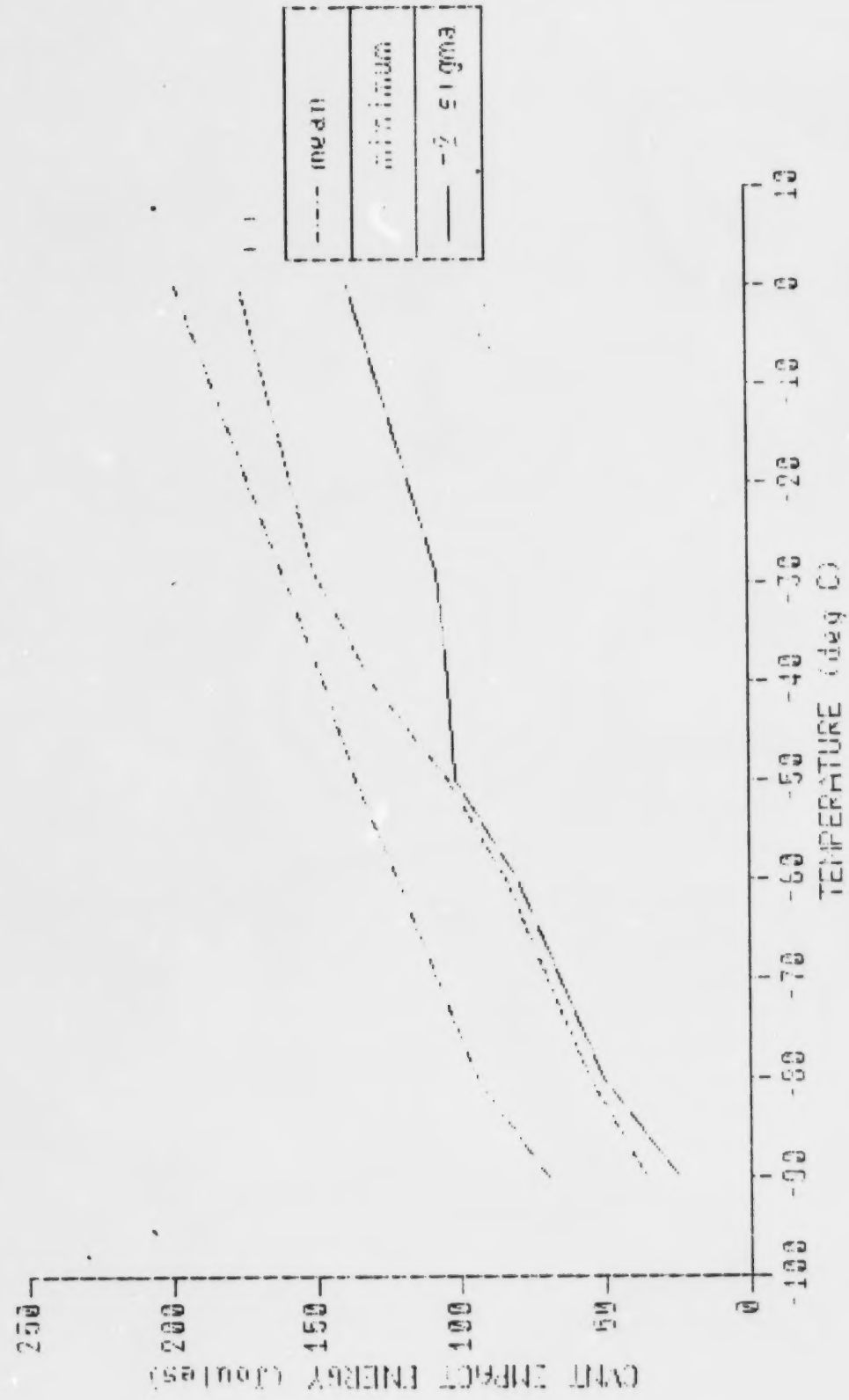

Figure 8: CVNT Impact Energy vs Temperature for 63 mm Plate

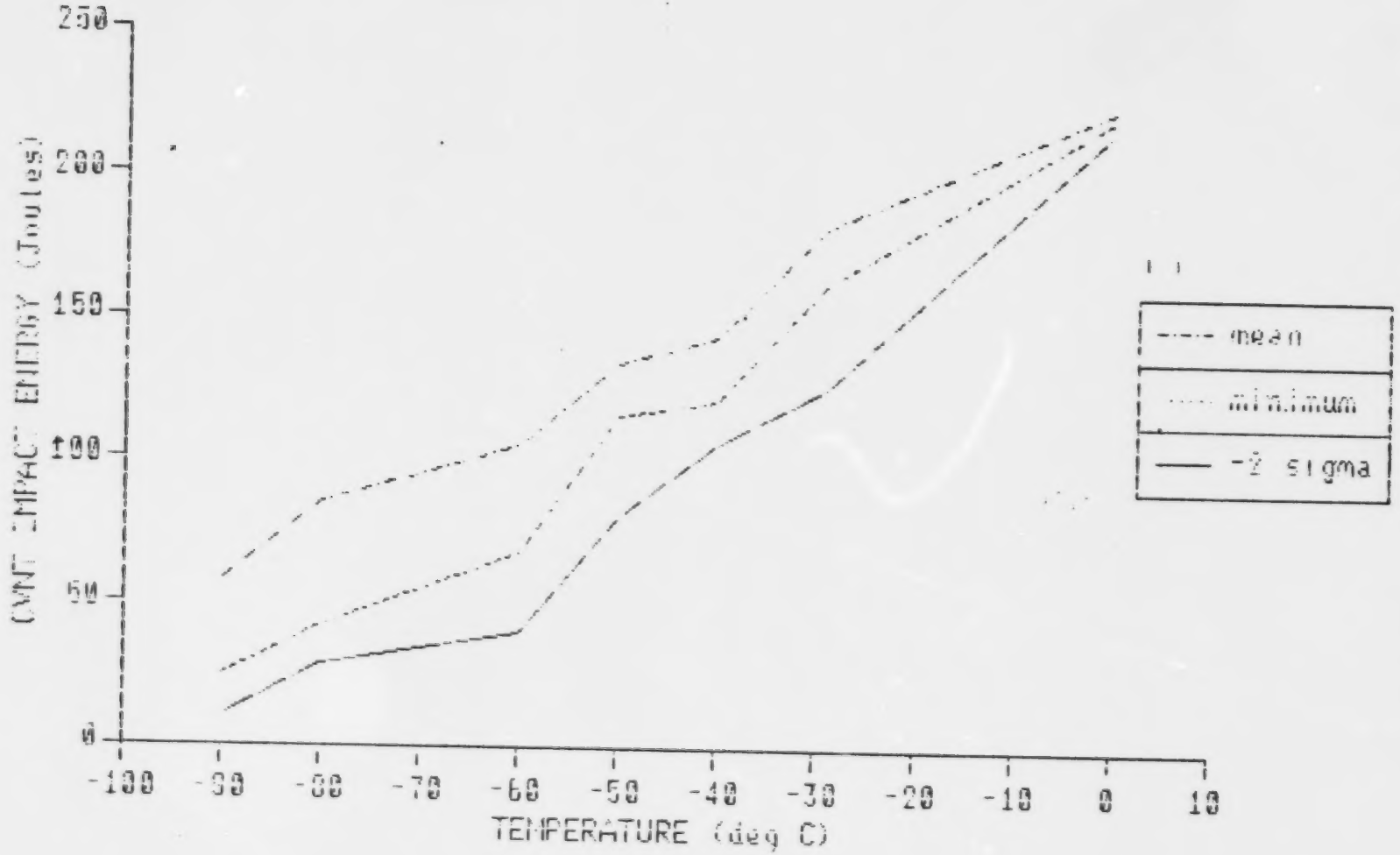

Figure 9: CVNT Impact Energy vs Temperature for 75 mm Plate

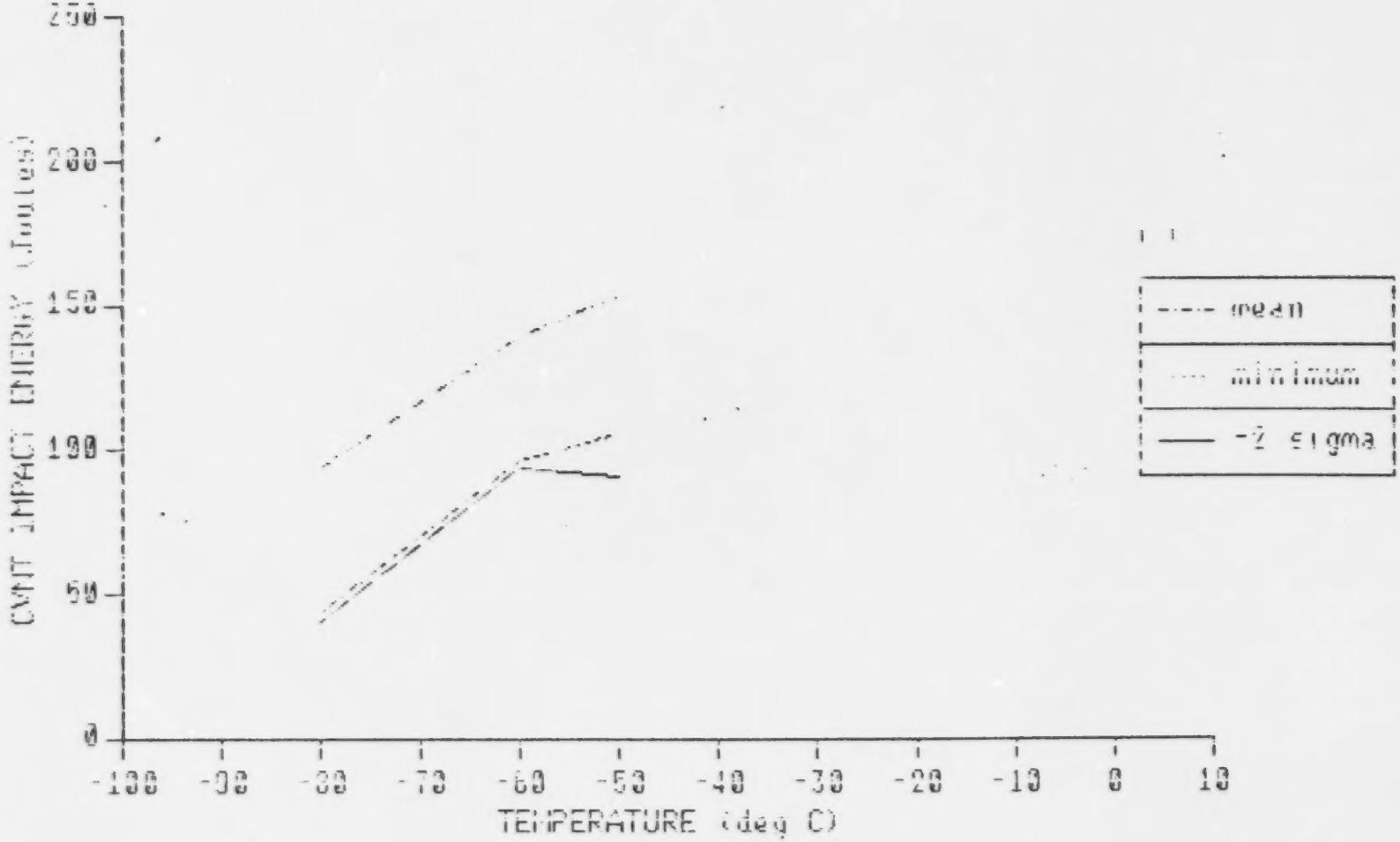

Figure 10: Frequency Histogram of CVNL Impact Energy at -60°C

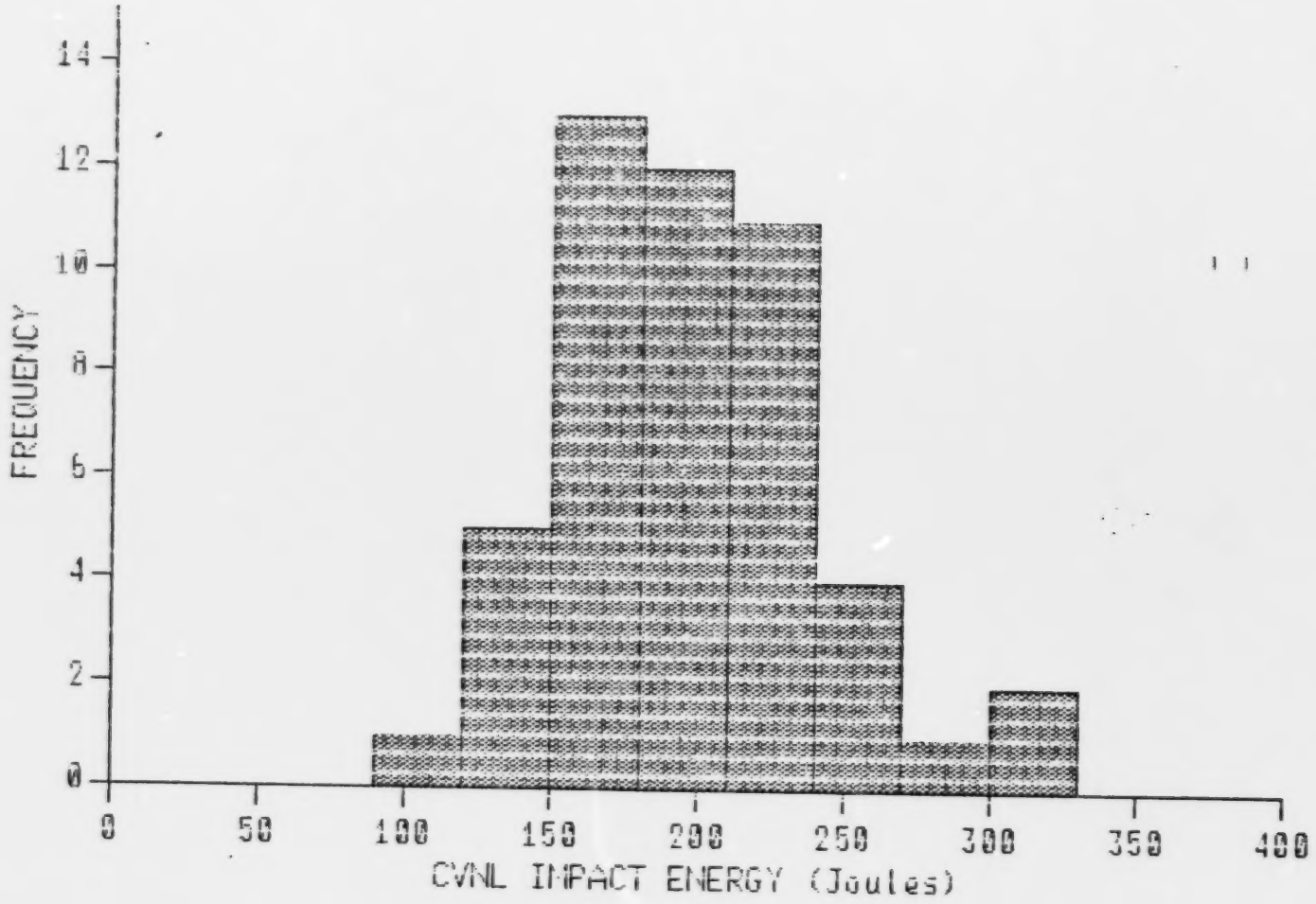

Figure 11: Percent Shear vs Temperature for CVNL and CVNT Impact Tests

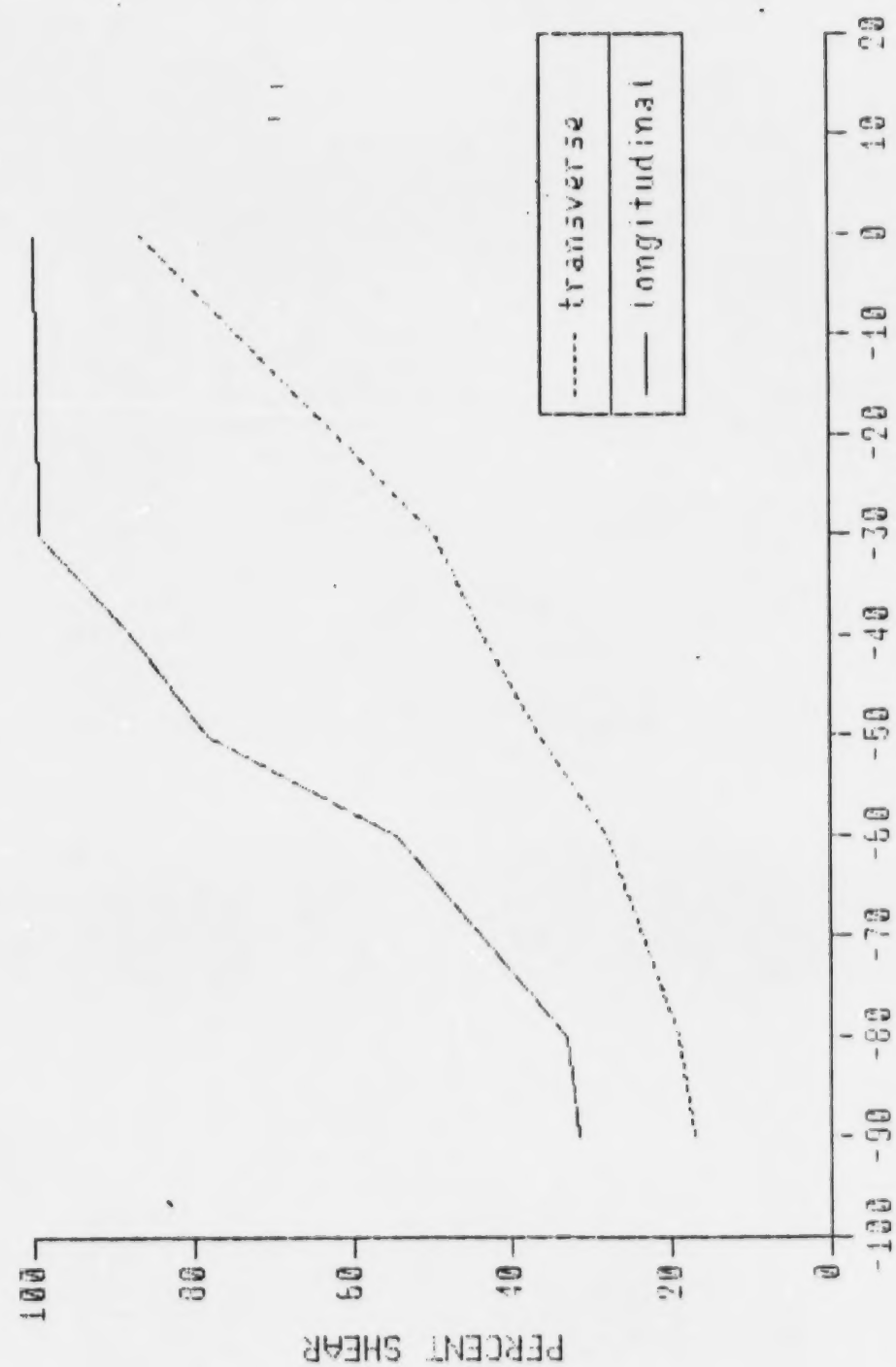

FIGURE 12a PHOTO MICROGRAPHS OF 25 mm and 50 mm PLATE THICKNESS

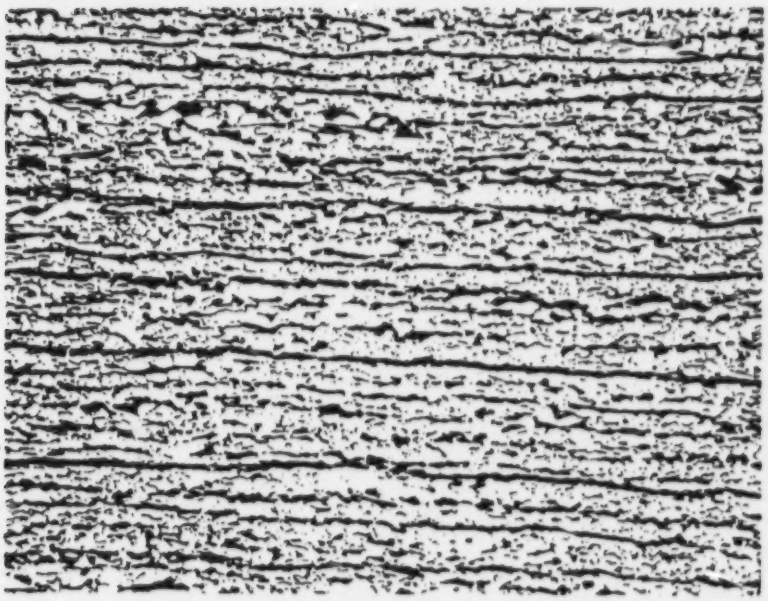

25 mm
Plate #32347

X100

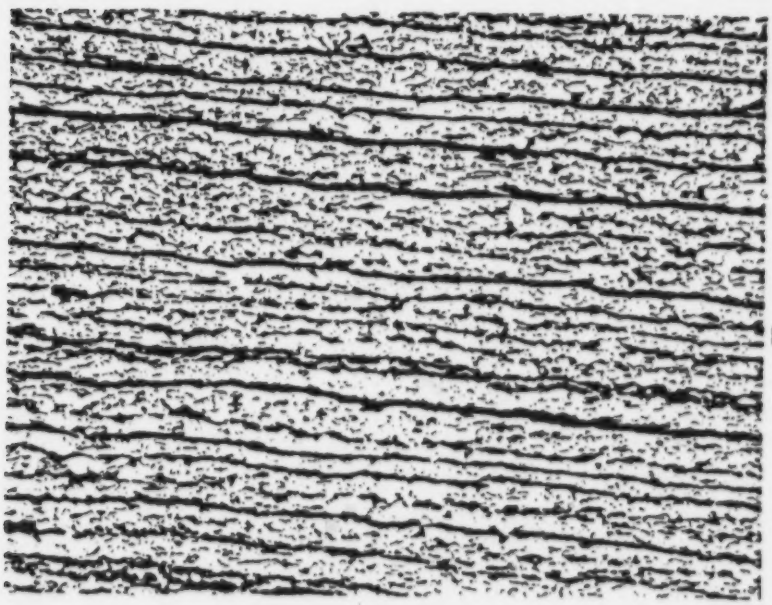

50 mm
Plate #32340

X100

FIGURE 12b PHOTO MICROGRAPHS OF 63 mm and 75 mm PLATE THICKNESS

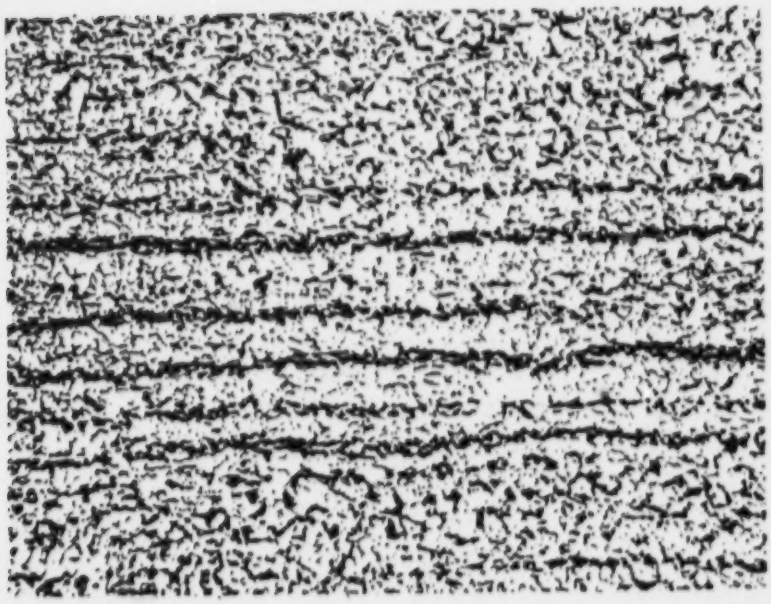

63 mm
Plate #32322

X100

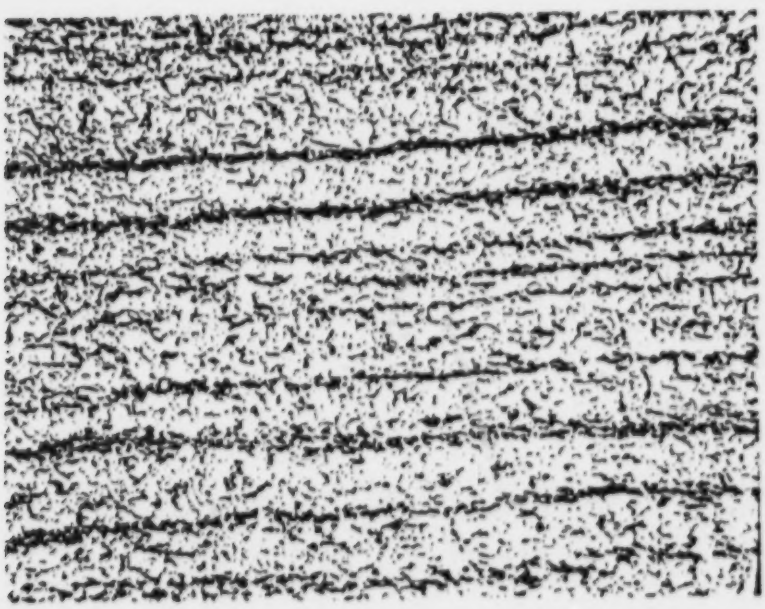

75 mm
Plate #32875

X100

FIGURE 13 CLEANNESS RATING PHOTO MICROGRAPHS

75 mm
Plate #32875

X100

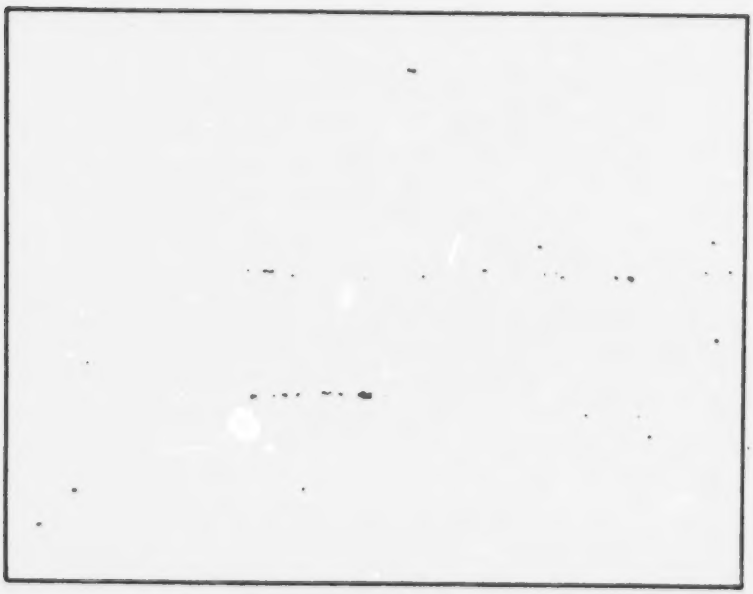

63 mm
Plate #32322

X100

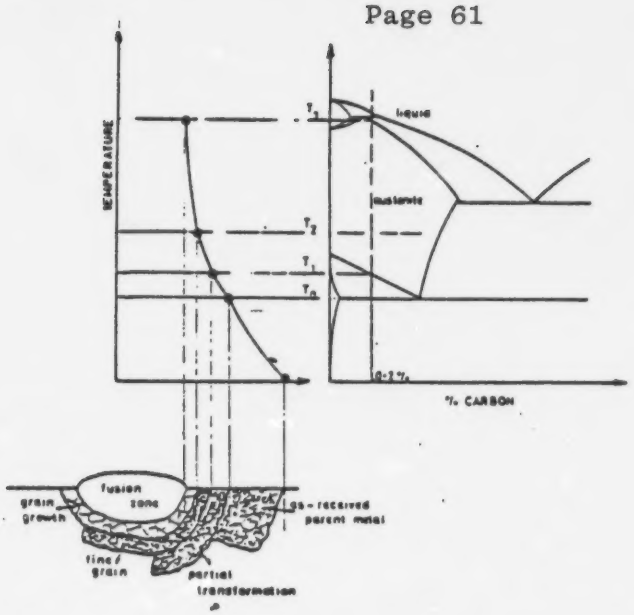

Figure 14: Schematic microstructure of 0.2% C steel weld

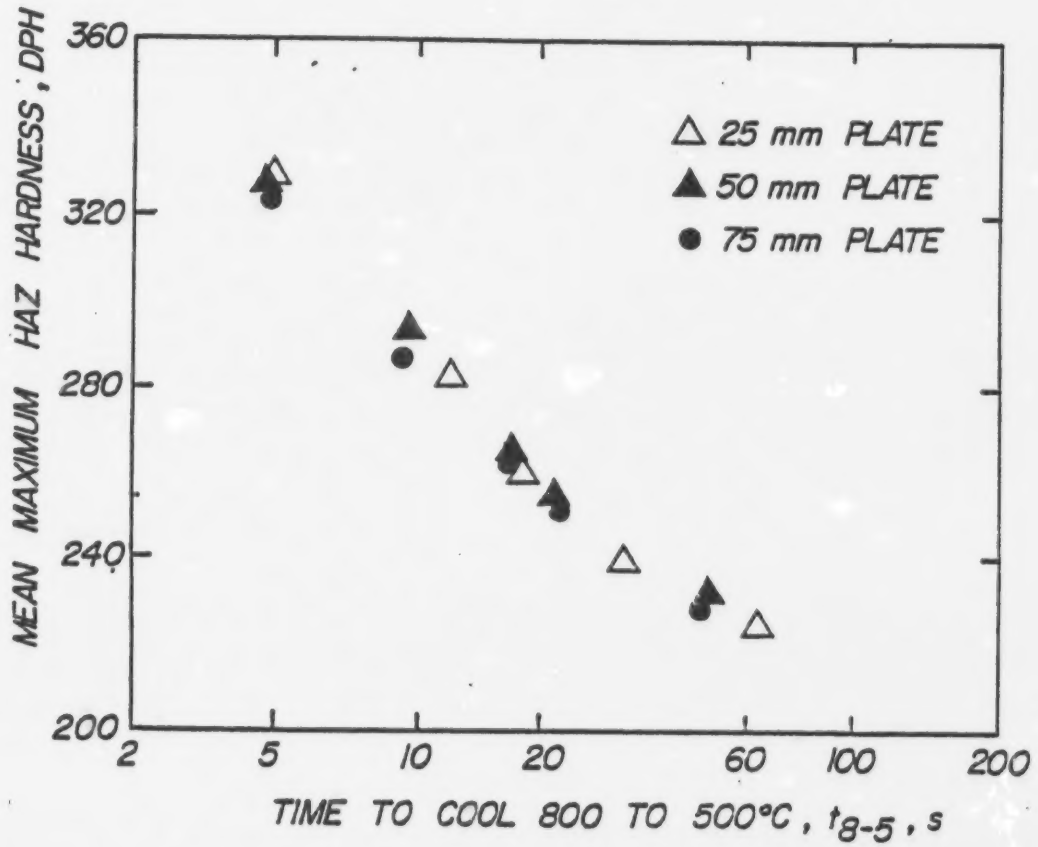

Figure 15: Hardening curve results showing HAZ hardness versus t_{8-5} for 25, 50 and 75 mm thick plates.

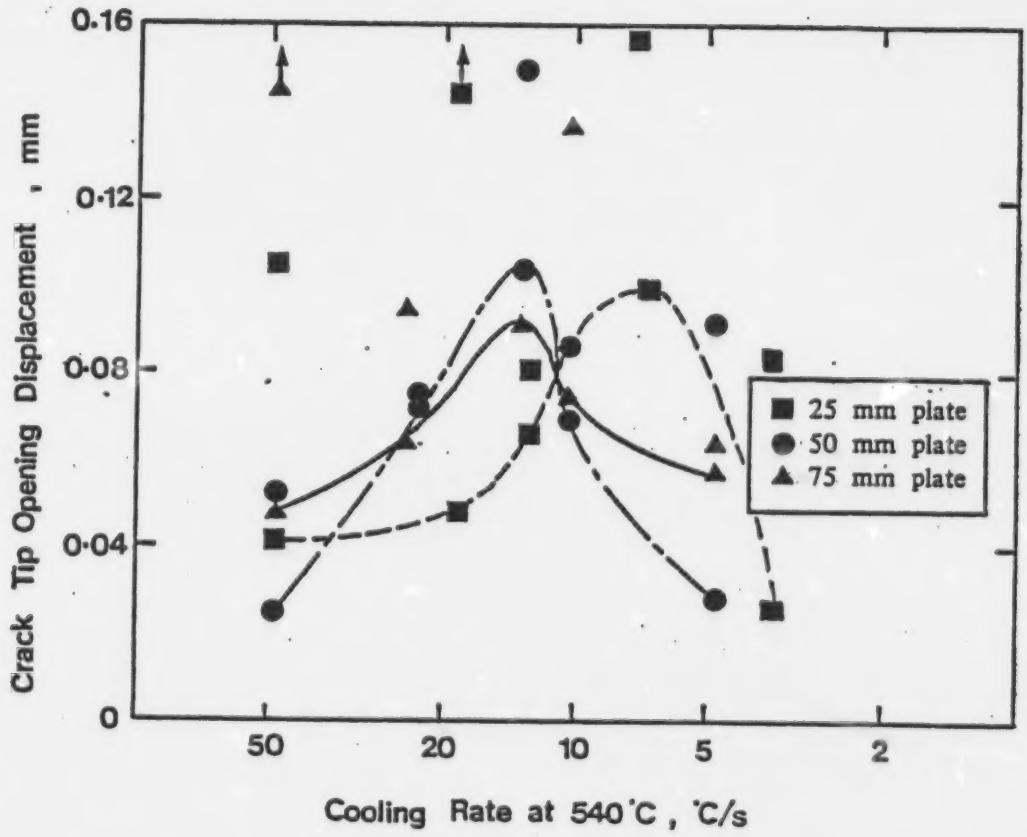

Figure 16: CTOD versus heat input for bead-on-plate welds. All testing conducted at -60°C.

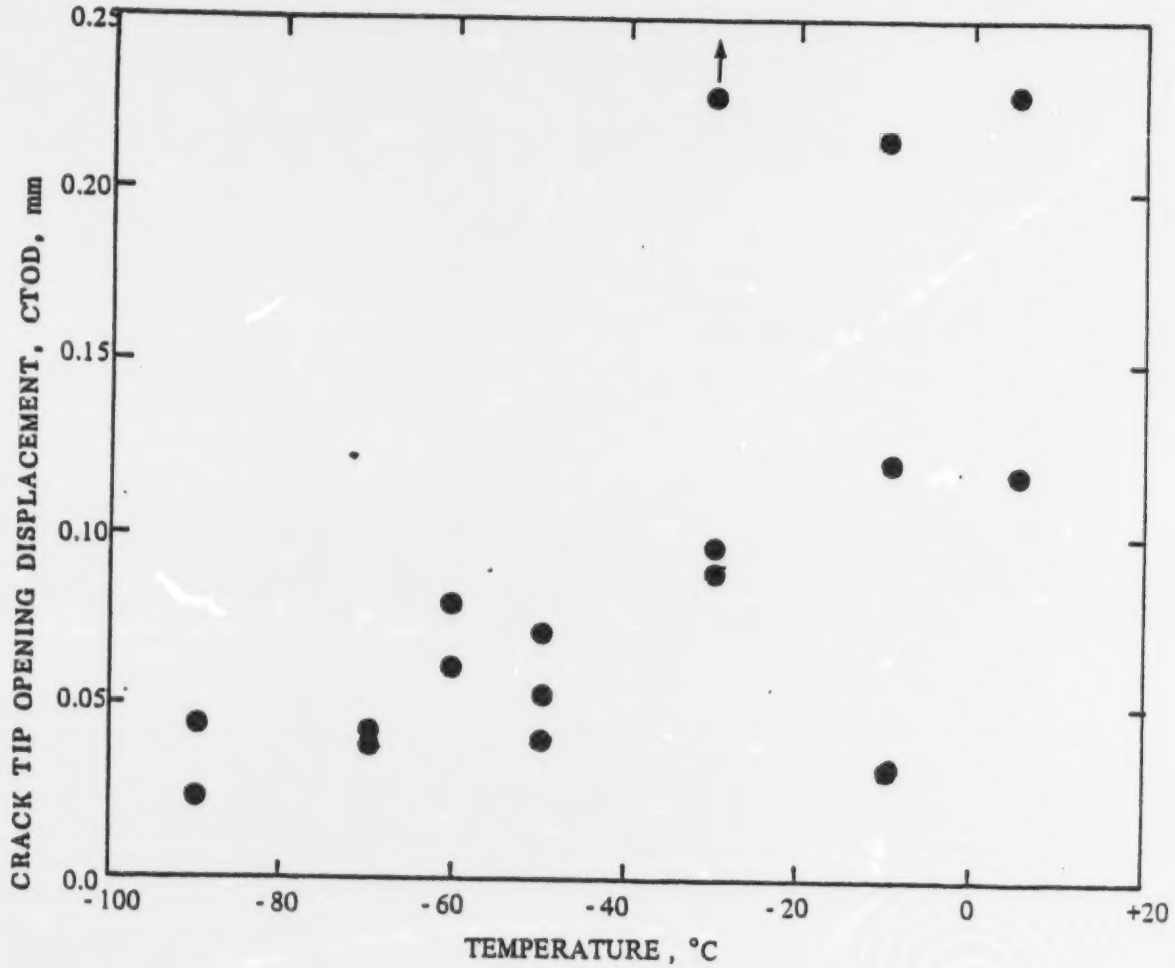

Figure 17: CTOD transition curve for weld 3A, bead-on-plate weld on 25 mm thick plate.

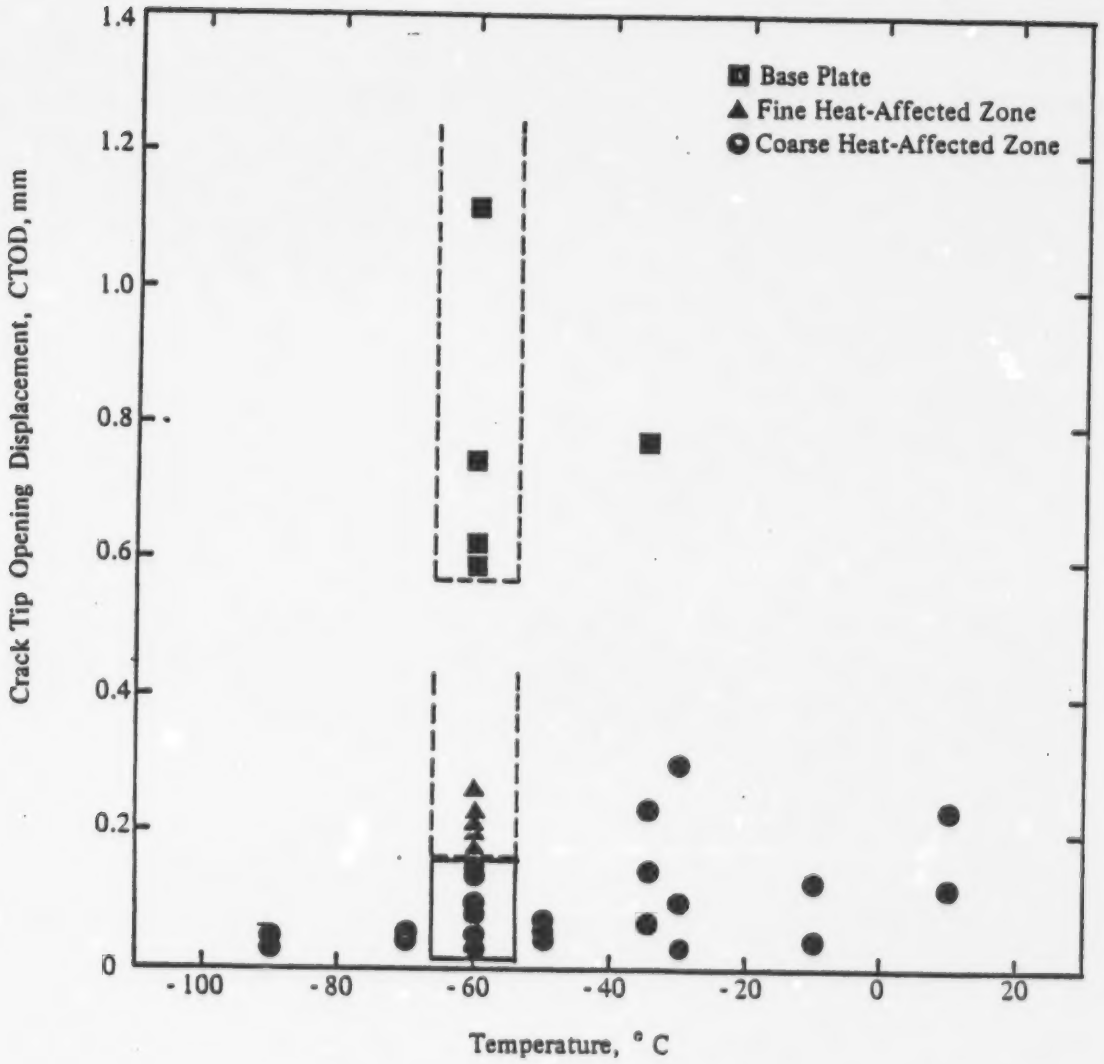

Figure 18: CTOD versus temperature for welds made using a heat input of 3 kJ/mm. Results include tests for bead-on-plate and K-prep welds.

	C	Mn	Si	Cr	Mo	V	Ni	Cu	Nb
A710	0·06	0·67	0·31	0·91	0·15	—	1·04	1·16	0·04
50E	0·16	1·42	0·30	0·02	—	—		0·03	0·04

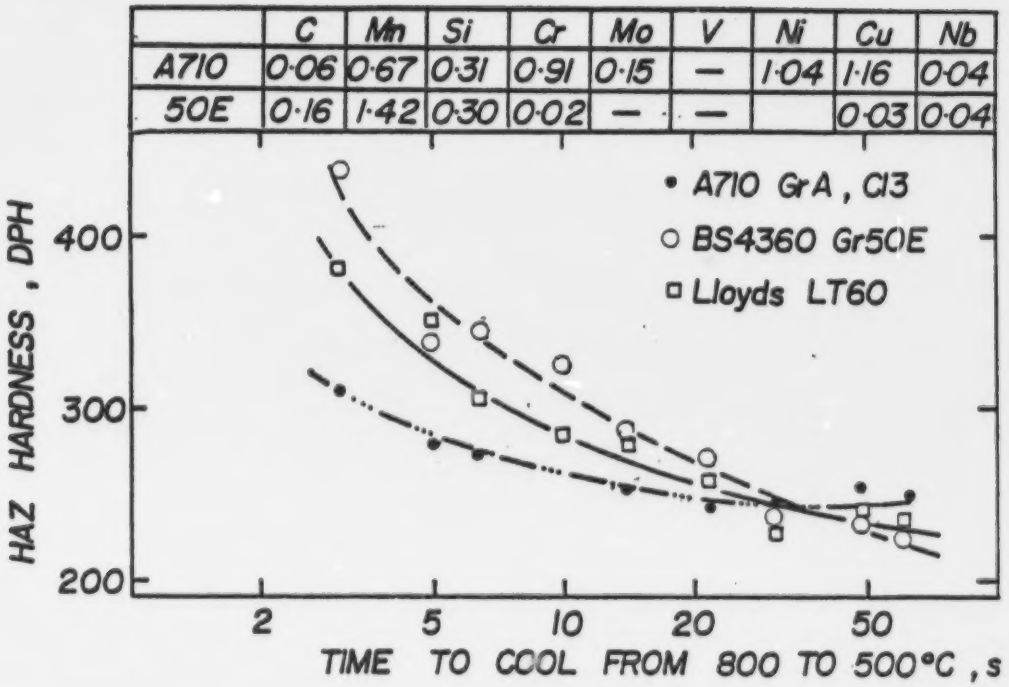

Figure 19: Hardening curve results for A710 Gr A C13, BS4360 Gr 50E, and Lloyd's LT60 steels.

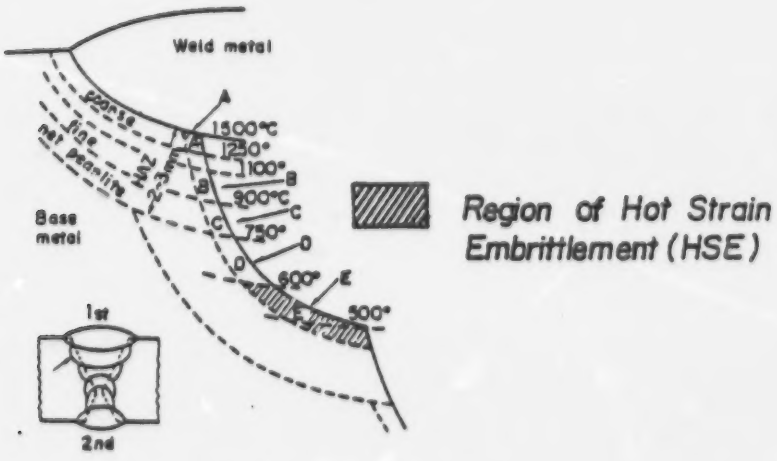

Figure 20: HSE area in multipass weld.

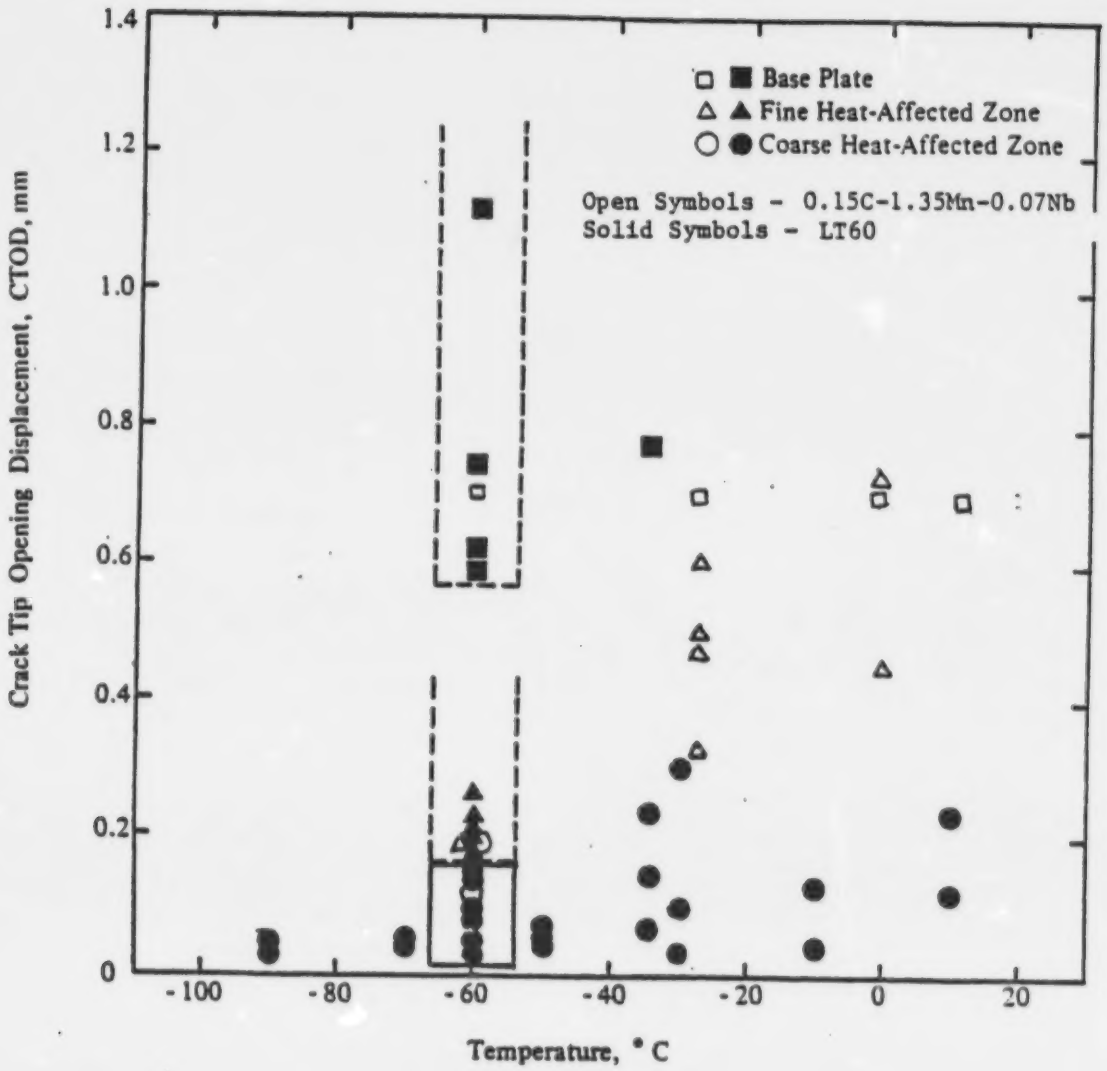

Figure 21: Comparison of CTOD results for LT60 steel and 0.15C - 1.35 Mn - 0.07 Nb steel, welded at 3 kJ/mm.

APPENDIX 1

WELDING INSTITUTE OF CANADA
INSTITUT DE SOUDAGE DU CANADA

391 BURNHAMTHORPE ROAD EAST, OAKVILLE, ONTARIO L6J 6C9. Tel. (416) 845-9881

STEELS AND THEIR FABRICATION FOR OFFSHORE AND ARCTIC VESSELS

Report RC142/2/84

Confidential to: The Algoma Steel Corporation Ltd.
Sault Ste. Marie, Ontario

Approved by

Dr. Alan G. Glover
Director of Technology

Prepared by: R. B. Lazor
T. W. Lau
A. G. Glover
J. C. Price

December 1983

STEELS AND THEIR FABRICATION FOR OFFSHORE AND ARCTIC VESSELS

by

R. B. Lazor, T. W. Lau, A. G. Glover and J. C. Price

Welding Institute of Canada

- EXECUTIVE SUMMARY

The principal objective of this work was to develop welding procedures for a candidate LT60 steel which would retain adequate heat-affected zone properties for the severe operating conditions foreseen in the Canadian Arctic and Sub-Arctic regions. The study consisted of a literature review of the weld properties of C-Mn microalloyed steels and a detailed examination of the microstructures and properties of the LT60 steel.

The literature review discussed the importance of fine grain size, precipitates to restrict grain growth in the coarse-grained HAZ, the significance of interstitials, and the overall microstructure in their effect on the HAZ properties.

The characteristic response of the steel to welding heat input was evaluated using hardening curves. Microstructural examinations and CTOD testing showed that optimum coarse-grained HAZ properties were obtained for heat inputs between 3 and 4 kJ/mm. However, the CTOD at the optimum heat inputs for these single pass welds was below 0.10 mm. The CTOD of full thickness welds completed using the same nominal heat input produced similar toughness values.

The weldability of 25 and 75 mm thick plates to Lloyds requirements was examined. The 25 mm plate was shown to be acceptable in terms of tensile and impact results. At the present time, there are no guidelines for acceptance of plates greater than 55 mm thick. However, the criteria for 55 mm plates was used to judge the acceptance of the 75 mm butt welds. The 75 mm butt welds produced acceptable tensile results, but impact values in the HAZ were subject to large differences and, in some regions, were below the Lloyds' requirements for the 55 mm plates. The region of maximum embrittlement was situated just outside of the visible HAZ. It is argued that strain-induced embrittlement is the most probable cause for the observed behaviour.

TABLE OF CONTENTS

		Page
	Executive Summary	(ii)
	List of Tables	(iv)
	List of Figures	(v)
1.0	Introduction	1
	1.1 Steel Requirements for Arctic Use	1
	1.1.1 Fracture Criteria for Ships and Structures	2
	1.2 Fracture Behaviour and Testing	4
2.0	Factors Controlling the Toughness of the Heat-Affected Zone of High-Strength Low-Alloy Steel Weldments	6
	2.1 Steel Development	7
	2.2 Heat-Affected Zone Characteristics	9
	2.3 Weld Metal Microstructure and Properties	10
	2.4 Microstructures	11
	2.5 Precipitates	13
	2.6 Inclusions	15
	2.7 Strain Aging	16
	2.8 Effects of Base Plate Composition and Heat Input	17
	2.8.1 Heat-Affected Zone Properties	18
	2.8.2 Grain Size Control	23
	2.9 Summary	24
3.0	Experimental Procedures and Results	25
	3.1 Materials	25
	3.2 Hardening Curves	26
	3.2.1 Metallographic Examination of Hardening Curve Welds	26
	3.2.2 Fracture Toughness Testing of Hardening Curve Welds	28
	3.3 Fracture Toughness of K-Preparation Welds	34
	3.4 Procedure Testing of Butt Weld Assemblies	36
4.0	Discussion	37
	4.1 Hardening Curve Results	37
	4.2 CTOD Fracture Toughness Testing	40
	4.2.1 Application of Results	42
	4.3 Procedure Testing of Typical Joints	42
5.0	Summary and Conclusions	47
6.0	Recommendations	48
7.0	References	50
	Appendix A Hardness Measurements of Hardening Curve Welds	88
	Appendix B CTOD Analysis and Results	91
	Appendix C Welding Procedure Data Sheets	94
	Appendix D Ultrasonic and Radiographic Test Results	95
	Appendix E Acceptance Criteria for Butt Welds	96

LIST OF TABLES

		Page
TABLE 1	External Hull Structure General Philosophy for Determination of Steel Grades	57
TABLE 2	Steel Plates for Fabricated Constructions	58
TABLE 3	Steel Types According to Applications	59
TABLE 4	Classification of Microstructures in Low Carbon Alloy Steel Weld Metal	60
TABLE 5	Chemical Composition and Mechanical Properties of Heat L1028	61
TABLE 6	Welding Parameters for Hardening Curves	62
TABLE 7	Summary of Hardening Curve Results	62
TABLE 8	Results of CTOD Testing of Coarse-Grained Hardening Curve Welds	63
TABLE 9	CTOD Results from K-Preparation Welds	64
TABLE 10(a)	Properties Obtained from Butt Weld Procedure on 25 mm Plate	65
TABLE 10(b)	Properties Obtained from Butt Weld Procedure on 75 mm Plate	66

LIST OF FIGURES

		Page
1.	Results of CTOD tests on parent material, HAZ, and weld metal of C-Mn steel weldment:	67
2.	Effects of testpiece geometry on CTODs measured in the transition regime.	68
3.	Typical notch orientations used for weldment testing.	69
4.	Schematic microstructure of 0.2% carbon steel weld.	70
5.	Schematic illustration of effects of microstructural parameters on HAZ toughness.	70
6.	Effect of M-A content on fracture appearance transition temperature.	71
7.	Effect of welding thermal cycle on HAZ Charpy V transition temperature of 3 HSLA steels.	71
8.	Hardening curve results showing HAZ hardness versus t_{8-5} for 25, 50 and 75 mm thick plates.	72
9.	Microstructures from hardening curve weld HAZ's for 25 mm plate.	73
10.	Microstructures from hardening curve weld HAZ's for 50 mm plate.	74
11.	Microstructures from hardening curve weld HAZ's for 75 mm plate.	75
12.	CTOD specimen showing notch and fatigue precrack.	76
13.	CTOD fracture surface showing fatigue precrack, coarse-grained zone, and columnar weld metal.	76
14.	CTOD versus heat input for hardening curve welds.	77
15.	CTOD transition curve for weld 3A, bead-on-plate weld on 25 mm thick plate.	78
16.	A-Welding in the flat position, high degree of HAZ refinement: B-welding horizontal, vertical, low degree of HAZ refinement.	79
17.	CTOD versus temperature for welds made using a heat input of 3 kJ/mm. Results include tests for bead-on-plate and K-prep welds.	80

List of Figures (Cont'd)

		Page
18.	Completed butt weld sections from 25 and 75 mm plates.	81
19.	Typical hardening curve for a C-Mn steel.	82
20.	Hardening curve results for A710 Gr A Class 3, BS4360 Gr 50E, and Lloyds LT60 steels.	82
21.	Relation between cooling time and the fraction of M-A constituent.	83
22.	Hot Strain Embrittlement (HSE) area in multipass weld.	83
23.	HAZ CTOD data for 0.15C-1.35 Mn-0.07 Nb steel, 25 x 25 mm section specimens.	84
24.	Comparison of CTOD results for LT60 steel and 0.15C - 1.35 Mn - 0.07 Nb steel.	85
25.	Comparison of critical CTOD values between synthetic HAZ and weld fusion line.	86
26.	Microstructures from procedure welds.	87

STEELS AND THEIR FABRICATION FOR OFFSHORE AND ARCTIC VESSELS

Confidential to: The Algoma Steel Corporation, Ltd.
Sault Ste. Marie, Ontario.

1.0 Introduction

The discovery of offshore oil and gas in Canadian waters has provided the opportunity for Canadian companies to supply materials and equipment for development of these resources. The high quality steel products foreseen as being necessary for the severe operating conditions of Canadian Arctic and Sub-Arctic regions are presently being developed in Canada. The requirements needed for these steels are being addressed in the current CANMET sponsored 50-50 program. As a result of this effort, a candidate steel has been developed by The Algoma Steel Corporation, Ltd., to conform to Lloyds grade LT60.

The primary objective of the work described in this report is the development of welding procedures for this steel which will retain adequate heat-affected zone properties using procedures which are practical for Canadian shipyards. The specific application considered is a large icebreaking, liquified natural gas tanker. The report includes a literature review and descriptions of basic metallurgical observations and welding trials to ascertain the suitability of LT60 steel for Arctic construction.

1.1 Steel Requirements for Arctic Use

The steel requirements for welded ship and offshore construction adopted by regulatory bodies (ie Lloyd's, ABS, DnV) are based on theoretical design criteria which include fatigue and fracture mechanics and also give consideration to production techniques. The philosophy behind the selection of steel grades for the various parts of a ship is outlined in Table 1. This table illustrates that areas of a structure which are subject to impact and abrasion, or experience partial or periodic immersion, tend to require higher quality steels. The properties of approved steels listed in Table 2 show the trend towards higher impact energy requirements at lower test temperatures as the applications become more demanding.

Steels of the LT60 grade are specified for structural parts which are subject to periodic immersion with the actual grades being determined on the basis of design air temperatures. The design air temperature for Arctic applications is expected to be at least -40°C, and some arguments have been presented for the use of a design temperature as low as -60°C. Nonetheless, the properties of LT60 represent a satisfactory choice for the most stringent requirements currently envisioned.

The structural materials for fixed structures are practically all specified as C-Mn steels and C-Mn microalloyed steels. These steels are supplied in normalized, controlled rolled and thermomechanically treated, or quenched and tempered conditions. The recommended steel types according to the importance of the application as specified by DnV is outlined in Table 3. This table shows the main applications of the steel types as well as the interpretations applied by other societies. The following quotations from Eide and others (3) explain the role of government in the end use of the structures and the steels used:

"The government regulations only give guidance to steel application, although special restrictions are being imposed on structural steel parts contributing significantly to the integrity of the whole structure".

"It is emphasized that the intention is to have the design deciding the classification and use of various steel types".

As with the requirements for welded ships, the higher grade steels are specified for the critical members. At the present time, the LT60 steel represents the latest technology in C-Mn steels for these applications.

1.1.1 Fracture Criteria for Ships and Structures

The design against brittle fracture in fixed structures adopted by governmental bodies and classification societies has been to specify minimum Charpy impact requirements; the aim being to prevent initiation of unstable fracture (3). This behaviour is ensured by either specifying high upper

shelf energy for arrest performance or by requiring a low transition temperature. This design procedure requires correlations between toughness requirements and practical experience. Extrapolation of Charpy requirements to the thicknesses found in critical parts of deep water platforms (>300 mm thick) has been considered insufficient and doubtful due to lack of relevant service data. To overcome this problem, fracture mechanics is now being used to assess the risk of brittle fracture.

A recent article by Pellini (2) outlines several factors which determine the selection of structural fracture criteria and considers the degree of structural reliability required for Arctic use. Consideration is given to environmental conditions, service temperature, and practical difficulties associated with repair of fractured members. Pellini notes that a separate analysis of structural reliability may be required for various parts of a structure, and incorporates concepts of redundancy. Fracture critical regions of primary or second-order importance, fracture of which can cause total failure or seriously affect the residual safety, should be designed on the basis of using fracture-arrest safe steels. Regions which are not fracture critical may be designed on the basis of fracture initiation prevention.

The concept of structural reliability outlined by Pellini is not the same as that adopted by The Welding Institute. Pargeter and Pisarski (4) present the rationale for their fracture philosophy with reference to the locally brittle HAZ, assuming that fracture initiation is favoured for defects in this region. A crack, once initiated, will either stop or continue to propagate, depending on the arrest properties of the steel and the energy available for fracture. Since the arrest toughness is significantly lower than the initiation toughness for most structural steels, arrest is unlikely unless the driving force decreases rapidly as the crack extends. These factors, combined with difficulties in designing to arrest criteria and difficulties in achieving steels with the necessary toughness, have led The Welding Institute to adopt the methodology of designing to prevent fracture initiation. This approach has been summarized by Harrison (5): "If the parent steel has not been selected to arrest running cracks, or if for other reasons an arrest approach is not viable, it becomes essential to know about the initiation resistance of all regions of welded joints and to assess the structure on the basis of the least tough of these regions".

When fracture mechanics testing is deemed necessary, the testing methods and strain rates are chosen to conform to those of the actual structure. The crack tip opening displacement (CTOD) technique is normally specified since the subsequent analysis is relatively straightforward and can account for residual stresses. This in turn requires a realistic test assembly to be prepared using thicknesses, consumables, and welding procedures representative of the actual structure. Tests are normally conducted on both the weld metal and the heat-affected zone at the lowest anticipated service temperature.

1.2 Fracture Behaviour and Testing

The initiation approach to fracture control adopted by the Welding Institute aims at ensuring that the toughness of the most brittle microstructure present in the fabrication is high enough to tolerate the maximum stresses to be imposed, in the presence of any defects that might remain after inspection. This philosophy has been extensively used for ferritic steels, which show a transition behaviour with temperature. This transition temperature is heavily influenced by thickness and strain rate, and hence the initiation approach must take these effects into account. In order to do this the fracture toughness of all of the microstructures within the weld region must be measured. The variation of toughness within a weldment is shown in Figure 1.

In order to assess the behaviour of the weldment, its material fracture toughness is required so that defect tolerance can be determined. Traditionally, this was carried out using linear elastic fracture mechanics (LEFM). However this is seldom applicable to welded structures except in very great section thicknesses. Because of the presence of tensile residual stresses and stress concentrations it is necessary for welded materials to be able to tolerate stresses up to or greater than the yield stress. This implies that full section thickness test pieces must not fail in a linear elastic manner at the minimum service temperature. Furthermore, when yield strains occur, the use of LEFM analyses for the structure itself is questionable. For these reasons the CTOD analysis was developed.

The CTOD test provides a measure of elastic-plastic fracture toughness, i.e.

the resistance to crack extension, which is unique to the specimen design and material sampled at the tip of the notch in a test, at the temperature and strain rate specified.

The CTOD test has been under development for many years and has culminated in a British Standard BS5762:1979 which defines a standard technique. The standard defines two testpiece geometries: a preferred t x 2t specimen and a subsidiary t x t specimen, where t represents the actual thickness of the specimen. The choice of testpiece or notch orientation depends primarily on the defect position. A subsidiary specimen is often specified when the significance of a particular defect is being evaluated. The preferred geometry is normally used, which gives a lower bound result as shown in Figure 2(a), unless the defect orientation is known, in which case the subsidiary testpiece can be used. The preferred testpiece has the highest constraint of the two, which partly accounts for the lower CTOD. The reduction of toughness with increased thickness for elastic-plastic toughness measurements also contributes to the observed difference with testpiece geometry. This effect of constraint is particularly important at low temperatures where fracture is controlled by cleavage initiation (see Figure 2(b)). However, if fracture initiates by ductile tearing, the CTOD is almost geometry independent. This difference is due to cleavage being stress controlled whereas microvoid coalescence (ductile tearing) is strain controlled.

In the upper shelf regime, fracture is controlled by a collapse mechanism and, as shown in Figure 2(c), the toughness is dependent on the total cross-sectional area. The CTOD at collapse tends to be higher for larger specimens because of the greater cross-sectional area, or ligament, of the testpiece. Plastically-induced fracture begins when a critical plastic strain is produced over a critical distance ahead of the crack tip. With the displacement of the crack tip being proportional to the strain in the volume element directly ahead of the crack (98), the larger specimens can accommodate larger applied loads and thus give a higher CTOD. Alternatively, the smaller the ligament, the smaller will be the CTOD at collapse, since it is the ligament that will restrict the amount of crack growth. This factor becomes important when analyzing for collapse behaviour and some limitation is normally placed on the defect size in order to prevent the flow stress from being exceeded in the remaining ligament.

The types of specimens most often used to measure CTOD of weldments are shown in Figure 3. A discussion on which type of specimen to be used for a particular defect is given by Dolby and Archer (97). The type E specimens have been successfully used to measure toughness of the narrow weld regions while type A specimens have been recommended (89) for providing representative values of HAZ fracture toughness. It is these latter two configurations which have been chosen for CTOD testing in this program, as will be discussed later.

One important factor in CTOD testing is the notch tip location, and this arises because the CTOD test is measuring initiation toughness. Measurements of HAZ toughness can be of value only if it can be envisaged that defects can form in these regions. The transformed HAZ, particularly the grain-coarsened region, is a potential site for hydrogen-induced cracks, liquation cracks and reheat cracks. In contrast, sub-critical HAZ embrittlement has been found to be significant only if welding is done in the presence of a strain concentrator. Hence, all regions of the weldment should be assessed to determine the lowest toughness region. It therefore becomes important to determine the exact notch tip location in the HAZ after testing. These factors have been reviewed by Pargeter and Pisarski (4). These authors particularly addressed the problem of testing the coarse-grained HAZ in thick section weldments. Their recommendation was the use of the inclined K-prep weld which gave more consistent coarse-grained HAZ assessments. However, one problem with this technique that has yet to be evaluated is the effect of welding electrode angle on the net heat input into the straight side and the distribution of coarse/refined HAZ along the length of the fusion boundary.

2.0 Factors Controlling the Toughness of the Heat-Affected Zone of High-Strength Low-Alloy Steel Weldments

A brief review of the development of steel in connection with welding and factors affecting the heat-affected zone (HAZ) toughness of high-strength low-alloy weldments will be presented. Emphasis is put on the effects of microstructures, microalloy elements such as niobium and vanadium, precipitates, and inclusions.

2.1 Steel Development

Traditional steels depend on carbon content for their strength. With the advent of welding, a problem associated with cracking in the HAZ of these high carbon structural steels was observed. Cracking in the HAZ is often due to the hardening of this region by the formation of martensitic microstructures during the rapid thermal cycle in welding. The transformation to martensite produces a highly stressed region which, combined with local hydrogen, further increases the likelihood of cracking.

Since the percentage and hardness of martensite increases with carbon content, high carbon often translates into poor weldability of the steels concerned and poor toughness of the welded structures. The term weldability is used in this summary to mean that there will be no cracking problems in the HAZ. Weldability of steels can be improved by lowering the carbon content and the use of low hydrogen electrodes. The strength of the steels, on the other hand, must be compensated by alloying.

Microalloyed steels, or high-strength low-alloy steels, were developed to meet the demand of good weldability and toughness, particularly for applications in low temperature environments such as linepipe constructions in the Arctic region and offshore applications. A high-strength steel is one having a yield strength of at least 300 N/mm2. In terms of British specifications, these are steels made to BS4360 Grade 50 or 55, with the carbon equivalent (CE) limited to 0.43% maximum. The requirement of good weldability has restricted these steels to be carbon-manganese type with a small addition of niobium and/or vanadium to ensure both grain refinement and precipitation hardening. Both grain refinement and precipitation hardening will contribute strength to the steel but grain refinement will also improve the toughness. Silicon, molybdenum and other alloys may be added for additional strength or better hardenability. Thinner plates are usually given a thermomechanical treatment (controlled rolling) while thicker plates (>50 mm) are usually normalized. All treatments are aimed at producing a fine grain size for better strength and toughness.

The HSLA steels exhibit improved properties compared to C-Mn steels because of the following features:

1) Fine grain size.
2) Dispersion strengthening by microalloy based precipitates.
3) Inclusion size and shape control.

The grain refinement due to the presence of microalloy based precipitates occurs by either a reduction in the hot rolled austenite grain size or by depressing the transformation temperature from austenite to ferrite so that the ferrite nucleation rate is increased. Both of these mechanisms are operable in the temperature range experienced during controlled rolling. The refinement of transformed microstructures is due to two mechanisms which often act concurrently: fine recrystallized austenite grains formed during rolling at intermediate temperatures and austenite deformation-induced recrystallization below the normal recrystallization temperature. Both of these effects enhance the nucleation of ferrite. Careful control of the rolling sequence can therefore produce uniformly recrystallized or uniform, heavily deformed austenite grains, either of which can transform to uniform, fine-grained ferrite structures.

The strength increment due to precipitation strengthening is obtained by choosing a microalloy addition and process variables that result in a large fraction of fine precipitates. The magnitude of strengthening by niobium carbonitride (NbCN) precipitation depends on the temperature at which precipitation occurs. No significant strengthening was observed when NbCN formed and coarsened at 1010°C. However, when precipitation occurred near the Ar_3 temperature the effect was very significant and was associated with very fine and coherent precipitates (83). Vanadium acts similarly to Nb except that the recrystallization retardation effect is weaker and the solution temperature lower. It is often added in addition to Nb to enhance precipitation of Nb in austenite. According to Rothwell and Bibby (95), in steels with roughly the same amount of each element (0.4 wt%), the Nb is most effective in retarding austenite grain growth while vanadium precipitates appear in the ferrite and provide additional age hardening.

The anisotropy of properties observed in carbon steels is reduced in HSLA steels either by lowering the sulphur content or by additions of calcium, zirconium, or rare earths. Low sulphur levels reduce both the size and number of sulphides and allow the Mn to combine with other elements. Sulphide shape control using Ca, Zr, and rare earths, reduces the inclusions' plasticity so that they do not elongate during rolling, and thus remain spherical, giving uniform properties in all testing directions.

Although the HSLA steels exhibit obvious benefits over the C-Mn steels in terms of strength and toughness, the microalloy additions have a strong influence on weldability, as will be discussed throughout this report.

2.2 Heat-Affected Zone Characteristics

The width of the heat-affected zone and the nature of the microstructures depend on the heat input and cooling as shown schematically in Figure 4 (104). Between T_2 and T_3, grain boundary migration and coalescence causes rapid grain growth leading to a grain-coarsened HAZ. In the lower austenite range (T_1 to T_2), a fine-grained structure is produced. The upper limit T_2 is controlled largely by grain refining elements such Al, Nb, V, and N. These form carbides and nitrides which prevent grain boundary migration but their usefulness reduces as the temperature is increased, since they go into solution. High yield strengths can be obtained by a uniform dispersion of precipitates throughout the matrix. Some of the strengthening may be lost if the precipitates are taken into solution in the high temperature HAZ near the fusion line (just below T_3). In addition they may be overaged, in lower temperature regions, in which case the precipitates coarsen, and the strength is reduced. In some cases the original properties can only be restored by reheat treatment. In the remaining portion of the HAZ between T_0 and T_1, pearlite in the original parent material begins to transform to austenite. If subsequent cooling is fast enough, and the material is high in carbon and microalloying elements, martensite may also be formed in this region.

Thus a composite picture can be constructed as in Figure 4 of a microstructure which varies continuously from the unaffected parent material at T_0, through fine-and coarse-grained phases to the fusion line, and finally to the cast structure of the weld metal.

The variations of toughness in the different HAZ regions is identified by the microstructural constituents where austenite grain size, microstructural classification, and precipitation effects are known to be significant (35, 79) (see Figure 5). It has been suggested that both polygonal ferrite and, in particular, upper bainite are detrimental to toughness. The recommended microstructure should contain fine, interlocking laths of acicular ferrite (80). In the coarse-grained HAZ, acicular ferrite is not commonly found because of the thermal cycles. On the other hand, the peak temperatures, and the subsequent cooling, in the fine-grained HAZ are such that structures similar to acicular ferrite are formed. This is aided by restricting grain growth by the presence of (Nb, V) carbonitrides.

2.3 Weld Metal Microstructure and Properties

Many studies have been made on the structure-property relationship in low carbon-manganese and HSLA steels. It is now generally agreed among researchers in this field that the optimum microstructure to be achieved is acicular ferrite. As Dolby (24) had indicated, both upper bainite and polygonal ferrite are clearly detrimental. Farrar et al (22) studied the toughness of weld metal in terms of the transition temperature and found that the transition temperature decreased with increasing amounts of acicular ferrite. The presence of upper bainite was found to be deleterious. They attributed the high toughness of acicular ferrite to the high angle boundaries between grains while the low angle grain boundaries in bainite provide an easy cleavage path. Similar results were observed by Levine and Hill (25) who studied steels containing high niobium (>0.02%) and steels with low niobium and vanadium. Charpy V-notch tests were used to assess toughness and the Charpy fracture surface was correlated with microstructures. Their results showed that steels containing high niobium consisted of lath structures (upper bainite), some acicular ferrite and little or no proeutectoid ferrite. In steels containing vanadium and low niobium, the microstructure consisted of proeutectoid ferrite and acicular ferrite. In both cases, fracture mostly started at the proeutectoid ferrite or the lath structure and was associated with featureless trans-columnar fracture, indicating low toughness. On the other hand, when cracks propagated through the acicular ferrite region, frequent change of direction was observed, indicating good toughness.

Studies concerning the effect of martensite-austenite, M-A, structure (23, 26), have shown that it decreases toughness values. Figure 6 (26) indicates that with increases in M-A content, the Fracture Appearance Transition Temperature (FATT) increases.

2.4 Microstructures

Factors that are important in assessing the toughness of the HAZ will be briefly reviewed in this section. It must be stressed that all these factors are interrelated and their combined effect on the HAZ toughness may not be a simple superposition.

The effects of gross microstructures (i.e. ferrite, bainite, and martensite), precipitates, inclusions, and grain size on toughness are examined in this section. The compositions of the HSLA steels are such that they produce ferrite-pearlite microstructures under normal steel finishing procedures. However, after welding, a variety of microstructures can result in the HAZ of the base plate due to the rapid thermal cycles experienced in the various regions of the HAZ. There has been much confusion in the nomenclature of the various microstructures. Recently, a Japanese committee has proposed a classification of microstructures in low-carbon, low-alloy steel weld metal (20). Their terminology is shown in Table 4. Some of the confusion was due to the difficulty in differentiating upper bainite from ferrite sideplates. However, using electron microscopy at higher magnification, the two structures can be readily distinguished, ferrite sideplates consist of a single ferrite grain, while upper bainite is composed of several laths and has a higher dislocation density. Also, acicular ferrite is now recognized as a distinct microstructural form of ferrite having a transformation temperature above the start temperature of bainite for steels of similar composition (21), and it is not a form of martensite as was once suggested (22). The M-A structure in Table 4, first termed by Coldren et al (23), is composed of pools of martensite in carbon-enriched untransformed austenite. Its presence is associated with the difficulty of pearlite or martensite formation in low carbon steels.

Rothwell et al (28) have observed alignments of M-A particles along the prior austenite grain boundaries in the HAZ. They suggested that the presence of a brittle phase at these high angle boundaries which are generally associated with transformation stresses, may aid the propagation of a crack from one grain to another. Their observation that tougher steels (which contain less M-A particles) contain a considerable number of non-propagating microcracks, while less tough materials have few microcracks, is taken as an indication that microcracks in the steels containing a greater proportion of M-A have a high probability of finding an easy mode of extension across the first one or two high-angle boundaries and therefore becoming hyper-critical. Consequently, M-A constituents would lower the toughness of the HAZ. Kikuta et al (29) have observed that the quantity of cementite is important to toughness in the HAZ. The amount of cementite increases as the cooling rate increases (i.e. decreases in cooling time through the 800°C - 500°C range), and as the amount of cementite increases, the transition temperature decreases. They stated that toughness is a function of several factors, namely the effective grain size, hardness and the amount of cementite.

There are other studies on the effect of microstructures on toughness. Chung et al (30) introduced a HAZ toughness indicator which depends on notch acuity, normalized grain size (a ratio between the maximum grain size and the distance from the fusion line) and the distance from the fusion line over which the ratio $H_V/H_{V(m)}$ remains constant. $H_V/H_{V(m)}$ is the ratio between the hardness at a point in the HAZ to the hardness of the parent metal containing 100% martensite as its microstructure. This suggested that the extent of the HAZ which consisted of martensite as the major component is important in determining the toughness. Marquet et al (31) suggested that the transition zone in the HAZ provided the greatest difference in microstructures between steels with good weldability and those which are less weldable. The transition zone of the most weldable specimen which they obtained consisted of a mixed microstructure made up of small bainitic blocks surrounded by proeutectoid ferrite. This type of structure was not observed in steel specimens classified as less weldable.

These last two studies recognized that the HAZ consists of a gradient of microstructures. Therefore a quantitative approach as was attempted by several workers in connection with weld metal would have additional difficulty (27, 32, 33). Marquet et al (31) have stated that quantitative characterizations of microstructures in welded joints often lack reliability, particularly when restricted to optical metallography. Furthermore, the gross microstructures alone will not determine the toughness of the HAZ. As will be shown presently, precipitates and inclusions also have significant effects.

2.5 Precipitates

The importance of precipitates in assessing the HAZ toughness increases in the presence of elements such as niobium, vanadium, and titanium as these alloy elements readily form carbide or nitride precipitates. These microalloy elements are used for strength and grain refinement in low-alloy structural steels. In normalized or controlled rolled plate the precipitates do not appear to be detrimental. This is partly due to their size and distribution, and partly due to the fact that their beneficial grain refining action outweighs their detrimental aspects. However, after the thermal cycle associated with welding, the grain refinement effect is lost in the coarse-grained region of the HAZ. During the heating cycle, some of the precipitates will dissolve back into the austenitic matrix due to increased solubilities at high temperatures. The extent of dissolution and the temperature at which this occurs depends on the solubilities of these carbide/nitride particles in the steel at a given temperature. During the cooling cycle, some of these may re-precipitate out. Whether or not precipitates reappear on cooling depends on the composition of the steel, the type of precipitates concerned, and the cooling rate. This information has been reviewed by Graville (34). If precipitates reappear in a continuous row-like manner, or as fine dispersions, low toughness and high hardness will result(32).

The high HAZ hardness of niobium and/or vanadium bearing steels was attributed to the above-mentioned precipitation hardening process by some workers (7-9, 14, 35), although in some cases no concrete evidence of the presence of precipitates was observed (7, 8). Hannerz (7) suggested that this was due to fine, continuous precipitates which are below the resolution

limit of the electron microscope. Weatherly (35) stated that this is due to the use of thin foil technique which has certain limitations. Using carbon replica techniques, Weatherly was able to observe fine precipitates of about 50Å in size, which he was not able to identify conclusively when using thin foils. Fine dispersions of precipitates have also been observed by other workers (9, 14). Easterling and Spilling (9) stated that the precipitates which they observed were coarser than the continuous mode and were the result of reprecipitation on cooling in the ferrite phase or at the moving $\gamma - \alpha$ grain boundary. They further stated that the hardening effect was also aggravated by the interaction of the precipitates and the dislocations. The high dislocation density is a result of the low transformation temperature due to the effect of niobium. Hrivnak (14) discussed the types and locations of precipitates he observed after welding. He stated that precipitation of MX particles on dislocations in the HAZ increased its transition temperature, although it also hardened this region. However, it is fair to state that the exact nature of precipitates is largely unknown, due to the many possible compositions of these precipitates and the various thermal cycles possible in the HAZ. Progress in this area has been described by Gray (36).

Precipitates not only interact with dislocations, but they also can be used to restrict grain boundary movement and therefore retard grain growth. Small grain size not only provides good strength, but also improves toughness. The impact transition temperature in ferrite can be described quantitatively by an equation of the form (37):

$$\beta T = \ell n\beta - \ell nC - \ell nd^{\frac{1}{2}},$$

where β and C are constants,

T the ductile-brittle transition temperature, and

d is the grain diameter

This is in agreement with the observation of Otterberg et al (38). They used several steel compositions (C-Mn, Si, Nb, V and Nb-Al steels) and subjected steel samples to simulated thermal cycles typical of those encountered in welding and studied the effects of prior austenite grain size, the width of polygonal ferrite and the distance between Widmanstatten ferrite sideplates on the impact transition temperature (ITT). It was proposed that the ITT increases as a function of the square root of the maximum possible inscribed crack length in the polygonal ferrite.

In steel manufacturing, nitrides and/or carbides of niobium and/or vanadium are most commonly used for the purpose of grain refinement, and this process involves two mechanisms. In producing plates <50 mm thick containing a small amount of alloy elements, small precipitates (<50 Å) are important to retard recrystallization (36) while others have suggested that solute atoms are responsible (8). Delayed recrystallization caused by either precipitates or solutes allows heavy deformation of the austenite phase during rolling and induces more ferrite nucleations, thereby producing fine ferrite grains. In steels containing larger amounts of niobium and vanadium, small precipitates may be difficult to obtain. On the other hand, in producing thick plates (>50 mm), it is difficult to accumulate sufficient strain in the plates. In both cases, larger precipitates (<0.1μ) are used to retard austenite grain growth. Hence, fine ferrite grain size is a direct result of fine austenite grains. In welding, as mentioned earlier, the HAZ will undergo a rapid thermal cycle. However, there will not be sufficient strain for enhanced nucleation and therefore grain refinement via this route is not possible. On the other hand, grain growth retardation at high temperatures may be possible. This depends on whether the precipitates are stable or not at the high temperature concerned. Hrivnak (14) indicated that vanadium carbide will dissolve rapidly when heated above 900°C. Similarly, niobium and aluminum carbonitrides will dissolve above 1150°C. When these precipitates are dissolved, they can no longer retard grain growth. Therefore, steels which use these precipitates for grain refinement will have coarse grains in regions heated above these temperatures. Dolby and Saunders (15) have shown that at regions close to the fusion line, there is no difference between the grain size of a material containing grain-refining elements and one that does not. However, in regions which are heated to lower temperatures, the fine grains of grain-refined materials are maintained and therefore the toughness is superior to non-grain-refined materials.

2.6 Inclusions

The inclusion levels in steels are closely related to the oxygen and sulphur levels in the steels. It is well known that inclusions have a significant effect on the fracture behaviour of weld metals (39 - 41). However, in the base metal and therefore the HAZ, the oxygen level is usually very low and the

effects of inclusions are less important. Nevertheless, lameller tearing is closely associated with inclusions in the base material. Many studies have been done in this area and related papers have been collected by Skinner and Toyama (42). Factors that are important in controlling lamellar tearing were reviewed by Kaufmann et al (43). The mechanism by which lamellar tearing occurs during welding is well understood (44, 45). Tearing is triggered by decohesion of non-metallic inclusions under through-thickness stresses generated by weld contraction. Elongated silicates and sulphides are most damaging, and they tend to initiate tears near the weld or just outside the HAZ. It is also now realized that lamellar tearing is not solely a material problem (46) but a design-materials-fabrication problem. In connection with the HAZ toughness, it is sufficient to state that the amount of inclusions should be miminized and their shape controlled, so as not to provide an easy path for crack initiation.

2.7 Strain Aging

The occurrence of strain aging is a fairly general phenomenon in steels and no commercial carbon steels are completely free from its effect. This embrittlement occurs in the thermally-strained zone outside the transformed heat-affected zone. Strain aging has been associated with steel composition and especially free nitrogen content (75). The free interstitial solute atoms diffuse to produce atmospheres around moving dislocations. The resultant drag on these requires the dislocations to multiply to sustain the applied strain rate, which increases the dislocation density and reduces the toughness. It has been noted that restraining the plates will reduce the strain and thus the embrittlement (4). Investigations on a series of C/Mn steels showed that, contrary to the usual behaviour of semi-killed C/Mn steels, greater embrittlement was obtained in the transformed HAZ than in the thermally strained zone in the case of a fully-killed, aluminum-treated 0.17% C, 1.4% Mn steel (76). This comparison shows that the presence of aluminum is beneficial in lowering the interstitial nitrogen content and reducing the strain aging susceptibility of the steel. Low heat input welds were mentioned as being more susceptible to strain aging than high heat input welds, these latter welds having poor toughness in the transformed regions. As a final note, this type of embrittlement can be removed by post-weld stress relief (77).

It has been shown in this section that the gross microstructures, prior austenite grain size, precipitates and inclusions all have effects on the toughness of the HAZ.

2.8 Effects of Base Plate Composition and Heat Input

One of the major aims in welding research is to predict weldment properties from the material composition and the welding procedure. One of the earliest and relatively successful attempts was the use of a carbon equivalent equation to assess the susceptibility of HAZ cracking. Graville (34) studied the hardening curves of a wide range of steels in order to determine whether control of HAZ microstructures through cooling rate was a possible approach of avoiding cold cracking. Using a carbon equivalent formula, steels were classified into three zones. Zone 1 materials are low-carbon, low-alloy steels which are not susceptible under most conditions. Zone 3 steels are high-carbon, high-alloy steels which are susceptible under all conditions of welding. Steels in Zone 2 have high carbon but low alloys and cracking can be controlled through proper cooling. This approach is important from a practical point of view as will be discussed later, and can be used to assess weldability. However, it often does not reveal the actual mechanisms involved. Alloy elements can affect the properties of steels through their action as solutes, precipitates and interaction with other elements. While the effects of precipitates were discussed in the last section, the other two factors will be examined here.

Alloy elements are added for many purposes; to increase hardenability, to increase strength and to increase corrosion resistance are a few examples. Alloying elements may be classified into two main groups. Group 1 are elements which dissolve in ferrite and group 2 are elements which combine with carbon or nitrogen to form simple or complex carbides, nitrides or carbonitrides. Group 2 elements are usually added in very small quantities (<0.1%) and are commonly called microalloy elements in welding literature. Solutes that dissolve in ferrite can be either substitutional atoms such as manganese and nickel, or interstitial atoms such as carbon and nitrogen. Substitutional atoms strengthen the matrix through symmetrical distortion of the solvent lattice and their strengthening power is usually small. Interstitial

atoms interact with dislocations and markedly increase the strength and also cause strain aging of the material (47). Both substitutional and interstitial atoms may be segregated to grain boundaries and help to retard recrystallization and grain growth (8). Alloy elements will change the γ-α transformation temperature. This corresponds to shifting the CCT curve in an upward or downward direction. A lower transformation temperature will result in finer transformation products and a higher dislocation density. Fine structures can improve toughness but dislocation hardening will not. Alloying usually increases the hardenability of steels which correspond to moving the CCT curve towards the right. As described earlier, different transformation products will have different intrinsic toughness properties. Alloy elements can influence toughness through their interactions with each other. Aluminum and titanium additions can improve toughness of a steel. This is not only due to the formation of nitride particles which restrict grain growth, but also due to the removal of interstitial nitrogen from the matrix.

2.8.1 Heat-Affected Zone Properties

Numerous studies (6 - 13) have been made to assess the effects of niobium and vanadium on the toughness of weldments. Some workers (6 - 9) have shown that niobium and/or vanadium additions will lead to poor toughness in the weldment,(HAZ and weld metal) some have shown that such additions are beneficial (10, 11) and others indicate that no difference in toughness can be observed, at least for small additions (12, 13). Nevertheless, recent trends in steel composition are moving towards lower niobium and vanadium. This is mainly due to the recognition that excessive niobium or vanadium additions, in relation to the remaining alloy content, will lead to precipitation hardening and poor toughness in the HAZ (9). Grain size has a very significant effect on toughness and it is ideal if the fine grain size of the parent metal is maintained in the HAZ after welding. During the thermal cycle of welding, niobium and/or vanadium carbonitride particles near the fusion line will dissolve into the austenite matrix, and are therefore not able to retard grain growth. Hrivnak (14) and Dolby and Saunders (15) have indicated these carbonitride particles will dissolve above 1200°C. Steels containing titanium were studied by the Japanese (16 - 19) with the aim of limiting the extent of the coarse-grained heat-affected zone. These studies showed that the

dispersion of titanium nitride particles (16 - 18) and calcium oxide particles (19) limited the coarse-grained zone size and improved the toughness of the HAZ. Titanium nitride and calcium oxide particles are effective due to their high dissolution temperature. Kanazawa (16) showed that the dissolution of titanium particles is small up to 1400°C. Further studies on these steels are necessary to provide detailed information on HAZ toughness after welding.

It is seen that the effect of composition on impact toughness is quite complicated, and several mechanisms have to be considered. It is fair to say that the effects of solutes on toughness are not well understood. This aspect may be quite important in welding. During the cooling cycle, the HAZ often becomes supersaturated with solutes and no precipitates are formed. In general those substitutional solutes which produce appreciable strengthening are detrimental in that they increase the impact transition temperature. The effects of interstitial solutes are even less clearly established because of complications arising from interactions with dislocations or other substitutional solutes. However, it must not be supposed that all solutes are detrimental to toughness, nickel is an example of a beneficial alloy. The effects of substitional solutes on impact toughness may be associated with their effects on deformation twinning in the ferrite, i.e., possibly through their effects on stacking-fault energy (48). The mechanisms by which an alloying element affects the transformation characteristics are not well understood. However, scattered information of the effects of certain elements is available. Some of this is reviewed by Chamberlain (49) and Dolby (50) in connection with weldments.

Among the traditional alloying elements that are important in HSLA steel production manganese is one that has been studied quite extensively. It is known that manganese will lower the transformation temperature (51) and refine microstructures (52). Evans (53) showed that in the reheated region of multi-pass welds, an increase in manganese content increases the amount of acicular ferrite. The austenite grain size of the coarse- and fine-grained regions was also refined, and optimum impact properties were attained at a manganese level of 1.5%.

Watkins (76) has surveyed the toughness of microalloyed steels in various regions of the heat-affected zone. He gives evidence that the coarse-grained zone of single pass welds has lower toughness than that of multipass welds,

and that the toughness is improved in the fine-grained region. In his summary on testing of Nb treated microalloyed steels, he concluded that the most seriously embrittled region was the grain-coarsened heat-affected zone and that the loss of toughness was most severe at high heat inputs. In these cases the microstructure contains significant quantities of upper bainite which has a detrimental effect on toughness. The prior austenite grain size is increased and this governs the unit size of the transformation product. The preferred microstructure is a mixture of low carbon lower bainite and martensite and control of the heat input is necessary to avoid excessive embrittlement due to the formation of large unit structures of upper bainite. The loss of toughness noted in the grain-coarsened HAZ from the formation of bainitic and martensitic products is regained somewhat by tempering in multi-pass welding, provided that precipitate growth is minimal. The best transition temperatures are obtained with autotempered martensite and bainitic microstructures with fine lath spacing. The presence of nickel is beneficial in this effect (78). Figure 7 shows the effect of welding thermal cycle on HAZ Charpy V-notch transition temperature of HSLA steels containing niobium.

The effects of silicon on the mechanical properties of steels were reviewed by Hannerz (54). When working with plain carbon-manganese steels (0.15% C-0.8% Mn), he observed a beneficial effect of silicon on the transition temperature. A minimum transition temperature was obtained at 0.4% silicon. However, with niobium bearing steels, no such effect was observed. This observation was explained by Hannerz using the solution softening concept. It is known that silicon solution softens steels at low temperatures (55) and it is this phenomenon which is responsible for the improved toughness in C-Mn steels. However, the precipitates in the Nb bearing steel raised the yield strength and in turn the transition temperature was raised to above room temperature where the solution softening effect of silicon no longer existed, and therefore silicon was not beneficial. Silicon is also known to raise the $\gamma - \alpha$ transformation temperature (56, 57) and promotes the higher temperature morphologies, such as grain boundary ferrite, resulting in a coarse-grained microstructure (58). However, information on the effects of silicon on HAZ properties is very limited and further work is needed, especially in view that there is a trend to increase silicon content in base material for strength and hardenability (58).

A considerable amount of work has been done on the effects of microalloy elements such as niobium and vanadium on microstructures in connection with weld metal (27, 50, 60). Niobium is generally associated with the reduction of grain boundary ferrite and promotes either acicular ferrite or ferrite side-plates. However, when the weld metal is studied, additional factors such as type of consumables used and oxygen level may mask the real effects of niobium. This aspect was recognized by Dolby (61) when he stated that the best weld metal toughness of niobium bearing steel will be found using consumables which give a high proportion of acicular ferrite. Hence, it is not clear whether the promotion of acicular ferrite and the decrease of ferrite side-plates attributed to niobium and summarized by Dolby (61) is dependent on such external factors or not.

When the HAZ is studied, it is seen that heat input is important with respect to the effects of niobium. This may be associated with the precipitation effect at higher heat inputs. Dolby (62) showed that in microalloyed steels with carbon content higher than 0.12%, the toughness of HAZ at low heat input (2 kJ/mm) is quite insensitive to niobium content. At high heat input (>3.5 kJ/mm) the decreased toughness of these steels was attributed to the formation of coarse ferrite side-plates. However, as mentioned earlier, fine precipitates have been observed by some workers. It may well be that the loss of dissolved niobium due to precipitation promotes the formation of ferrite side-plates. In steels with lower carbon contents, Graville and Rothwell (63) showed improved toughness in the HAZ with niobium up to 0.14% at low heat input (1.4 kJ/mm) using dynamic fracture initiation tests. They further stated that as heat input goes up, toughness deteriorates and that the effect of cooling rate dominates the effect of composition. Sawhill et al (64) worked with steels containing molybdenum and observed improved toughness in the HAZ with niobium additions up to 0.05%. This was attributed to a slight decrease of bainite packet size under the conditions employed. On the other hand, Rothwell et al (65) worked with carbon manganese steels (C in the 0.075% to 0.095% range) and observed no toughness changes except at a high heat input (4.4 kJ/mm). However, niobium did reduce the width of the bainitic ferrite laths and the size of the carbide aggregates they observed. The deterioration of toughness at high heat input was attributed to precipitation hardening, in agreement with the observation of Hannerz (7).

Dolby (62) suggested that the precipitation hardening process may be avoided by proper alloying so as to depress the $\gamma - \alpha$ transformation temperature. This requires further investigation. It is clear, however, that a high heat input will decrease the toughness of niobium alloyed steel as other studies also support this observation (66, 67).

The effect of vanadium was studied by Sawhill et al (64). They concluded that the addition of vanadium up to 0.06% had no significant effect on microstructures or HAZ toughness. Similar results were observed by Rothwell et al (65) with vanadium additions up to 0.09%. They also observed that the addition of molydenum to niobium containing steels decreased the amount of grain boundary polygonal ferrite, refined the bainitic structures, promoted the formation of M-A particles at slow cooling rates and increased the amount of martensite at high cooling rates. However, the corresponding transition temperature is relatively unchanged except at high heat inputs where the detrimental effect of niobium is accentuated by molybdenum. When V-Nb steels were considered it was observed that vanadium had little effect except that a higher martensite content was observed in the HAZ with fast cooling rates.

Recently, the addition of titanium to steel has received increasing attention. Titanium precipitates not only prevent grain growth at relatively high temperature, but it was observed that these precipitates, either as nitride particles (68, 69) or as oxide particles (70) promote the nucleation of acicular ferrite. Titanium is often added in conjunction with boron to weld metals (27, 71, 72), and has been observed to improve weld metal toughness. Mori et al (73) stated that the beneficial effect is due to the following two reasons:

1) During the terminal transient solidification of weld metals, boron is capable of reducing free nitrogen while titanium protects boron from oxygen.
2) During the $\gamma - \alpha$ transformation, active boron, segregated to austenite grain boundaries, retards the nucleation of proeutectoid ferrite and titanium oxide promotes the nucleation of acicular ferrite intragranularly, thus producing homogeneous fine microstructures within the weld metal.

Most of the studies on titanium were done in connection with the weld metal. The effects of titanium on HAZ toughness, particularly when titanium is in solid solution are not clear, although it is known that titanium can promote bainite formation (13) and a coarse microstructure (57). However, titanium precipitates can retard grain growth as described earlier.

From the above discussion, it is evident that the effects of heat input are very important in determining the HAZ toughness. Christensen et al (74) studied the effects of heat input (0.9 kJ/mm to 2.1 kJ/mm) on the HAZ microstructures. Experimental steels (Nb-Al) were used and the quantity of martensitic structures were measured as a function of distance from the fusion line. The percentage of martensitic structures was seen to increase with decreasing heat input. Excessive heat input will always degrade toughness in the HAZ, especially in steels that contain microalloy elements where precipitation hardening is detrimental. Graville and Rothwell (63) have stated that the effects of heat input outweigh that of the steel composition. From an economic point of view, particularly when thicker and thicker sections are being welded, it is worthwhile to look into steel compositions which can be welded with high heat input without loss of HAZ toughness.

2.8.2 Grain Size Control

Work has been done aiming to improve the toughness of the HAZ through grain size control. One approach was to alloy steels with elements which produce precipitates with low solubilities even at relatively high temperatures. Kanazawa et al (16) showed that steels containing fine titanium nitride precipitates gave good toughness values in the HAZ even when high heat inputs (10 kJ/mm) were used. It was shown that the amount of soluble titanium in the steels they studied remained unchanged up to 1250°C, indicating no dissolution of titanium nitride precipitates. Also, the fine grain size of the base plate was maintained even when heated up to 1400°C. The austenite grain size was correlated to the volume fraction of precipitates with diameters smaller than 0.05μ and remained undissolved at 1400°C. The larger the number of these precipitates, the more refined were the austenite grains in the HAZ. This approach was taken further by Nakanishi et al (19) who used low sulphur, titanium and calcium treated steels. They observed that

titanium nitride and calcium oxisulphide particles in these steels could restrict grain growth in the grain-coarsened region. They showed that the solubility of calcium oxisulphide particles was several orders of magnitude smaller than titanium nitride at 1350°C. They therefore concluded that the dissolution of calcium oxisulphide particles is minimal at high temperatures and that these undissolved particles were still functional in preventing grain growth. The titanium nitride particles shown by the authors were less than 0.1μ in size but there was no indication of the effective particle size for the calcium oxisulphide particles. All calcium oxisulphide particles displayed were several microns in diameter.

Ikawa et al (17) studied the effect of precipitate size in the parent metal on grain growth in the HAZ of steels containing aluminum nitride. It was shown that fine precipitates of aluminum nitride dissolved rapidly when heated above 1350°C. On the other hand, coarse precipitates of aluminum nitride only dissolved gradually when heated above 1350°C. Thus if the precipitates in the base metal are small in size but large in quantity, a narrow, coarse-grained HAZ would result. However, the grain size of the coarse-grained zone will be quite large. This is due to the rapid dissolution of precipitates close to the fusion line which reduces the resistance to grain growth. Further away from the fusion line, the small precipitates are more efficient in restricting grain growth. If the precipitates in the base metal are coarse, the coarse-grained zone is wider but the average grain size is smaller than in the previous case. This is due to the less efficient grain growth retardation of coarser precipitates and slower dissolution rate of these particles near the fusion line, respectively. This study shows that the grain size of the HAZ can be controlled, at least to a certain extent, by controlling the size of precipitates in the base plate.

2.9 Summary

It is known that HAZ toughness is a function of microstructure, composition and heat input. The problem is further complicated by the fact that there is always a gradient of microstructures across the HAZ. The quantity and location of microstructures are also important. For example, the alignment of

M-A particles along prior austenite grain boundaries may be significant. The effect of alloy elements, both in solid solution and as precipitates, is not totally clear. The possible interactions amongst alloys have been even less studied. However, the possible mechanisms which are important in determining the HAZ toughness have been adequately pointed out. From the discussion on composition, it is clear that the ideal base material would be one that possesses a fine grain size, has stable precipitates to prevent grain growth during welding, contains a minimal of interstitial elements and would transform to good microstructures after the welding cycle.

3.0 Experimental Procedures and Results

3.1 Materials

The steel used for the welding studies was made to meet the requirements of Lloyds LT60. The chemical composition of the plates as reported for heat number L1028, is given in Table 5. The steel was rare earth treated and cast into 1700 mm x 810 mm ingots, which were hot rolled to the final thickness and normalized. The reported mechanical properties of the three plates are also listed in Table 5. In subsequent discussions the 25 mm thick plate will be referred to as plate A, the 50 mm plate as plate B, and plate C will designate the 75 mm thick plate.

The minimum values for Lloyds requirements are 41 J at -60°C for impact energy and 355 N/mm2, 490-610 N/mm2, and 22% for yield, ultimate, and elongation, respectively. From Table 5, it is evident that all plate thicknesses meet the minimum requirements of Lloyds LT60 grade for mechanical properties and chemical composition.

The 25 mm and 75 mm plates had full-thickness CTOD samples (t x 2t and t x t, respectively) machined such that their principal axes were transverse to the principal rolling direction, and the fatigue crack was therefore along the rolling direction. All testing was done in accordance to BS5762:1979 at -60°C, and the results are given in Table 5. The first 25 mm sample exhibited fully ductile behaviour while all of the remaining tests failed in an elastic-plastic manner.

3.2 Hardening Curves

The nominal welding conditions for the five welds are listed in Table 6. The cooling cycle for the lowest heat input is comparable to manual welding with a 4 mm diameter electrode on thick plates without preheat. The highest heat input represents realistic welding conditions for actual construction projects. The weld number in Table 6 refers to the nominal heat input in kJ/mm. This number is subsequently used throughout the report as a prefix ahead of the letter designation for plate thickness to keep track of the results (ie 1A, 2A, 3A refer to heat inputs 1, 2 and 3 kJ/mm respectively, on plate A). Numbers after the letter will refer to a particular section of the weld. The thermal histories of the welds as they cooled to room temperature were recorded using Pt/Pt-13% Rh thermocouples which were mechanically plunged into the molten weld pool. The time to cool between 800°C and 500°C, t_{8-5}, was obtained for each weld, see Table 7.

Four sections from each weld were removed for hardness measurements which were done using a Vickers diamond point indenter with a 5 kg load. The maximum hardness of the coarse-grained HAZ was recorded for each weld, with all of the values being given in Appendix A, while the average values are included in Table 7. The average values for each heat input are plotted against cooling cycle in Figure 8. All of the results can be represented by the same curve, which is expected, since the plates were all rolled from the same heat of steel.

3.2.1 Metallographic Examination of Hardening Curve Welds

The heat-affected zones of these welds were examined to assess what microstructural changes could be attributed to various heat inputs. The prior austenitic grain size was determined by counting the number of grain boundaries intercepted over a distance of 120 mm at a magnification of 500X. At the same time, a qualitative assessment was made of the relative proportions of various microconstituents. The microstructures of these regions were typical of those found in steels but differences in prior austenite grain structures, thermal cycles, and inclusions made some aspects of the microstructures

unique. The ferritic transformation products were classified as grain boundary allotriomorphs, lath or plate morphologies and intragranular idiomorphs. In addition, bainitic and martensitic structures were often observed. When quantitative measurements of microstructures were conducted, the different categories were defined at the beginning of the examination to avoid confusion over semantics. In the present study, the classification of microstructures followed those used in previous studies (7, 34).

The basic morphologies were categorized as follows. True grain boundary ferrite (TGB) was the name given to all blocky ferrite on the grain boundary. It is identified by its relatively coarse appearance and also by the fact that a series of grains adjacent to one another could be seen which would often form a ring surrounding a prior austenite boundary. This structure is termed grain boundary allotriomorphs or proeutectoid ferrite in the literature. Side grain boundary ferrite (SGB) is a morphology which appears to grow from grain boundaries as laths or plates, eventually trapping long islands of M-A. This structure develops at high temperatures from the TGB as a result of a carbon diffusion-controlled transformation (35). Laths with a similar appearance have been observed within austenite grains, remote from the grain boundaries (34). It was proven that these ferrite laths nucleated within the grains and that there were only a few orientations of ferrite laths within any one austenite grain. This microstructure was classified as intragranular allotriomorphs although it has been termed Widmanstatten ferrite in some reports. At lower temperatures, the quenched welds generally contained large percentages of sideplate morphology which was also noted to contain a small number of high angle boundaries. When the ferrite transformations were complete, it was difficult to determine whether the ferrite sideplates or laths had nucleated at a grain boundary or within a grain. Since both the nucleation locations resulted in similar M-A spacings with large ferrite grains, and since similar mechanical properties can be expected (36), they were classified together as lath structure (LS) for the microstructural analysis. As the cooling rates increase, the structure remains the same but the ferrite lath width and effective grain size decreases. No distinction was made in the examination on the details of the lath structure. At the faster cooling rates, martensite readily formed as well.

In summary, although there are many subtleties in the appearance of the microstructures, three categories were chosen to quantify the results. These categories are proeutectoid ferrite (PF), lath structure (LS), and martensite (M).

The results of the semi-quantitative metallographic examination of the hardening curve welds are presented in Table 7 and typical microstructures for the 25, 50, and 75 mm plates are shown in Figures 9, 10 and 11, respectively. All of the welds at 1 kJ/mm have 80% martensite and 20% lath structure, this changes to 50% martensite and 50% lath structure at 2 kJ/mm, and at the highest heat inputs the heat-affected zones are essentially lath structure with some limited areas of proeutectoid ferrite. From a metallurgical viewpoint, the optimum balance in structures is obtained for the intermediate heat inputs, 2 to 3 kJ/mm, in which the HAZ is comprised of 50% martensite and 50% lath structure. At lower heat inputs, the risk of hydrogen cracking is increased because of the higher martensite content and hardness, whereas at higher heat inputs the formation of coarse lath structures is detrimental to toughness.

3.2.2 Fracture Toughness Testing of Hardening Curve Welds

The effect of welding heat input on the fracture behaviour was examined using CTOD test methods as outlined in BS5762:1979. Examples of various load-displacement graphs and methods of calculating CTOD values are outlined in Appendix B.

The question as to whether fracture toughness of the heat-affected zone is related to the initiation or the propagation of a crack allows one to determine the type of testing to be used. In reviewing cases of failures (88), it is observed that initiation can be shown to occur in the HAZ but that the crack propagates most often in the baseplate. This has been attributed both to the superior weld metal toughness of mild steel weldments and the residual stress distribution. Because of the many examples demonstrating that fracture initiation is the critical event in the HAZ, it was concluded that a test procedure which measures crack initiation is preferred to one which measures crack propagation.

Two t x t specimens were tested for each of the hardening curve welds. The notch was extended by fatigue pre-cracking into the coarse-grained heat-affected zone. Specimens for the lowest heat inputs (1A, 1B, 1C) were 6 mm x 6 mm while the remaining specimens were 7.5 mm x 7.5 mm. All of the notches were made in the baseplate and then grown towards the weld as shown in Figure 12.

An alternative method of notching the CTOD samples is given by specimen E in Figure 3. The results of testing with fracture initiation both towards and away from the weld metal were reported (97) to have no detectable effect, for the particular consumables and plate investigated. However, the authors noted that the toughness of the region beyond the tip of the notch may control the initiation event since it is enveloped by the plastic zone. If this region was of lower toughness, than one could conceivably report unrepresentative CTOD values. They conclude (97) that initiation directed away from the weld metal is preferred to preclude the expected low measurements in the weld metal. Following their hypothesis, it is conceivable that the hardening curve results could possibly be measuring the weld metal values only. This would be the case if the toughness of the bead-on-plate weld metal was lower than the HAZ toughness. To examine this concern load-displacement curves were analyzed and CTOD values were calculated for the weld metal on samples 3A1 and 3A3. The drop in the load-displacement curve of each test is referred to as a pop-in. A pop-in occurs when testing specimens of mixed microstructures of variable toughness when a cleavage crack, which has nucleated in a low toughness region, runs into a region of higher toughness. A similar effect can occur because of the high compliance of the test frame. In the present case, however, it is considered that the subsequent rise in load after the pop-in confirms that the new crack tip location is within a region of higher toughness. Subsequent examination of the fracture surface confirmed that the pop-in was representative of the coarse-grained HAZ CTOD, 0.074 mm, while the subsequent CTOD was a measure of the weld metal toughness, 0.22 mm. With the weld metal giving values three times greater than the HAZ, the values reported for the hardening curves do reflect measurements of the coarse-grained region.

The fatigue precracking operation was originally to be conducted using a Manlabs constant amplitude precracker, but the narrow region into which the crack was to end precluded its use. To obtain greater control, all precracking was done on a servo-hydraulic testing machine.

The procedure for preparing the CTOD samples from the hardening curve welds required the greatest effort. After the specimen width, B, was obtained by grinding, both surfaces were polished and etched to ascertain the exact fusion boundary position. The fusion boundary was then marked at the mid-depth of the specimen, W/2, and the final machining was completed.

In CTOD testing, assumptions must be made on the anticipated disparity between surface and midpoint measurements of fatigue crack growth. Past experience with similar sized samples was that one could expect the crack to be 0.25 mm deeper at the centre of the sample compared to the edges. On this premise, the precracking was continued until the crack had advanced 60% of the dimension 'a'. Scribe lines were located on each specimen after examination on a stereo microscope for the depths of the rough saw cut, the starter notch saw cut, and the position of the fusion boundary.

The validity of using the 0.25 mm difference between surface and internal measurements was verified on the first series of bead-on-plate results for the 25 mm plate. The observed depth range of the fusion boundary was compared to the measured fatigue crack front and it was generally found that the 0.25 mm assumption was acceptable. However, further correlation showed that better results could be obtained if the depth of fatigue crack growth could be matched to the heat input as below:

Heat Input, kJ/mm	Depth of CGHAZ from fusion boundary, mm
1	0.35
2	0.40
3	0.45
4	0.45
5	0.45

In subsequent testing, these values were used to monitor the fatigue crack growth on both sides of the test specimen. In most cases, the crack growth was considered complete after it had advanced 60% of dimension 'a'.

The final confirmation between HAZ size and crack growth was obtained by comparing measurements on polished sections to details on the CTOD fracture surface. The width of the coarse-grained HAZ was measured from the polished sections at 200X magnification. The resulting measurements, shown below are within $\pm$ 0.025 mm on the actual sample. This error is due to the difficulty in determining the demarcation between the coarse- and fine-grained zones.

Heat Input, kJ/mm	Width of Coarse-Grained Zone, mm	
	Measured	Average
1	0.225,0.200,0.275	0.233
2	0.175,0.325,0.325	0.275
3	0.310,0.300,0.340	0.317
4	0.416,0.425,0.450	0.430
5	0.425,0.420,0.380	0.408

These measurements show that subtracting 0.25 mm from the previous table will put the crack tip from 0.10 to 0.20 mm away from the fusion boundary, and thus it will supposedly lie in the middle of the coarse-grained HAZ. Although good behaviour was anticipated, each sample was etched and examined for the exact positions of the fusion boundary and crack tip before testing.

The subsequent examination of the fracture surfaces on the stereo microscope confirmed the positioning of the crack tip. The brittle behaviour of the CTOD tests produced shiny cleavage facets which clearly showed the position of the fusion boundary. In the weld metal the columnar austenite grains could be seen to be very different from the coarse-grained regions. A typical fractured surface is seen in Figure 13. The fatigue precrack, initiation in the coarse-grained zone, and brittle propagation through the columnar weld metal are very evident.

The measured CTOD values themselves also indicated how successful the precracking had been. A high CTOD value compared to the other results immediately indicated that initiation did not occur in the coarse-grained zone. An example of this is given by specimens 2A2 and 2A4. The width of the coarse-grained zone is approximately 0.3 mm for this heat input. In 2A2, the fatigue crack was just outside of the coarse-grained zone, while in 2A4 the precrack was within 1 mm of the fusion boundary. The measured CTOD values of 0.203 and 0.048 mm for 2A2 and 2A4, respectively, demonstrated the magnitude of the difference that could be observed with notch tips located outside of the coarse-grained region.

Although considerable care was taken to ensure that the crack tip was located in the exact region of interest, it has been indicated (97) that the notch tip does not necessarily have to be located in the region of lowest toughness. In the heat-affected zone there is a steep microstructural gradient and the precise location of fracture initiation is not readily apparent from the fracture surface. Nonetheless, it is reasonable to assume that initiation will occur within the notch tip plastic zone where the interaction of applied strain and toughness becomes critical. Therefore, it is sufficient to ensure that the notch tip is located adjacent to the region and that the plastic zone envelops the region of lowest toughness. This argument, however, does not exclude the practice of locating the tip exactly in the region of interest which is currently being used.

At least two CTOD samples were tested at -60°C from each hardening curve weld. The results of the individual tests are given in Appendix B and summarized in Table 8 and Figure 14. As well as the testing at -60°C, a CTOD transition curve was determined for weld 3A between -90°C and 5°C (Figure 15).

The CTOD toughness from the hardening curve welds are plotted against cooling rate in Figure 14. The lines in the figure represent the lowest bound toughness for the 25, 50, and 75 mm thick plates. These lowest bound values show that there is an optimum toughness at intermediate cooling rates, which corresponds to heat inputs of 3 to 4 kJ/mm. The metallographic

examination of these welds showed that the highest HAZ toughness corresponded to mixed martensite/bainite structures, approximately 50% of each. These results also indicate that the HAZ toughness decreases with plate thickness. However, since one would not expect lower toughness with increased thickness since all of the plates were normalized, the trend to lower toughness could be due to cooling rate effects. The thicker plates cool slightly faster which produces a greater percentage of martensite, and hence a lower overall toughness. The quantitative examination of the hardening curve heat-affected zones was not sufficiently detailed to discern these observed differences in toughness with thickness.

The toughness results from the hardening curve welds clearly showed that the largest CTOD values in the coarse-grained HAZ were obtained at intermediate heat inputs, 3 to 4 kJ/mm. The optimum toughness was measured for microstructures which contained a 50% martensite/50% lath structure mixture which, from a metallurgical view, was the optimum combination. The hardening curve CTOD values confirm this position. Based on these CTOD values, it was decided to use a nominal heat input of 3 kJ/mm for each pass of the full thickness welds on the K-preparation joints and the butt joints. The results of testing on these welds will be described in following sections.

The CTOD evaluations of the effects of heat input on the hardening curve welds involved testing only at -60°C. This temperature was expected to lie within the lower shelf regime and thus the results would represent the worst case. A transition curve was subsequently determined for weld 3A to examine the variation of toughness with temperature. The details of testing are given in Appendix B while the CTOD values are plotted against temperature in Figure 15. The lower shelf CTOD of approximately 0.05 mm was maintained up to -50°C, above which temperature the CTOD value increased. As discussed above, the line in the figure gives the lowest bound toughness.

3.3 Fracture Toughness of K-Preparation Welds

A series of K-preparation welds were made from each plate using a nominal heat input of 3 kJ/mm and a maximum interpass temperature of 150°C (see Appendix C for details). This joint configuration was chosen so that the fatigue crack notch tip could be accurately grown into the region of interest for subsequent testing. The specimen type and notch locations as proposed for testing are summarized below. The surface notched specimens were required because of limitations in the capacity of the testing machine. Three specimens were to be tested for each case.

Specimen Type	Fatigue Crack	Plate Thickness, mm		
		25	50	75
t x 2t	through-thickness	Coarse HAZ	-	-
t x 2t	through-thickness	Fine HAZ	-	-
t x t	surface	Coarse HAZ	Coarse HAZ	Coarse HAZ
t x t	surface	Fine HAZ	Fine HAZ	Fine HAZ

The attainment of a planar zone on the vertical side of the K-prep was difficult to obtain using methods representative of good welding practice. When the capping passes were deposited the depth of penetration and the necessary bead placement resulted in a weld looking as if it had been prepared using a butt weld joint. It was therefore not possible to place a through-thickness notch such that testing was in a single region, either coarse-grained or fine-grained. The actual testing was for a combination of the two and is referred to as a 'mixed zone'. When the fatigue crack lies in such a 'mixed zone', the critical event will be controlled by cleavage initiation in the region of lowest toughness along the crack front (for plane strain conditions), which has been found to be the coarse-grained HAZ from the hardening curve results. On the other hand, the surface notches were located such that the fatigue crack tips were in the region of interest, either the coarse-grained or fine-grained zones.

An alternative welding method for CTOD testing of K-prep welds involves tilting the plate to be welded so that the angle of attack and degree of bead overlap are the same on both sides of the joint (4). This method is somewhat similar to the approach used to improve the HAZ toughness by tempering the previous weld HAZ by overlapping the weld beads. The amount of refinement produced in various welding positions is shown in Figure 16. With tilting the plate, the amount of tempering is increased and the toughness is improved in most steels (76). It is therefore considered that tilting is not exactly representative since it may not typify the worst possible toughness, and welding of the K-preps was done in the flat position.

A technique often used for CTOD testing of weld zones in thick sections is that of precompressing the material below the fatigue crack starter notch. The recommended practice requires the application of 1% strain. This value is based on the assumption that the residual stress in the surface beads is tensile while the remainder of the bead is in compression. By precompressing the specimen, it is assumed that the tensile surface stresses go to zero and that there is a uniform stress field across the specimen in which the crack is expected to grow. In actual fact though, many studies have shown that the surface is most often in compression and that a very high tensile residual stress exists through the thickness. Precompression may therefore cause compressive yielding on the surface which most likely would be balanced by increased tensile stresses at mid-thickness. The resultant stress distribution would be worse than before the precompression and its benefit would therefore be questioned. Past experience has also shown less scatter in CTOD values when precompression was not used. A final note worth mentioning is that the 1% precompression requires a previous knowledge of the yield strength of the material being precompressed. This is not always possible. In view of the arguments presented above, it was decided not to precompress the CTOD samples tested in this program.

The CTOD specimens were tested in the as-welded condition. The 25 mm weld was tested at -60°C, -35°C, and -10°C, while the 50 and 75 mm welds were tested only at -60°C. The complete results are given in Appendix B, which includes the specimen measurements and loading curves. The

interpretation of the CTOD values for these K-prep welds showed that a distinction could be made between the coarse-grained and fine-grained regions, as shown in Figure 17. The values in this figure include some of the results from the hardening curve weld transition curve to complement the lower bound values. Since most of the points refer to lower shelf CTOD values where specimen size and geometry effects are less significant than in the transition zone, comparing all of the results without correction is not expected to influence the outcome. The low toughness of the coarse-grained zone is evident through most of the temperature range, although there is a slight improvement at +10°C. The fine-grained region exhibits improved toughness at -60°C compared to the coarse zone and the lone result at -10°C suggests that the toughness improves rapidly between -60 and -10°C. A final point worth noting from Figure 17 is the large difference between the baseplate toughness and that of the weld zones at -60°C.

3.4 Procedure Testing of Butt Weld Assemblies

Butt welds were made using 25 and 75 mm plates to examine the weldability of the LT60 steel. The welding procedures used are detailed in Appendix C. The root passes were deposited using Tibor 22 wire and OP121TT flux, the roots were back gouged to sound metal, and then filled using SD2 2Ni wire with OP121TT flux. All welding was conducted parallel to the principal rolling direction.

When welding had been completed, the 25 mm plate was radiographically inspected to ASME Section IX and the 75 mm plate was examined ultrasonically. Details of the inspection are given in Appendix D. The radiograph met the specification and no reflectors were apparent at DAC sensitivity settings for the ultrasonic test.

Full thickness cross-weld tensile specimens were removed from each weld. The results are listed in Table 10.

Photographs of cross-sections from the completed butt welds are shown in Figure 18.

Standard 10 mm x 10 mm Charpy impact specimens were machined transverse to the welding direction with the notches perpendicular to the plate surface and located at several positions across the weld as shown in Table 10. Accurate positioning of the Charpy notches required etching of the finished blanks to reveal the fusion boundary, locating the notch, and then cutting the specimens to length. The fusion line position conforms to the Lloyds Registry of Shipping Rules for Welding and Inspection (90). One set of 15 specimens was prepared from the 25 mm plate while two sets were prepared from the 75 mm plate. The weld metal specimens for the 75 mm weld were tested at -80°C while all other testing was done at -60°C. All of the results from the weldability tests are listed in Table 10.

The hardnesses across the heat-affected zones of the butt welds were measured using a Vickers diamond point indenter with a 5 kg load. The results of the traverses are also given in Table 10. The hardness at 5 mm from the fusion line, DPH 171, is only slightly higher than the unaffected baseplate at DPH 164.

The acceptance criteria for weldability testing is outlined in Appendix E.

4.0 Discussion

The weldability of the steel is discussed by referring to each phase of the experimental program. This involved examination of the basic response of the steel to welding thermal cycles using hardening curves and mechanical testing of procedure qualification welds.

4.1 Hardening Curve Results

The maximum hardness in the heat-affected zone is one of the most important parameters to estimate the resistance of a steel to hydrogen cracking. The value of this parameter reflects a necessary selection of materials and welding conditions to prevent cracking, and is often referred to when describing the weldability. A general form of this index has been given by Arata and others (99):

$$H_V = F\ f(\tau) + f(E) + F_O$$

where $f(\tau)$ and $F(E)$ are functions of cooling time and composition, respectively, and F_O is a constant which relates to the basic hardness of the metal. In graphical form, the above expression is called a CCTSH (Continuous Cooling Transformation Structure Hardness) curve (99) or, more simply, a hardening curve.

The variation in hardness with cooling time is shown for a typical steel in Figure 19. The critical cooling times at which the quantity of martensite becomes 100%, T_{m100}, and 0%, T_{mo}. For times longer than T_{mo}, the structure is completely bainitic, and the hardness remains constant. The hardness between these two times is closely connected to the quantity of martensite in the structure and is affected by the welding conditions.

The hardness, apart from being closely related to the structure, gives an indication of the resistance to hydrogen cracking and toughness. At fast cooling times ($<T_{m100}$), the structure is very susceptible to hydrogen-induced cracking while at long cooling times ($>T_{mo}$), the microstructures are completely bainitic and exhibit poor toughness. Therefore, a hardening curve is used to specify welding procedures such that the cooling of the HAZ is at some optimum value between T_{m100} and T_{mo}.

A part of this current EMR-sponsored project has been involved with examining this LT60 steel and two others (an A710 GrA, Class 3 and a BS4360 Gr50E steel) using a hardening curve approach at AMCA (94). The results obtained in this study are plotted along with those from AMCA in Figure 20 and show very good agreement. The curves in Figure 20 show the comparative hardening behaviour of the three steels. The A710 steel is less hardenable than the LT60 steel while the BS4360 50E steel is more hardenable, based on the maximum hardness. Apart from the hardness at fast cooling rates, the slope of the hardening curve gives an indication of the resultant HAZ properties.

The precise metallurgical conditions which control toughness are difficult to identify. Austenite grain size, which is certainly of paramount importance, will be controlled by effective net heat input, alloying additions, and precipitation effects. When bainite is present, then cracks can propagate readily across ferrite-ferrite boundaries within a bainitic colony. The critical fracture initiation event would thus be the extension of a microcrack across a high-angle boundary. Previously, (35, 80) it has been noted that M-A (martensite-austenite) particles tend to be "trapped" in linear arrays at such boundaries. It is not suggested that cracks are likely to propagate preferentially along such arrays, and indeed this has never been observed in our previous fractographic studies. However, the presence of a brittle microconstituent at high angle boundaries with associated transformation stresses, may be expected to aid the propagation of a crack from one grain to another in much the same way as grain boundary carbides are found to do in polygonal ferrite structures.

The mechanism of formation of M-A, rather than carbide aggregates or the discrete, lath-boundary carbides typical of classical upper bainite, is not known exactly. In general, with the range of conditions typical of welding, a reduction in transformation temperature, whether as a result of increased cooling rate or alloying, will tend to promote M-A. In the case of alloying, it appears that, while interstitial diffusion is fast enough for the austenite to become increasingly enriched as transformation progresses, there is little partitioning of substitutional alloying elements. It is also probable that at a given transformation start temperature, the formation of M-A is more likely to occur as the carbon content decreases. This is probably the result of a reduction in the rate of carbon enrichment, so that there is less probability of the necessary carbon content for the nucleation of carbides being established before the temperature has fallen below the carbide formation range.

In a recent study which is still ongoing (96), Japanese researchers examined the formation of M-A in Ni-Cr-Mo, low-carbon steels and related this to the toughness using Charpy tests. Their main results showed that both coarsening of the structure and the presence of M-A contributed to loss of

toughness, with the M-A exerting a smaller influence on the toughness deterioration at long cooling times. SEM studies of the structures showed that the morphology of the bainite changed from elongated to massive shapes with increasing cooling time, and at even longer times changed to a decomposed ferrite and carbide aggregate. In their observations they also noted that the M-A consisted of martensite, twinned martensite, and retained austenite. An overiew of their work could be summarized by saying that toughness is adversely affected at low heat inputs primarily by the M-A constituent, while at high heat inputs the coarsening of the microstructure overrides the loss of toughness due to the M-A distribution. The relation of the cooling time to the fraction of M-A in Figure 21 shows the increase in M-A and subsequent decomposition with heat input. It is expected that a similar sequence of transformations would also be observed in HSLA steels.

A final factor that has to be taken into account is changes in the dispersion of fine carbides, either niobium or vanadium. Such changes could be brought about by interactions between the niobium and vanadium or any other carbide formers, or could simply result from the fall in transformation temperature with increasing alloying. The interaction between these factors has yet to be resolved.

4.2 CTOD Fracture Toughness Testing

Measurements of CTOD have become increasingly important in recent years with the introduction of fracture mechanics methods which evaluate allowable defect sizes. Past experience has indicated that the base metal CTOD is generally lower than that of the weld metal. When measuring the baseplate toughness in the HAZ, the crack tip location is crucial to obtain the minimum CTOD, particularly in multipass welds.

The initial HAZ regions subjected to reheating from subsequent passes undergo additional microstructural changes which result (100) in the following structures (see Figure 22): a coarse-grained region (A), fine-grained (B), granular pearlite (C), and coarse structures (regions D and E), During reheating from subsequent passes, the plastic deformation due to the

rotational distortion of the joint promotes dynamic strain aging, or hot strain embrittlement, in the regions A to E described above. Using surface-notched specimens, Tanaka et al (101) found that the CTOD was the minimum in regions A and E. Region A is the coarse-grained HAZ while E has been reheated to about 500 or 600°C. These results confirm that the coarse-grained HAZ regions are the most embrittled.

The narrow regions of the HAZ make it very difficult to accurately locate the notch tip and obtain a representative CTOD measurement. This problem was described by Gittos and Dolby (102) when they tried to measure the toughness of the coarse-grained zone of a 0.15C - 1.35 Mn-0.07 Nb steel as a function of heat input. The results of their experiments shown in Figure 23 show that their success rate for evaluating the coarse zone CTOD was very low, as was described in their text. The CTOD for 2 kJ/mm are particularly questionable in that the coarse-grained zone has even better toughness than the parent plate. In succeeding articles, such as reference (62), the results are presented as being representative of coarse-grained measurements only and are therefore somewhat misleading. The fine-grained values from the original work (102), however, are reasonable when they are plotted along with the results of the LT60 steels, as in Figure 24. This figure shows the transition behaviour of the coarse-and fine-grained regions, as well as the baseplate.

The concensus developed over the years for HAZ testing has been that numerous repetitions must be made to obtain the minimum CTOD value, or any region for that matter. The results of testing (100) on the various HAZ regions, A to E in Figure 22 are shown in Figure 25. The scatter in the results is evident and this confirms the requirement of testing many specimens. Also shown in their results are CTOD values for Gleeble samples with single thermal cycles, and Gleeble samples which are subsequently strained to 5% and reheated. The authors conclude that this technique is therefore suitable for establishing the lower bound results with a minimum of testing.

The important point to note in the results of Figure 25 is that the CTOD at

-50°C is between 0.10 and 0.50 mm for the lower bound results. These agree well with the LT60 values and some of the coarse-grained results of Gittos and Dolby (102) as in Figure 23. Although the compositions are slightly different in these examples, they do show that the heat-affected zones of single pass and multipass welds can produce extremely low CTOD results at testing temperatures below 0°C.

4.2.1 Application of Results

The CTOD test has been developed to determine a fracture toughness measure of the significance of a particular defect in a known stress field. However, to apply CTOD to a structure it is necessary to complement it with other results such as for wide plate tests. Although detailed, this procedure in itself may not be sufficient since it may be relevant to only one part of the structure. This part of the structure may or may not be redundant which, in itself, implies a particular fracture criteria. Therefore, failure of part of the overall fabrication may or may not lead to catastrophic failure. All of these factors must then be considered when determining the structural integrity of a welded structure.

4.3 Procedure Testing of Typical Joints

The mechanical testing of butt-welded joints was done to determine the acceptability of LT60 steel for welded construction, particularly for the fabrication of Arctic icebreakers. The minimum requirements listed by Lloyds' were used as the acceptance criteria (see Appendix E).

A 2% nickel wire and a fully basic flux combination, which is approved by Lloyds for the welding of LT60 steels, was selected for the investigation. Because of its susceptibility to strain aging (81), particularly in the root passes, it was only considered satisfactory for the joint fill-up. Fortunately, the development of the titanium-boron-molybdenum wires provided a solution to the problem of not being susceptible to strain aging and possible embrittlement. These were primarily developed for the high heat input welding of microalloyed structural steels and compatibility with the deoxidation charac-

teristics of fully basic fluxes. Their success depends on controlling microstructure and strength at an overall lean alloy composition, ie without excessive solid-solution alloying (82). The critical elements are titanium, which serves a dual role as a deoxidizer and nitride former, and boron (protected during welding) which is rendered 'active' in the final transforming weld metal. A very small percentage of 'active' boron in the weld metal (0.001%) can completely dominate the transformation behaviour of the weld deposit, allowing a fine acicular ferrite to be readily achieved. Hence, this consumable was selected for the root and back side passes. However, it should be mentioned that the re-heated Mn-Mo-Ti-B weld metal suffers a loss in toughness at nitrogen contents less <50 ppm over the as-welded weld metal. The Charpy transition temperature can rise to -40°C for weld metals containing 0.3% Mo subjected to reheating compared with -80°C in the as-welded condition (83). Consequently, a high molybdenum containing weld metal is not very suitable for heavy section fill and cap passes where very high toughness is required. The 0.2% Mo-Ti-B and 2% nickel consumable should therefore be the best combination if used for heat inputs up to 5 kJ/mm.

The tensile specimens failed in the baseplate, above the minimum specified value and showed the soundness of the weld metal.

The impact energies for the 25 mm plate (Table 10(a)) gave good weld metal results, 80 J average, a low of 51 J in the coarse-grained HAZ, and an improvement in the baseplate away from the weld. Referring to the acceptance criteria in Appendix E (27 J at -60°C for weld metal and 31 J at -60°C for the fusion line), the 25 mm butt weld exceeds the minimum requirements.

The Charpy values for the 75 mm plate are listed in Table 10(b). At the testing locations for the butt weld procedures, Lloyds requirements specify that the weld metal must attain a minimum 27 J at -80°C and 31 J for the fusion line at -60°C. The weld metal toughness at -80°C is only 14 J and improves to 43 J average at -60°C for the testing position at the top of the weld. The corresponding HAZ measurements show acceptable impact results for the coarse-grained HAZ, 40 J average, but the 5 mm position average

energy of 29 J is below the acceptable value of 31 J. This variation in Charpy results was repeated for the root position of the 75 mm plates. The weld centreline gave very poor results, 8 J at -80°C, there was an improvement in the coarse-grained HAZ, 70 J average at -60°C, and then a marked reduction at the 3 mm position, 17 J at -60°C. In strictly interpreting the requirements in Appendix E, the butt weld for the 75 mm plate does not satisfy Lloyds requirements, if the present limit of 55 mm is extended for the 75 mm plates. This raises a question as to the criteria set forth by the regulatory bodies and specifically, whether they are realistic. The distinction for testing is made on the basis of thickness with the present requirements being set at $\leq$35 mm and $\geq$35$\leq$55 mm. Historically, these values have been set on the basis of extensive experience in construction and reported results. In recent years, the use of thicker plates has become possible with improvements in steelmaking technology but, as yet, the field experience does not permit one to specify with certainty what acceptable impact energies are necessary to prevent brittle fracture. Accepting this position, the above results for the 75 mm plate do however give a cause for concern and the possible causes for poor toughness are addressed in the following paragraphs.

The weld metal impact energies can, in part, be related to observable structure and degree of bead overlap. Comparing the weld results at -60°C from the top of the weld, the high energy for the 25 mm weld, 80 J, is associated with mainly refined regions whereas the 75 mm weld tested a large proportion of as-welded metal which gave a lower toughness, 43 J. The dilution of the Tibor deposit into the 2 Ni capping pass may have also contributed to the higher toughness of the 25 mm weld. The microstructures of the capping passes from the 25 mm and the 75 mm welds are shown in Figure 26 (a) and 26 (b), and the structure from the Tibor root is also included as Figure 26 (c). The 2 Ni welds contain significant areas of ferrite with aligned M-A, while the Tibor root is predominantly acicular ferrite with only small areas of grain boundary ferrite. The microstructure of the 25 mm weld capping pass is intermediate between these two structures and suggests that dilution of the Tibor deposit into the capping pass influences the resultant microstructure, and hence properties.

The high proportion of refinement at the weld root position for the 75 mm weld, however, did not improve the toughness; the Charpy energy was 8 J at -80°C at the root compared to 14 J at -80°C at the top position. The poor root toughness was most likely caused by the heating of this region during deposition of the subsequent passes or during back gouging; Ti-B weld metals are known to suffer toughness degradation in those instances. Whereas the Tibor deposit gave good as-welded properties, heat treatments have been shown to markedly reduce the absorbed energy (84). The lower toughness was shown (84) to result from Nb carbonitride precipitation which was observed after stress relief.

A cause for concern was the poor toughness of the HAZ of the 75 mm plate, especially for the notches located at E, 29 J, and J, 17 J. Examination of the microstructures at these locations showed that the root of the notch was located just outside of the spheroidized region and thus the maximum temperature was below 400°C. Reductions of toughness in this area have been attributed to strain aging, providing that sufficient interstitial solute is present, either carbon or nitrogen (85). Strain aging due to nitrogen is prevented if the ASA:N $\geq$ 2:1. In the present material, the ASA:N ratio is greater than 3:1 and thus one would not expect strain aging due to nitrogen. Segregation of carbon which can be attributed to production methods (ie. continuous casting), has been known to cause strain age embrittlement in the centre of the plate. Microstructures and grain sizes were uniform through the thickness and segregation of alloying elements was not observed. With embrittlement due to solute interaction being unlikely, the possibility of toughness degradation due to local strain was examined.

Comparing a restrained flat-butt joint to a free rotation T-butt joint, Marshall (87) showed that the restrained weld met requirements of 34 J at -40°C while the unrestrained weld did not. The lowest toughness values were observed at the fusion line +10 mm position where the 34 J transition temperature was 60°C higher than the parent metal. In contrast, positions at 5, 10 and 15 mm from the fusion line gave higher toughness values at -60°C than the parent metal for the restrained weld. To examine the effects of work hardening due to strain alone (87), specimens were strained up to 20%, which corresponded

to a hardness increase of 30 DPH. The low toughness values were associated with hardness increases for the T-butt near the root and it was suggested that work hardening was the cause.

The hardnesses outside of the visible HAZ were measured for the 75 mm plate at the surface and the root at 177 and 193 DPH, respectively, compared to 183 DPH in the baseplate. The lower hardness at the surface could be within plate variations or it could possibly indicate aging of precipitates. The 10 DPH increase at the root however, does support Marshall's views on strain hardening and lower toughness, and is the most probable cause for embrittlement.

The main effect of plastic straining, which can be caused by forming or thermally-induced strains, is to increase the strength with a concurrent loss of toughness. The detrimental effect on impact properties is typical for most pressure vessel steels, and the maximum allowable strain before heat treatment is necessary ranges from 2.5 to 10% (105).

In fabricated structures, the local thermally-induced strains due to welding make the problem more acute since the magnitude of the strain is increased. Also, as the plate thickness increases, the overall restraint of the plates becomes greater, and strain-induced toughness degradation is again increased. In some grades a normalizing treatment may be necessary to restore properties. In most C-Mn steels, stress relief at normal temperatures ($\sim$ 625°C) can recover a substantial part of the toughness lost to strain-induced effects. For C-Mn microalloyed steels, however, stress relief may reprecipitate microalloy carbides and carbonitrides which can lead to significant toughness losses (77). At the present time, there is no clear indication on what type of treatment is the best way to proceed to recover toughness. This is primarily due to conflicts in opinions on the nature of the embrittlement. To confuse the issue even further, the problem of strain-age embrittlement has been related to the embrittlement encountered in low-carbon steels which have been strained while at temperatures around 250-300°C, called blue brittleness (106). The interaction of carbon and nitrogen with dislocations

exerts a dragging force on them which increases the yield strength and corresponding lowers toughness. Additions of titanium, aluminum, and possibly niobium and vanadium can interact to form nitrides on nitrides, thus decreasing the drag on dislocations, and possibly eliminate blue brittleness.

In the preceeding discussion, various theories have been put forward on the cause for embrittlement in the heat-affected zone. Each of the mechanisms has been related to the chemical composition of the baseplate and recommended procedures have been identified to restore the toughness. The present state of knowledge, however, is such that no one mechanism can be clearly isolated, but it is hoped that by narrowing down the possibilities can lead to a solution in the near future.

5.0 Summary and Conclusions

The weldability and heat-affected zone properties of C-Mn microalloyed steels was reviewed with particular reference to the influence of alloying elements. The review has also outlined some of the fracture design philosophies which are used for welded structures and the significance of various toughness measurements. From the literature review, the best HAZ characteristics would be obtained for a steel which has a fine grain size, stable precipitates to prevent grain growth, a minimal amount of interstitial elements, and which transforms to a microstructure which is a balance between between martensite and bainite.

The main emphasis of this work has been to develop welding procedures for a particular heat of LT60 steel which would retain adequate heat-affected zone properties. The laboratory examination included a study to ascertain the overall welding characteristics and procedure qualification butt weld trials. The main points which were determined in the course of the work are listed as follows:

1. The change in microstructure and hardness of the LT60 HAZ with different heat inputs can be used to determine welding procedures for optimum mechanical properties. For this steel, a heat input of 3 to 4 kJ/mm resulted in the best CTOD values and the corresponding microstructure was a 50/50 mixture of martensite/bainite.

2. Careful control of the fatigue precracking operation in CTOD testing is necessary to ensure testing of selected HAZ regions. Also, the lower bound CTOD values must be reported to provide a clear picture of the results.

3. The coarse-grained heat-affected zone CTOD of C-Mn microalloyed steels is the region of lowest toughness.

4. Low toughness measured in the baseplate adjacent to the spheroidized region of the HAZ has been attributed to strain-induced hardening.

5. The CTOD testing of multipass welds indicated that tempering from the deposition of subsequent passes did not improve the toughness over that of single pass welds.

6. Charpy measurements of the approved Lloyds consumables were significantly below the minimum acceptable requirements.

7. Impact results for the HAZ of butt weld procedure qualification tests confirmed that regions of low toughness are a concern with C-Mn microalloyed steels.

6.0 Recommendations

A number of interesting problems and questions arose during the course of this project which warrant further examination. Many of these have been mentioned throughout the text, and are identified below:

1. Investigate procedures or methods which could prevent strain-induced hardening in the baseplate adjacent to the visible heat-affected zone.

2. Review the toughness requirements which have been proposed for Arctic structures and vessels, and develop realistic requirements for structures fabricated with 75 mm thck plates.

3. Examine the heat-affected zone toughness of other candidate steels (such as the Ni-Cu A710 Cl3 or Lloyds 1/2% Ni steels) which also have acceptable baseplate properties at -60°C.

4. Examine the reasons for loss of toughness during stress relief of C-Mn microalloyed steels and make recommendations on chemistry requirements to optimize stress-relieved properties.

5. Investigate the HAZ of welds made in C-Mn microalloyed steels and how the microstructures and properties are influenced by composition.

6. Conduct a study on consumables which can be used to produce acceptable properties at low temperatures and which would not be susceptible to toughness degradation during stress relief.

7.0 References

1. B. Rapo, "Steels for Arctic Use - Classification Requirements", Workshop on Fracture Toughness of Steels for Arctic Use, Ottawa, October 12/13, 1983.

2. W. S. Pellini, Guidelines for Fracture Safe and Fatigue Reliable Design of Steel Structures, (Cambridge, UK: The Welding Institute), 1983.

3. G. H. Eide, K. O. Vilpponen, and others, Review of Steels Used in the Construction of Offshore Structures, Det norske Veritas Report 82-0086, Oslo, Norway, April 1982.

4. H. G. Pisarski and R. J. Pargeter, "Fracture Toughness of Weld Heat-Affected Zones in Steels Used in Constructing Offshore Platforms", proc. Welding in Energy Related Projects (Toronto: Pergamon Press), 1983.

5. J. D. Harrison, "Methods of Fracture Testing and Assessment of Test Results", Welding Institute Seminar Avoiding Brittle Fracture in Steel Fabrication, Atlanta, Georgia, November, 1975.

6. M.W.F. Cane and R.E. Dolby, "Metallurgical Factors Controlling the HAZ Fracture Toughness of Submerged Arc Welded C-Mn Steels",Welding Research International, Vol 4 (3), 1974, p 51.

7. N. E. Hannerz, "Effect of Cb on HAZ Ductility in Construction HT Steels", Welding Journal, Vol 54 (5), 1975, p 162-s.

8. N. E. Hannerz and B. M. Jonsson-Holmquist, Metal Science J., Vol. 8 (7), 1974, p 228.

9. K. E. Easterling and P. J. Spilling, Scan J. of Metallurgy, Vol 1, 1972, p 179.

10. E. G. Signes and J. C. Baker, "Effect of Columbium and Vanadium on the Weldability of HSLA Steels", Welding Journal, Vol 58 (6), 1979, p 187-s.

11. J. Jesseman and G. C. Schmid, "Influence of Some Steelmaking Variables on Ship Plate Weldment Toughness", Welding Journal, Vol 58 (8), 1979, p 239-s.

12. E. Levine and D. C. Hill, "Toughness in HSLA Steel Weldments", Metal Construction, Vol 9 (8), 1977, p 346.

13. Y. Yoshino and R.D. Stout, "Effect of Microalloys on the Notch Toughness of Line Pipe Seam Welds", Welding Journal, Vol 58 (3), 1978, p 59-s.

14. I. Hrivnak, Zvanacske Spravy, 1974, p 1.

15. R. E. Dolby and G. G. Saunders, "Metallurgical Factors Controlling the Heat Affected Zone Fracture Toughness of Carbon:Manganese and Low Alloy Steels", IIW Doc IX-891-74.

16. S. Kanazawa, "Development of New Steels for High Heat Input Welding", IIW Doc IX-952-76.

17. H. Ikawa, H. Oshige, Y. Mekuchi and S. Noi, "Effect of Precipitates on Austenitic Grain Growth of Steel in Weld-Heat Affected Zone", Transaction of the Japanese Welding Society, Vol 9 (2), 1978, p 23.

18. M. Suzuki et al, Proceeding "Second International Conference on Offshore Welded Structure, Nov. 1982", British Welding Inst. 1982, paper 16.

19. M. Nakaniski et al, IIW Doc IX-1281-83.

20. Committee of Welding Metallurgy of Japanese Welding Society, IIW Doc IX-1282-83.

21. T. Kasugai and M. Inagaki, Journal of Japan Welding Society, 1974, p 52.

22. R. A. Farrar, S. S. Tuliani and S. R. Norman, "Relationship Between Fracture Toughness and Microstructure of Mild Steel Submerged-Arc Weld Metal", Welding and Metal Fab., February 1974, p 68.

23. Coldren et al, Symposium "Steel Strengthening Mechanisms", Climax Moly. Co. 1969.

24. R. E. Dolby, "Research Member Seminar, Amsterdam", British Welding Inst., June 1975, p 15.

25. E. Levine and D. C. Hill, Met. Trans. A., Vol 8A, Sept 1977, p 1453.

26. L. J. Habraken and M. Economopoulus, "Bainitic Microstructures in Low Carbon Alloy Steels and Their Mechanical Properties", Sym. Transformation and Hardenability in steels, Climax Moly Co., 1969.

27. J. G. Garland and P. Kirkwood, "Towards Improved Submerged Arc Weld Metal", Metal Construction 1975, Vol 7 (5), p 275.

28. A. B. Rothwell, A. Glover, J. T. McGrath and G. C. Weatherly, "Heat-Affected Zone Toughness in High-Strength Pipeline Steels", Weldments: Physical Metallurgy and Failure Phenomena, Proc of the Fifth Bolton Landing Conference (Schenectady, NY: General Electric Company, 1978), p 257.

29. Y. Kikuta, T. Araki, A. Ohkubo, M. Yoneda and H. Tsuji, "Contribution of Cementites to Notch Toughness in Structural Steel Welds", Trans. of Japan Welding Society, Vol 9 (2), 1978, p 76.

30. S. Chung, H. Takahashi, M. Suzuki, "Microstructural Gradient in HAZ and Its Influence Upon HAZ Fracture Toughness", IIW Doc IX-1063-77.

31. F. Marquet, J. Defourny, C. Marique, M. Lamberigts and A. Bragard, "A Weldability of Structural Steels Evaluation of the Heat Affected Zone Properties", IIW Doc IX-1028-77.

32. J. M. Gray, "Weldability of Niobium Containing High Strength Low Alloy Steel", Welding Research Council, Bulletin 213, 1976.

33. A. J. Pacey and H. W. Kerr, Proceedings of the Fifth Bolton Landing Conference, August 1978, p 285.

34. B. A. Graville, "The Physical Metallurgy of the Weld Heat Affected Zone in Steels", Technical Report, Concordia University, 1978.

35. G.C.Weatherly, "Heat-affected Zone Toughness of Welded Joints in Micro-alloy Steels", Editors D.W.C. White and K. Winterton, CANMET Report 79-6, Section 3B.

36. J. M. Gray, " The Effect of Niobium on Transformation and Precipi tation Process in HSLA Steels", Moly Corp. U.S.A. 1975.

37. F. B. Pickering, Physical Metallurgy and the Design of Steels (London, UK: Applied Science Publisher Ltd., 1978) p 16.

38. R. Otterberg, R. Sandstrom and A. Sandberg, "Influence of Widmanstatten Ferrite on Mechanical Properties of Microalloyed Steels", IIW Doc IX-1127-79.

39. P. D. Blake, "Oxygen in Steel Weld Metals", Metal Construction, Vol 11(3), 1979, p 118.

40. T. H. North, H. B. Bell, A. Nowicki and I. Craig, "Slag/Metal Interaction Oxygen and Toughness in Submerged Arc Welding", Welding Journal, Vol 57, 1978, p 63-s.

41. U. Ekstrom and K. Olsson, "Weld Pool Chemistry and Metallurgy" British Welding Institute, 1980, p 323.

42. D. H. Skinner and M. Toyama, "Through Thickness Properties and Lamellar Tearing (a Bibliography)", Welding Research Council Bulletin 232, Nov 1977.

43. J. Kaufmann, A. W. Pense and R. D. Stout, "An Evaluation of Factors Significant to Lamellar Tearing", Welding Journal, Vol 60 (3) 1981, p 43-s.

44. Y. Ito et al, Proceedings "Welding of HSLA (Microalloyed) Structural Steels", ASM, Nov 1976, p 583.

45. J. E. M. Jubb, "Lamellar Tearing", Welding Research Council Bulletin 168, Dec 1971.

46. Y. Ito, M. Ikeda, M. Nakanishi and A. Michishita, "Notch Toughness of Weld Metal for C-Mn-Nb Steel", IIW Doc II-657-73.

47. F. B. Pickering, Physical Metallurgy and the Design of Steels (London, UK: Applied Science Publisher Ltd., 1978), p 13.

48. ibid, p 15.

49. B. G. Chamberlain, Project RC14, Report, WIC 1981.

50. R. E. Dolby, British Welding Institute Report 14/1976/M.

51. P. L. Harrison, "Continuous Cooling Transformation Diagrams for Niobium Bearing Weld Metals" University of Southampton, 1979.

52. N. Christensen, "Transformation Behaviour of Carbon-Manganese Weld Metal an International Study", IIW Doc II-933-80.

53. G. M. Evans, "Factors Affecting the Microstructure and Properties of C-Mn All-Weld-Metal Deposits", IIW Doc II-957-81.

54. N. E. Hannerz, "Influence of Silicon on the Mechanical Properties and on the Weldability of Mild and High Tensile Structural Steels - Literature Survey and own Experimental Studies", IIW Doc IX-1169-80.

55. W. C. Leslie, Met. Trans. Vol. 3, 1972, p 5.

56. J. S. Kirkaldy, Met. Trans. Vol 4, 1973, p 2327.

57. D. J. Kotecki and R.A. Moll, "A Toughness Study of Steel Weld-Metal from Self-Shielded Flux Cored Electrodes - Pt II", Welding Journal, Vol 51 (3), 1972, p 138-s.

58. N. Bailey and R. J. Pargeter, "The Influence of Flux Type on the Strength and Fracture Toughness of Mild Steel Weld Metal", British Welding Journal, Aug 1979.

59. R. Lazor and A. G. Glover, Confidential Report, WIC.

60. E. Levine and D. C. Hill, "A Review of the Structure and Properties of Welds in Columbium or Vanadium Containing High Strength Low Alloy Steels", Welding Research Council Bulletin 213, Feb 1976, p 20.

61. R. E. Dolby, "Review of Work on the Influence of Nb on the Microstructure and Toughness of Ferritic Weld Metal", IIW Doc IX-1175-80.

62. R. E. Dolby, "HAZ Toughness of Structural and Pressure Vessel Steels - Improvement and Prediction", Welding Journal, Vol 58 (8) 1979, p 226-s.

63. B. A. Graville and A. B. Rothwell, "Effect of Niobium on HAZ Toughness Using the Instrumented Charpy Test", Metal Construction, Vol 7 (10), 1975, p 455.

64. J. M. Sawhill et al, Proceedings Welding of HSLA (Microalloyed) Steels, (Metals Park, Ohio: American Society for Metals 1976), 1976, p 255.

65. A. B. Rothwell, CANMET Report 79-6, edited by D.W.G. White and K. Winterton.

66. G. Bernard, F. Fause and P. M. Maitrepierre, Welding of HSLA (Microalloyed) Steels, (Metals Park, Ohio: American Society for Metals, 1976), p 187.

67. E. Miyoshi, S. Hasebe, K. Bessyo and Y. Yamaguchi, "Fracture Initiation Characteristics of Heat Affected Zone Assessed by COD Tests", IIW Doc IX-878-74.

68. Y. Ito and M. Nakanishi, "Study on Charpy Impact Properties of Weld Metal with Submerged Arc Welding", IIW Doc XII-A-113-75.

69. A. H. Koukabi, T. H. North and H. B. Bell, "Properties of Submerged Arc Deposits - Effects of Zirconium, Vanadium and Titanium/Boron", Metal Construction, Vol. 11(12), 1979, p 639.

70. I. Watanabe and T. Kojima, Journal Japan Weld Society Vol 49(11), 1980.

71. K. Shinmyo, S. Saito, N. Mori, T. Takami and R. Kono, "A New Submerged Arc Welding Flux for Offshore Structure in Arctic Use", IIW Doc XII-A-138-77.

72. K. Nagano et al, IIW Doc. XII-E-40-79.

73. Naomichi Mori, H. Homma, S. Okita and M. Wakabayashi, "Mechanism of Notch-Toughness Improvement in Ti-B Bearing Weld Metals", IIW Doc IX-1196-81.

75. A. C. deKoning, Loss of Ductility in Material Next to a Weld, IIW Doc IX-471-65.

76. B. Watkins, "The Significance of the Heat-Affected Zone in Fracture Initiation", IIW Doc IX 694-70/X-542-69.

77. R. B. Lazor and A. G. Glover, "Examination of Stress Relief Requirements", Welding Institute of Canada Report RC157/1/84.

78. G. Buchanan, C.J.G. Jensen and R.J.C. Dobson, Lloyd's Register of Shipping's Approach to the Control of the Incidence of Brittle Fracture in Ship Structures.

79. R. E. Dolby and J. F. Knott, JISI 1972, 210, p 857.

80. J. G. Garland and P. D. Kirkwood, British Steel Report No. Prod/832/1/76/c.

81. C. F. Berkhout, S. H. Van den Brink, "How Strain Aging Influences the Toughness of Some Weld Metals", Welding and Metal Fabrication, Vol 46 (5), 1978, p 347.

82. P. R. Kirkwood, An Improved Submerged Arc Welding Wire for the Seam Welding of High Strength X70 Line Pipe, British Steel Report T/WE/MISC/175/77/C.

83. P. L. Mangonon, Jr., and W. E. Heitmann, "Subgrain and Precipitation - Strengthening Effects in Hot-Rolled, Columbium - Bearing Steels", proc Microalloying 75 (New York, N.Y.: Union Carbide Corporation, 1977) p 59.

84. N. H. Croft, J. M. Gray and A. J. DeArdo, "Submerged Arc Weld Metal Toughness in Microalloyed Linepipe Steels - The Effects of Post-Weld Heat Treatment", presented at ASM Conference, Philadelphia, PA, October 1983.

85. J. D. Baird, "The Effects of Strain Ageing Due to Interstitial Solutes on the Mechanical Properties of Metals", as cited in (4).

86. J. D. Ray, personal communication.

87. V. G. Marshall, "Procedural Requirements for Welded Joints in Offshore Structures - A Question of Validity", Metal Construction, Vol 14 (10), 1982, p 528.

88. J. T. McGrath, Literature Review on Fracture Toughness Testing of the Heat-Affected Zone, Canadian Welding Development Institute, December 1975.

89. "Report on Methods for Fracture Toughness Tests for Weldments", IIW Doc X-716-73.

90. Provisional Steel Grades Distribution for LNG Carriers to Operate in Canadian Arctic at a Design Temperature of Not Less Than -43°C, Lloyds Registry of Shipping, Appendix A, Issue 2, Welding and Inspection.

91. B. A. Graville, The Principles of Cold Cracking Control in Welds, (Montreal, Canada: Dominion Bridge Company, Limited, 1975).

92. N. Bailey, "Welding Procedures for Low Alloy Steels", Welding Institute Report, July 1970.

93. K. Lorenz and C. Duren, "Evaluation of Large Diameter Pipe Steel Weldability by Means of the Carbon Equivalent", proc. Steels for Line Pipe and Pipeline Fittings (London, UK: The Metals Society, 1983), p 322.

94. AMCA Progress Report on CANMET 50/50 program, Ottawa, October 1984.

95. M. J. Bibby and A. B. Rothwell, Technical Memorandum No. 37, Noranda Research Centre, February 1975.

96. H. Ikawa, H. Oshige and T. Tanoue, "Effect of Martensite-Austenite Constituent on HAZ Toughness of a High Strength Steel", IIW Doc IX-1156-80.

97. R. E. Dolby and G. L. Archer, "The Assessment of Heat-Affected Zone Fracture Toughness", conf Instn Mech Engrs, paper C53/71, p 190.

98. A. S. Tetelman and A. J. McEvily, Fracture of Structural Materials, (New York, NY: John Wiley and Sons, Inc. 1967), p 278.

99. Y. Arata, K. Nishiguchi, T. Ohji, and N. Kohsai, "Weldability Concept on Hardness Prediction", Transactions of JWRI, Vol 8(1), 1979, p 43.

100. T. Horitani and others, "A New Method to Estimate the Minimum CTOD Value of Weld Fusion Line", as cited by H. Suzuki, "Weldability of Modern Structural Steels", 1982 IIW Houdremont Lecture, Ljubljana, Yugoslavia.

101. Tanaka and others, private communication, ibid.

102. F. Gittos, R. E. Dolby, "Predicting the HAZ Toughness of C and C-Mn Steels: Welding 25 mm Plate at 1-7 kJ/mm", Welding Research International, Vol 9(6), 1979, p 22.

103. H. G. Pisarski and M. G. Dawes, "Measurement of Crack Opening Displacement in Weldments with Particular Reference to Offshore Structures", The Welding Institute, 1980.

104. T. G. F. Gray, J. Spence, and T. H. North, Rational Welding Design. (London, UK: Newnes-Butterworths, 1975), p 105.

105. J.N. Cordea, "Niobium-and Vanadium-Containing Steels for Pressure Vessel Service", Welding Research Council Bulletin 203.

106. A.S. Tetelman and A.J. McEvily, Fracture of Structural Materials, (New York, NY: John Wiley and Sons. Inc., 1967), p 512.

TABLE 1

External Hull Structure General Philosophy for Determination of Steel Grades (1)

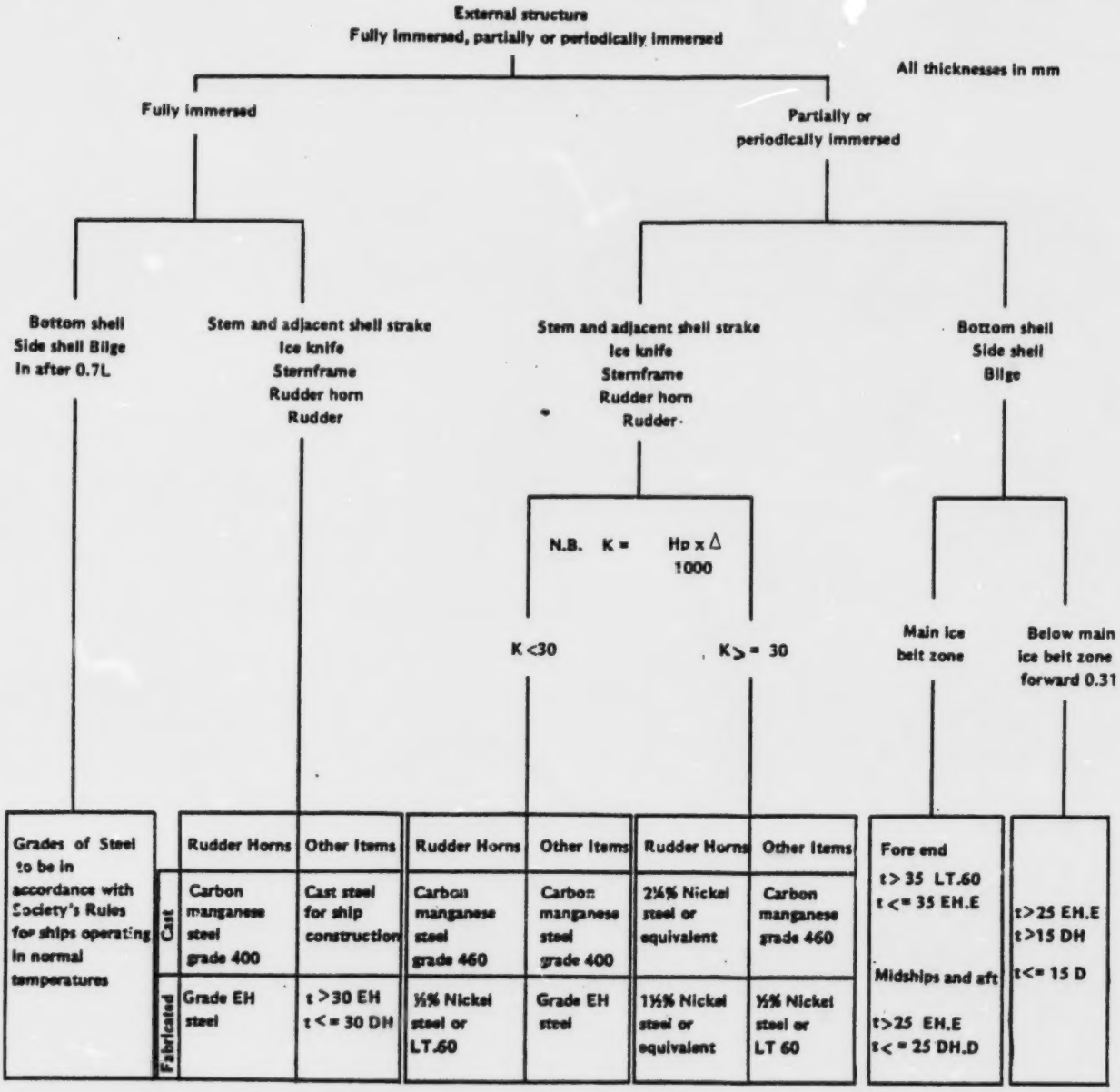

TABLE 2

Steel Plates for Fabricated Constructions (1)

STEEL PLATES FOR FABRICATED CONSTRUCTIONS						
Grade of Steel	Yield Stress N/mm^2 min.	Tensile Strength N/mm^2	Elongation on 5.65 S_o %min	Impact Test Temp. °C	Charpy V - Notch Impact Tests	
					Ships for liquefied gases	Other applications
C-Mn LT60	245 285 355	360-480 410-530 490-610	24 24 22	- 60	Plates - transverse tests Average energy 27 J min.	Plates, sections and bars - longitudinal tests when specified minimum tensile strength 450 $/mm^2$
½ Ni	245 285 355	360-480 410-530 490-610	24 24 22	- 60	Sections and bars - longitudinal tests Average energy 41 J min.	Average energy 27 J min. when specified minimum tensile strength 450 N/mm^2 Average energy 41 J min.
1½ Ni	275	490-460	22			
AG AH32	315	490-590	22			
AH32				0		31 J
DH32	315	49	22	- 20		31 J
EH32				- 40		31 J
AH34S				0		34 J
DH34S	340	440-590	22	- 20		34 J
EH34S				- 40		34 J
AH36				0		34 J
DH36	355	490-620	21	- 20		34 J
EH36				- 40		34 J
B	235	400-490	22	0		27 J
D	235	400-490	22	- 10		27 J
E	235	400-490	22	- 40		27 J

TABLE 3
Steel Types According to Applications (5)

CLASSIFICATION	FUNCTION	TYPICAL USE	PRINCIPAL REQUIREMENTS
SPECIAL STRUCTURAL STEEL (DnV) Class I (BV) Primary Components (Ger.Lloyd) Class A Steel (API RP-2A) Class A Steel (API RP-2A) Special Application Structures (ABS) Weld Class A members (USGS) Primary members (DoE)	MEMBERS ESSENTIAL/ CRITICAL FOR OVERALL INTEGRITY	can sections, deck to leg connections, cruciform joint of main girders main bracing in tubular structures Intersection of lattice type leg structures	- transverse impact property requirements - limits on C, CE, impurities alloy elements - through thickness ductility - ultrasonic examination – each item tested - high strain ageing resistance
PRIMARY STRUCTURAL STEEL (DnV) Class II (BV) Secondary Components (Ger.Lloyd) Class B (API) Primary Application Structure (ABS) Weld Class B members (USGS) Secondary members (DoE)	MEMBERS PARTICIPATING IN OVERALL INTEGRITY/ CARRYING PRIMARY LOADS	jacket legs, piles, bracings, main girders and beams riser support structure module support jack house supporting structure of vertical columns	- longitudinal test - impact requirements - restriction on CE, alloy elements and impurities - heat testing - good cold forming ability
SECONDARY STRUCTURAL STEEL (DnV) Class III (BV) Class C (API) or no class Secondary Application STructure (ABS) Weld Class C members (USGS) Others (DoE)	OTHER LOCAL STRENGTH ELEMENTS	OTHER stiffeners deck floors Internal framing upper platform decks equipment supports	- as per recongized steel standards for weldable grades - only impact testing in thicker sections (e.g. DnV fixed: 50 mm)

TABLE 4

Classification of Microstructures in Low Carbon Alloy Steel Weld Metal (20)

Principal Structures	Classification (Component Structures)
Ferrite	Grain boundary ferrite Ferrite allotriomorph Grain boundary polygonal ferrite Intragranular polygonal ferrite Ferrite sideplate
Pearlite	Pearlite Lamellar pearlite Degenerated pearlite Fine colony pearlite
Acicular ferrite (Fine grained ferrite)	Acicular ferrite
Bainite	Upper bainite Lower bainite
Martensite	Lath martensite M-A constituent

TABLE 5

Chemical Composition, Wt Percent and Mechanical Properties of Heat L1028

C	Mn	S	P	Si	Cr	Ni	Cu	Mo	Al	Nb	V
0.12	1.39	0.011	0.017	0.28	0.17	0.15	0.15	0.001	0.027	0.041	0.053

Description	Plate Number, thickness (mm)		
	32347, 25	32340, 50	33877, 75
Tensile Properties			
Yield Strength, MPa	403	397	372
Tensile Strength, MPa	510	524	506
% Elongation in 50 mm		32	30
in 200 mm	27		
Impact Properties, J			
Type, Direction	CVNL	CVNL	CVNL
Testing Temperature, °C	-60	-60	-60
Sample 1	151	120	165
Sample 2	203	163	137
Sample 3	225	238	219
CTOD Properties, mm			
Testing Temperature, °C	-60		-60
Specimen type	t x 2t		t x t
Sample 1	δ m = 1.120		δ u = 0.750
Sample 2	δ u = 0.620		δ u = 0.594

TABLE 6
Welding Parameters for Hardening Curves

Weld Number	Initial Plate Temperature °C	Voltage volts	Current amperes	Travel Speed mm/s	Nominal Heat Input kJ/mm
1	20	30	425	14.8	0.860
2	20	30	550	8.3	2.0
3	20	32	675	6.8	3.19
4	20	32	700	5.3	4.23
5	200	32	700	5.3	4.23

TABLE 7
Summary of Hardening Curve Results

Weld Code	Thickness mm	t_{8-5}, s	R_{540}(a), °C/s	HAZ Hardness	Grain Size g/mm (b)	Microstructural Category PF	LS	M (c)
1A	25	4.50	48.2	329	21.7	0	20	80
2A	25	11.55	18.8	282	15.8	0	50	50
3A	25	17.0	12.8	260	12.1	0	50	50
4A	25	29.5	7.4	239	9.71	0	90	10
5A	25	61.0	3.6	224	8.26	5	95	0
1B	50	4.35	49.9	326	22.7	0	20	80
2B	50	9.39	23.1	293	14.6	0	50	50
3B	50	16.2	13.4	264	11.9	0	50	50
4B	50	20.4	10.6	254	9.8	0	100	0
5B	50	46.6	4.7	231	7.3	3	97	0
1C	75	4.35	49.9	324	21.2	0	20	80
2C	75	8.88	24.4	287	13.2	0	50	50
3C	75	15.9	13.7	263	11.5	0	50	50
4C	75	21.0	10.3	251	10.5	2	80	15
5C	75	44.4	4.9	228	8.12	3	97	0

(a) $R_{540} = \frac{217}{t_{8-5}}$ for 3D cooling (Graville)

(b) grains/mm

(c) PF - proeutectoid ferrite
LS - lath structure
M - martensite

TABLE 8

Results of CTOD Testing of Coarse-Grained HAZ of Hardening Curve Welds

Weld	Test Temperature °C	CTOD Values	
		Average	Minimum
1A	-60	0.041 (1)*	0.041
2A	-60	0.048 (1)	0.048
3A	-90	0.034 (2)	0.023
	-70	0.042 (2)	0.041
	-60	0.074 (2)	0.066
	-50	0.055 (3)	0.041
	-30	0.163 (3)	0.091
	-10	0.125 (3)	0.033
	+ 5	0.177 (2)	0.119
4A	-60	0.130 (2)	0.099
5A	-60	0.026 (2)	0.076
1B	-60	0.038 (2)	0.025
2B	-60	0.072 (2)	0.071
3B	-60	0.127 (2)	0.104
4B	-60	0.077 (2)	0.069
5B	-60	0.060 (2)	0.028
1C	-60	0.048 (1)	0.048
2C	-60	0.079 (2)	0.064
3C	-60	0.091 (1)	0.091
4C	-60	0.105 (2)	0.073
5C	-60	0.061 (2)	0.058

* Indicates number of specimens tested.

TABLE 9

CTOD Results from K-Preparation Welds

Sample	Type	Temperature °C	CTOD mm	Comments Notch Location Expected	Actual
A7	tx2t	-10	δ_m = 0.716	C	invalid
A5	tx2t	-35	δ_u = 0.142	C	mixed
A11	tx2t	-35	δ_u = 0.234	C	mixed
A1	tx2t	-60	δ_u = 0.145	F	mixed
A3	tx2t	-60	δ_u = 0.066	F	mixed
A9	tx2t	-60	δ_u = 0.086	F	mixed
A2	txt	-60	δ_u = 0.076	C	C
A8	txt	-35	δ_c = 0.009	C	C
A4	txt	-60	δ_u = 0.076	C	C
A6	txt	-60	δ_u = 0.064	F	C borderline
A10	txt	-60	δ_u = 0.210	F	F
A12	txt	-60	δ_m = 0.716	F	F too far, baseplate
B1	txt	-60	$\delta_{u/c}$ = 0.076	F	F
B2	txt	-60	δ_c = 0.008	F	C
B3	txt	-60	δ_c = 0.005	F	F
B4	txt	-60	δ_u = 0.066	C	C invalid
B5	txt	-60	δ_u = 0.201	C	C invalid
B6	txt	-60	δ_c = 0.013	C	C
C1	txt	-60	δ_u = 0.066	F	F
C2	txt	-60	δ_u = 0.262	C	C high
C3	txt	-60	δ_u = 0.081	F	F
C4	txt	-60	$\delta_{u/c}$= 0.076	C	C
C5	txt	-60	δ_u = 0.033	F	F
C6	txt	-60	$\delta_{u/c}$= 0.028	C	C

TABLE 10 (a)

Properties Obtained from Butt Weld Procedure on 25 mm Plate

Tensile Properties						
Yield Strength, MPa					440	
Tensile Strength, MPa					612	
% Elongation					38	
Location of Fracture					Base metal	
Impact Properties, J		Sample				
Test Temp. °C	Notch Location	1	2	3	Avg	Hardness DPH_5
-60	A	98	64	77	80	
-60	A					
-60	B	78	40	53	57	229
-60	C	40	73	41	51	214
-60	D	90	90	92	91	190
-60	E	85	67	110	87	171

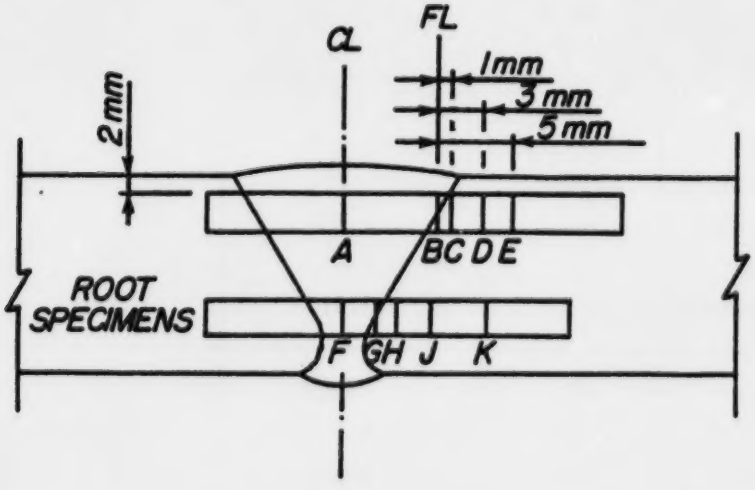

TABLE 10 (b)

Properties Obtained from Butt Weld Procedure on 75 mm Plate

Tensile Properties						
Yield Strength, MPa		356				
Tensile Strength, MPa		521				
% Elongation		29				
Location of Fracture		Base metal				
Impact Properties, J		Sample				
Test Temp. °C	Notch Location	1	2	3	Avg	Hardness DPH_5
-80	A	13	22	8	14	200
-60	A	39	46	44	43	
-60	B	48	46	27	40	202
-60	C	35	77	42	51	224
-60	D	42	50	57	50	196
-60	E	30	28	28	29	176
-80	F	6	7	10	8	212
-60	G	15	23	17	18	244
-60	H	64	35	111	70	254
-60	J	8	32	10	17	199
-60	K	80	88	76	81	193
baseplate						183

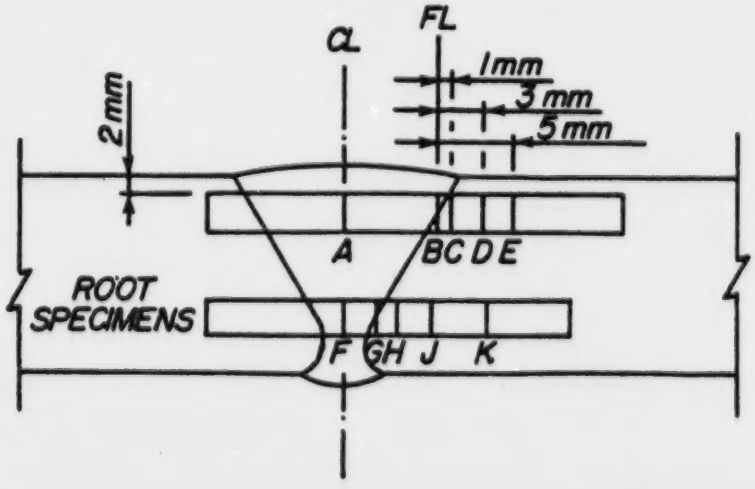

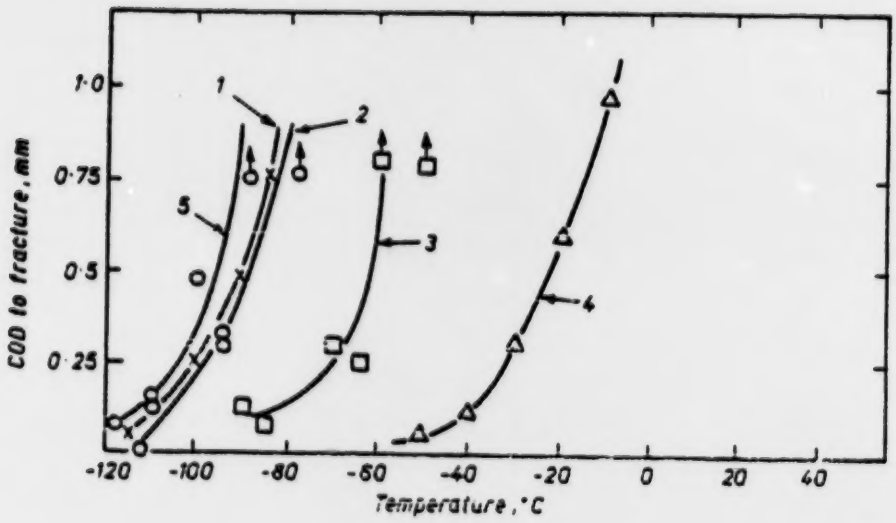

Figure 1. Results of CTOD tests on parent material, HAZ, and weld metal of C-Mn steel weldment: 1 - hot strained (250°C) parent material; 2 - fine-grained HAZ; 3 - coarse-grained HAZ; 4 - weld metal; 5 - plain material.

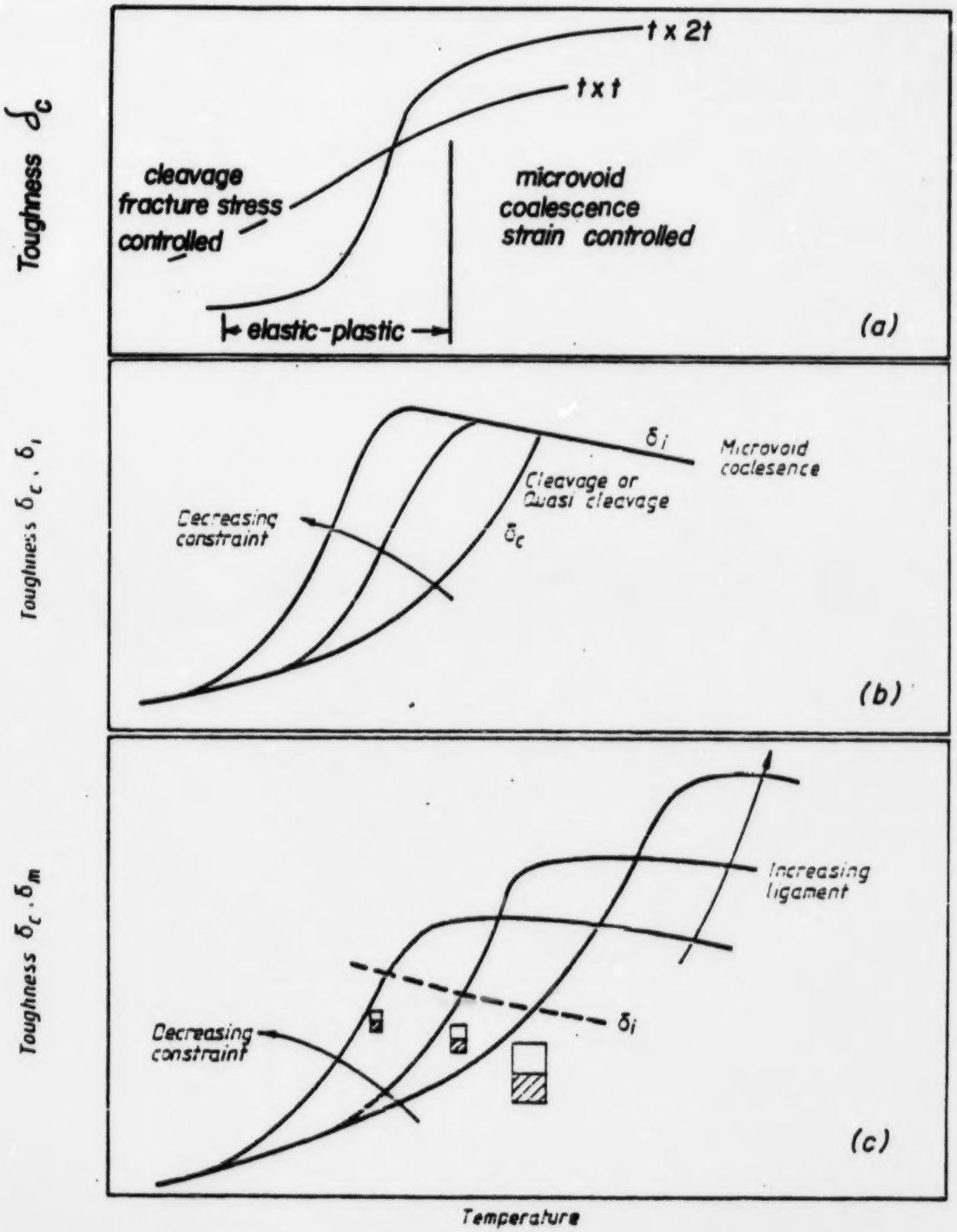

Figure 2. Effects of testpiece geometry on CTODs measured in the transition regime.

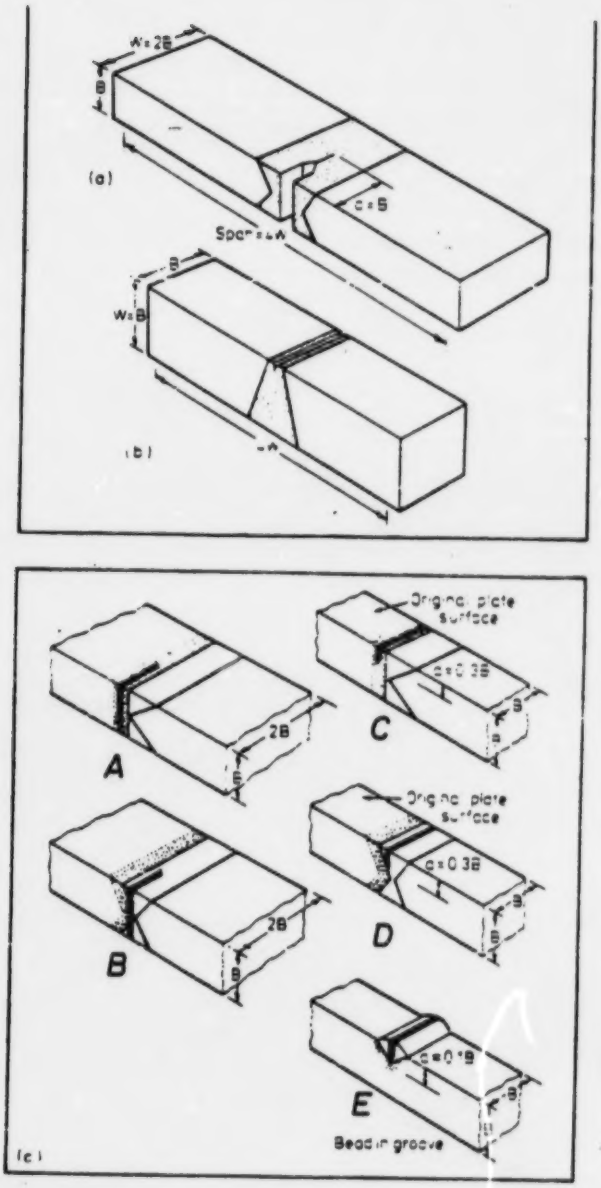

Figure 3. Typical notch orientations used for weldment testing: a) Preferred (with through thickness notch on weld centreline); and b) Subsidiary (showing notch orientation used to investigate suspected low root toughness in a single V or asymmetric double V weld) CTOD testpiece geometries (weld metal notches); c) Used to investigate HAZ toughness.

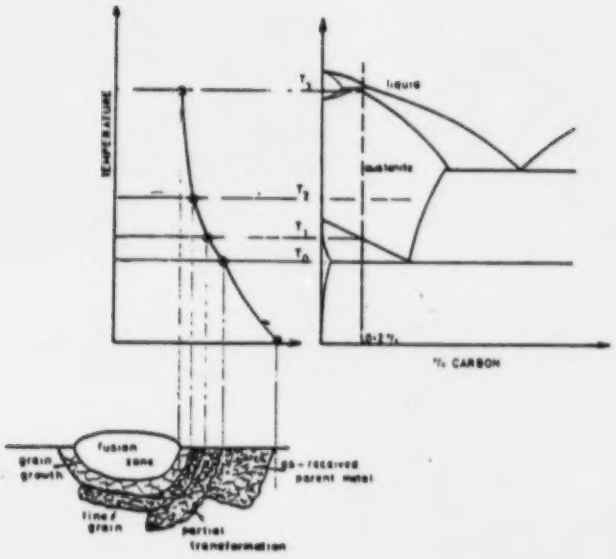

Figure 4. Schematic microstructure of 0.2% C steel weld (104).

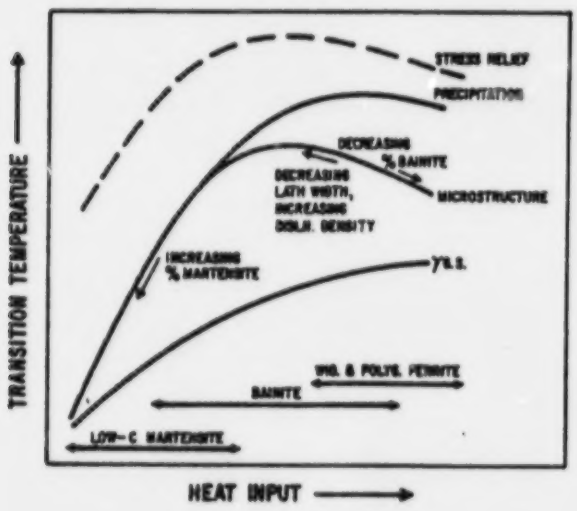

Figure 5. Schematic illustration of effects of microstructural parameters on HAZ toughness (35).

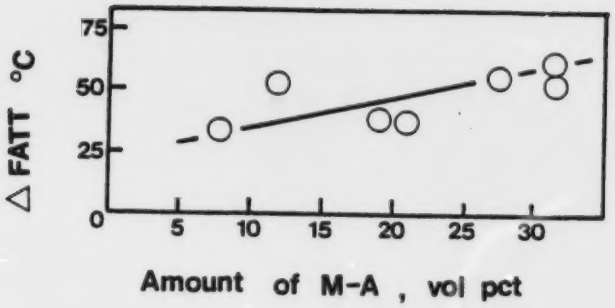

Figure 6. Effect of M-A content on Fracture Appearance Transition Temperature. Circled values indicate average calculated carbon content (26).

	C	Mn	S	Si	Al	Nb	Mo
B1	0.69	1.350	0.16	0.242	0.14	0.34	0.188
B4	0.160	1.465	0.10	0.325	0.39	0.43	0.210
B5	0.119	0.153	0.12	0.322	0.52	0.31	-

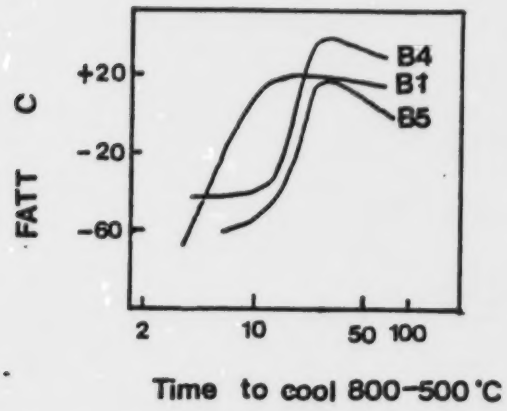

Figure 7. Effect of welding thermal cycle on HAZ Charpy V transition temperature of 3 HSLA steels (66).

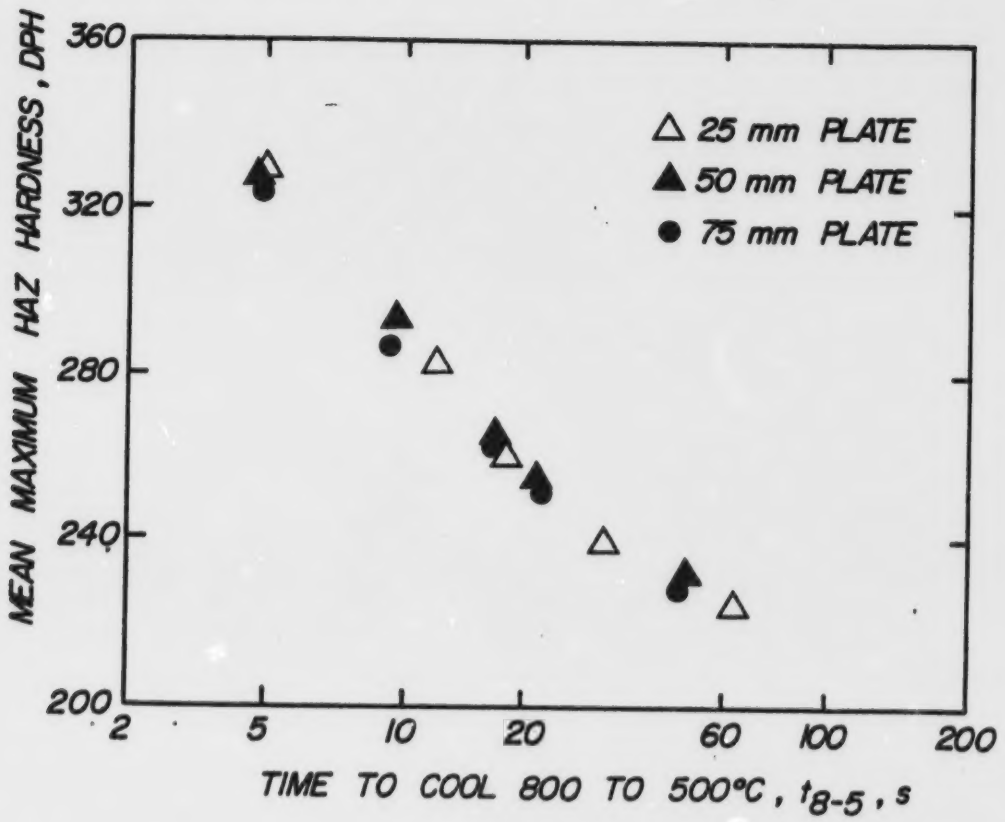

Figure 8. Hardening curve results showing HAZ hardness versus t_{8-5} for 25, 50 and 75 mm thick plates.

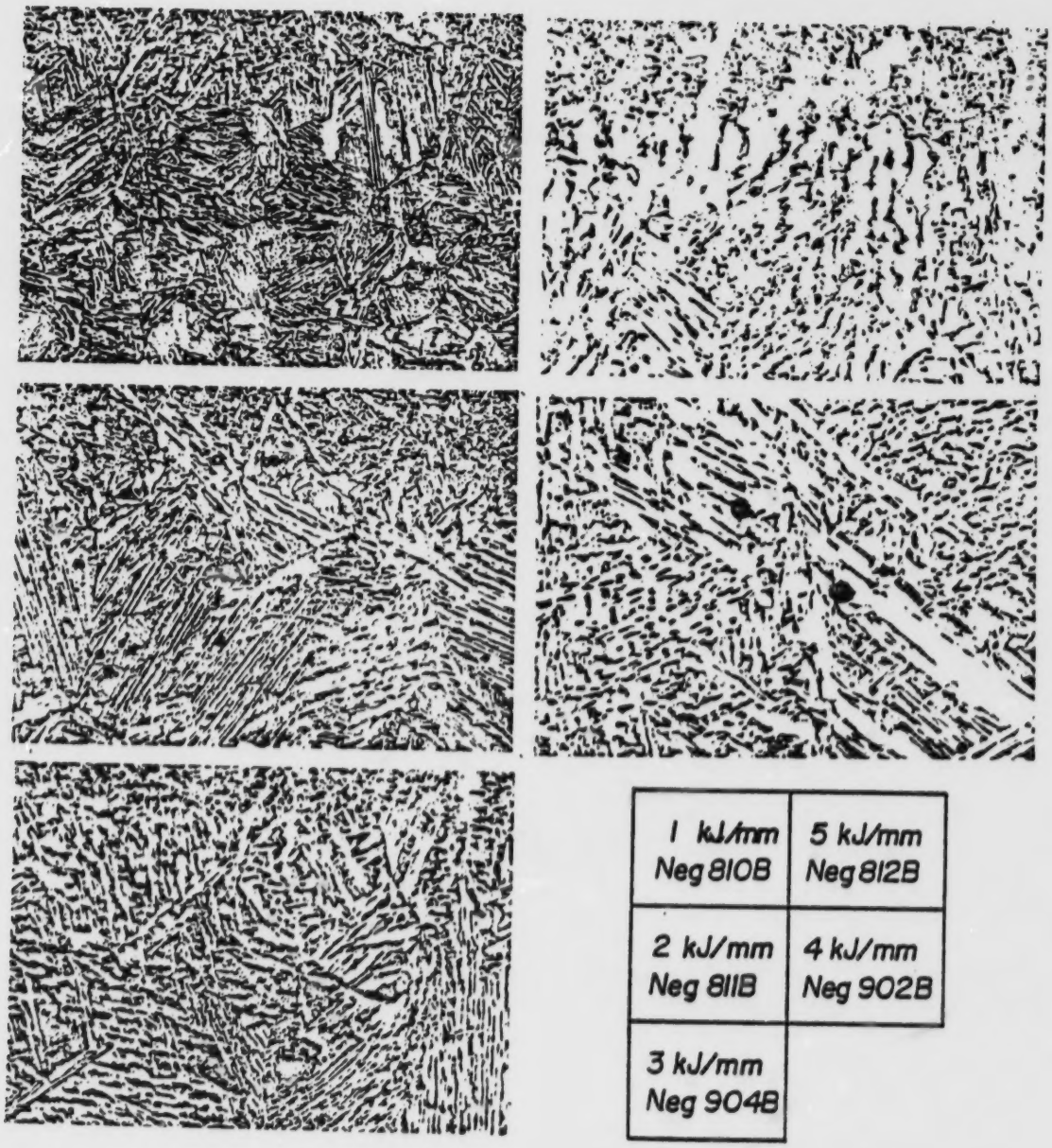

Figure 9. Microstructures from hardening curve weld HAZ's for 25 mm plate. 500 X mag. Counterclockwise from top left: 1, 2, 3, 4 and 5 kJ/mm.

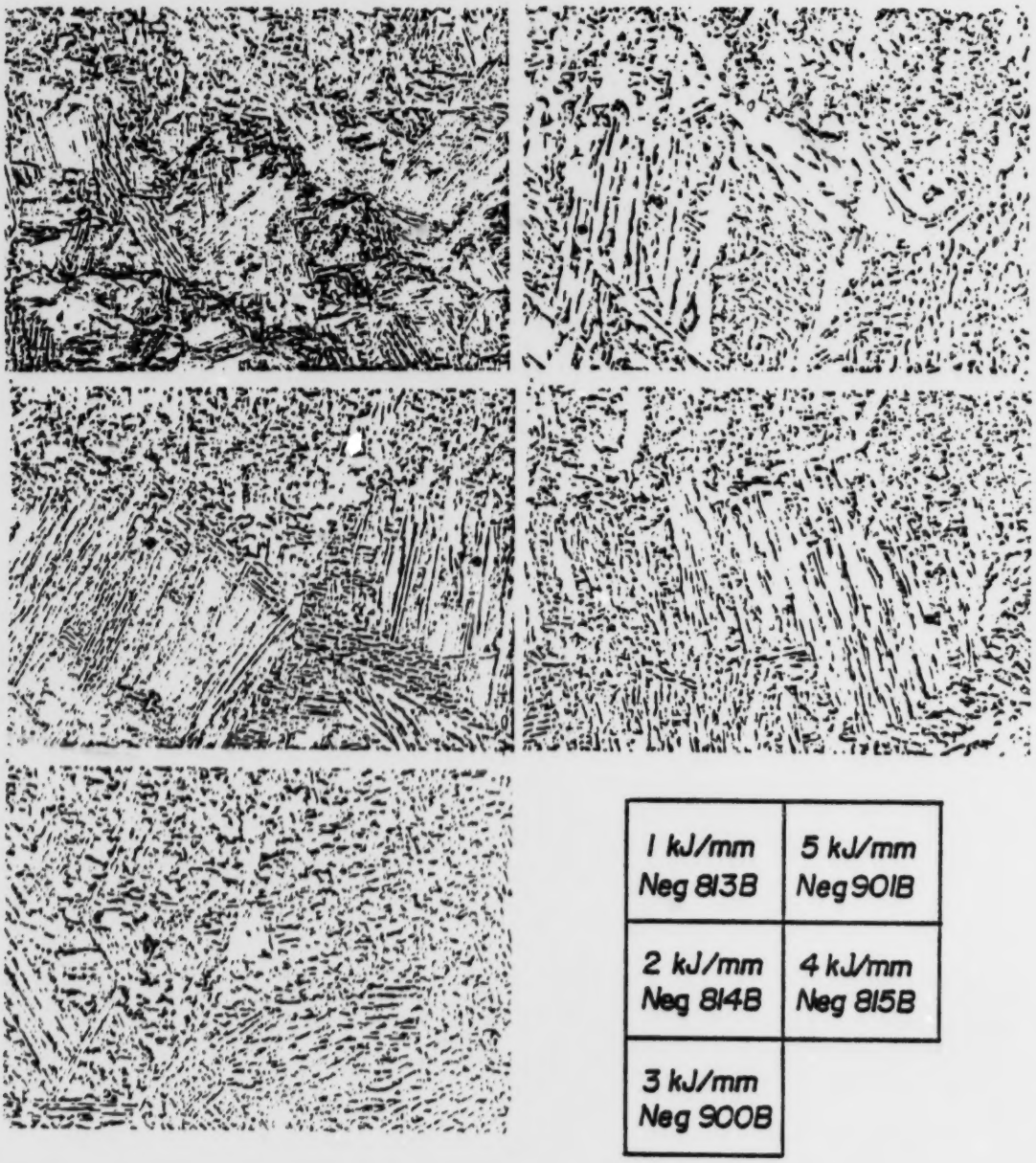

Figure 10. Microstructures from hardening curve weld HAZ's for 50 mm plate. 500 X mag. Counterclockwise from top left: 1, 2, 3, 4 and 5 kJ/mm.

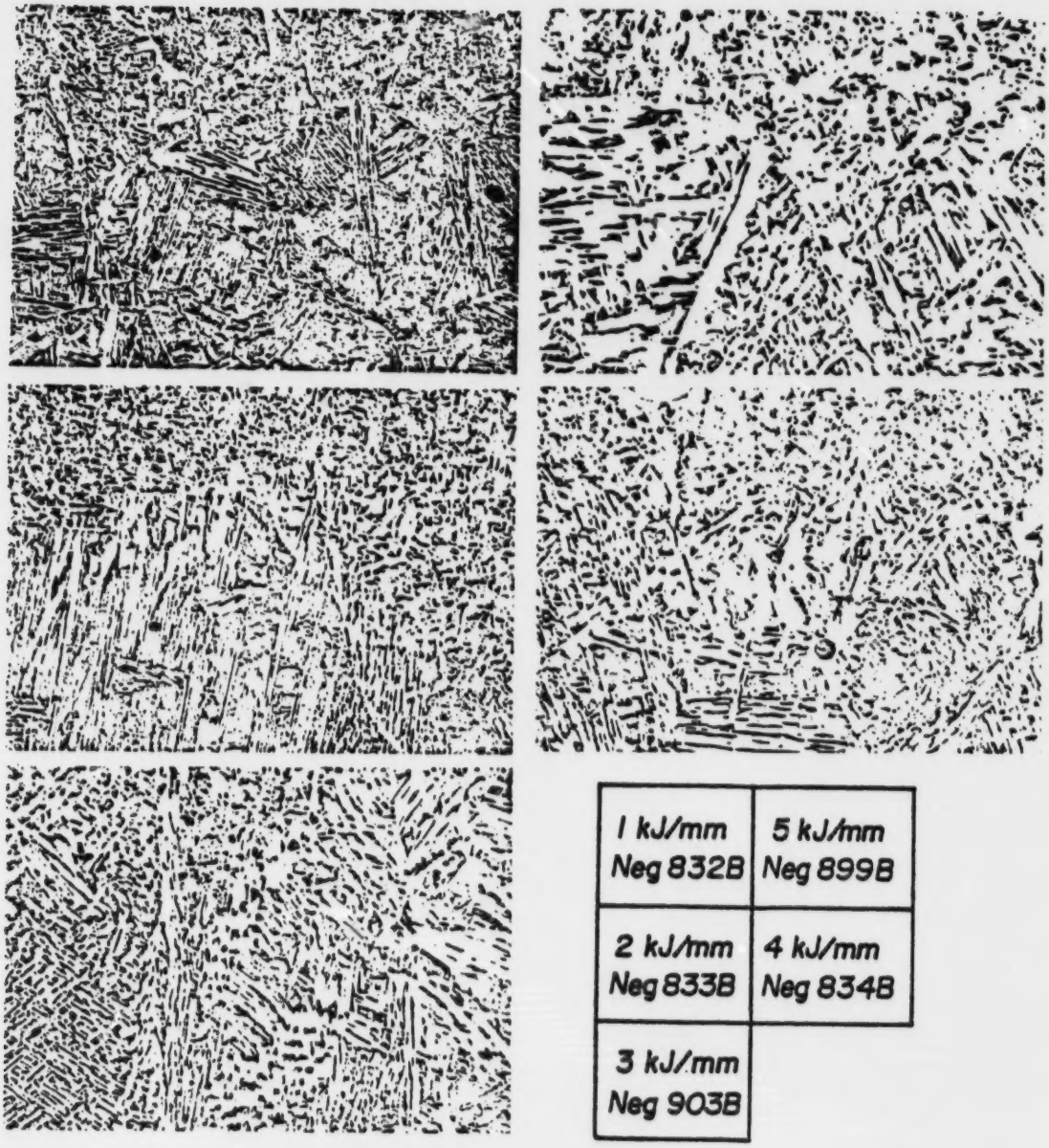

Figure 11. Microstructures from hardening curve weld HAZ's for 75 mm plate 500 X mag. Counterclockwise from top left: 1, 2, 3, 4 and 5 kJ/mm.

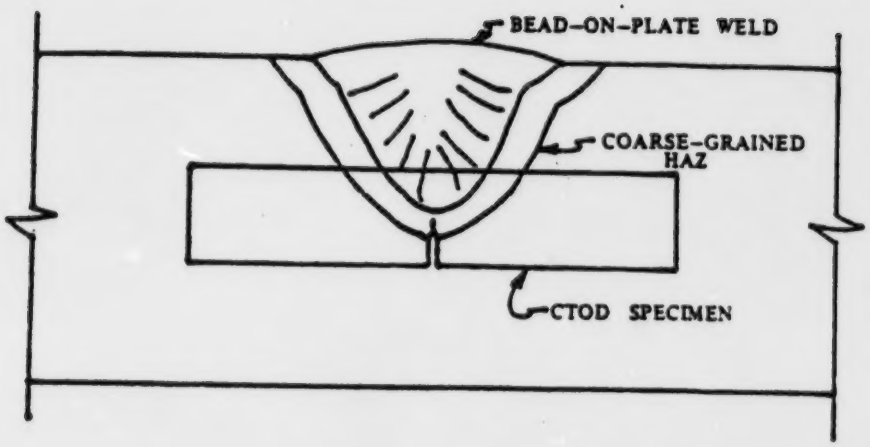

Figure 12. CTOD specimen showing notch and fatigue pre-crack.

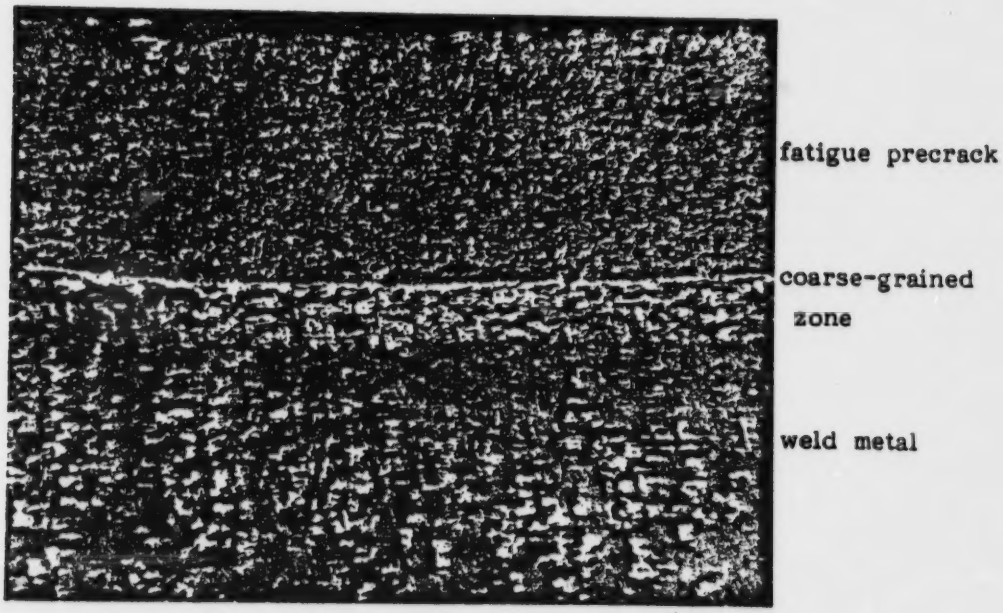

Figure 13. CTOD fracture surface showing fatigue precrack, coarse-grained zone, and columnar weld metal. 18 X, specimen 3A (3), Neg 905B.

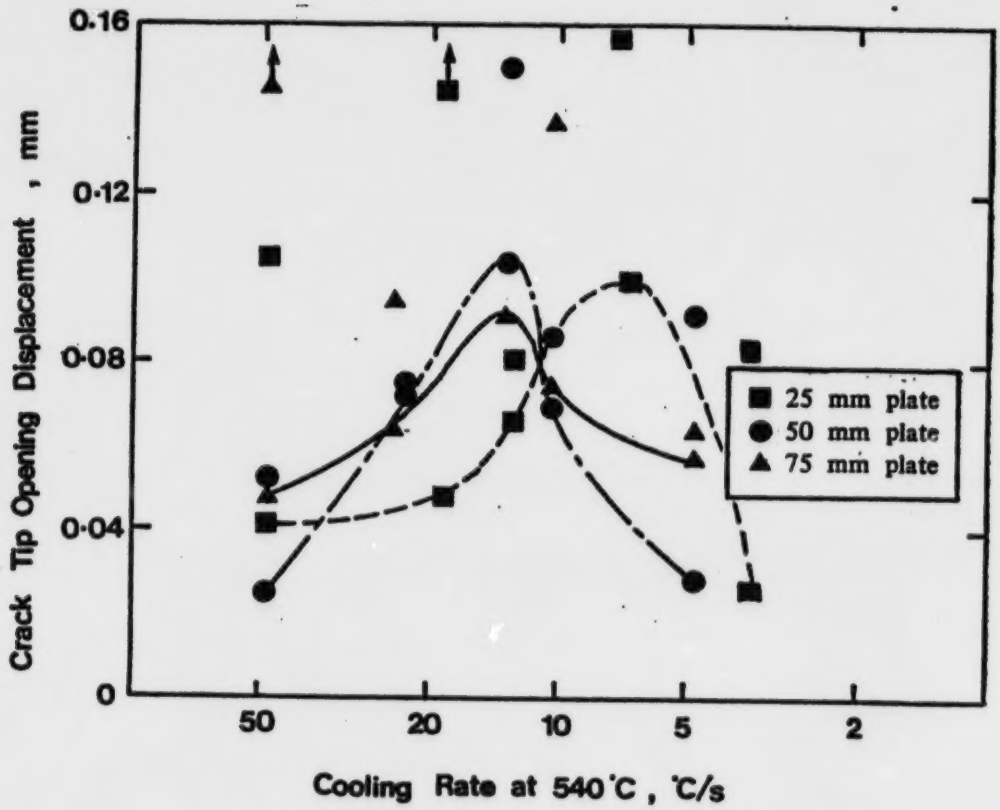

Figure 14. CTOD versus heat input for bead-on-plate welds. All testing conducted at -60°C.

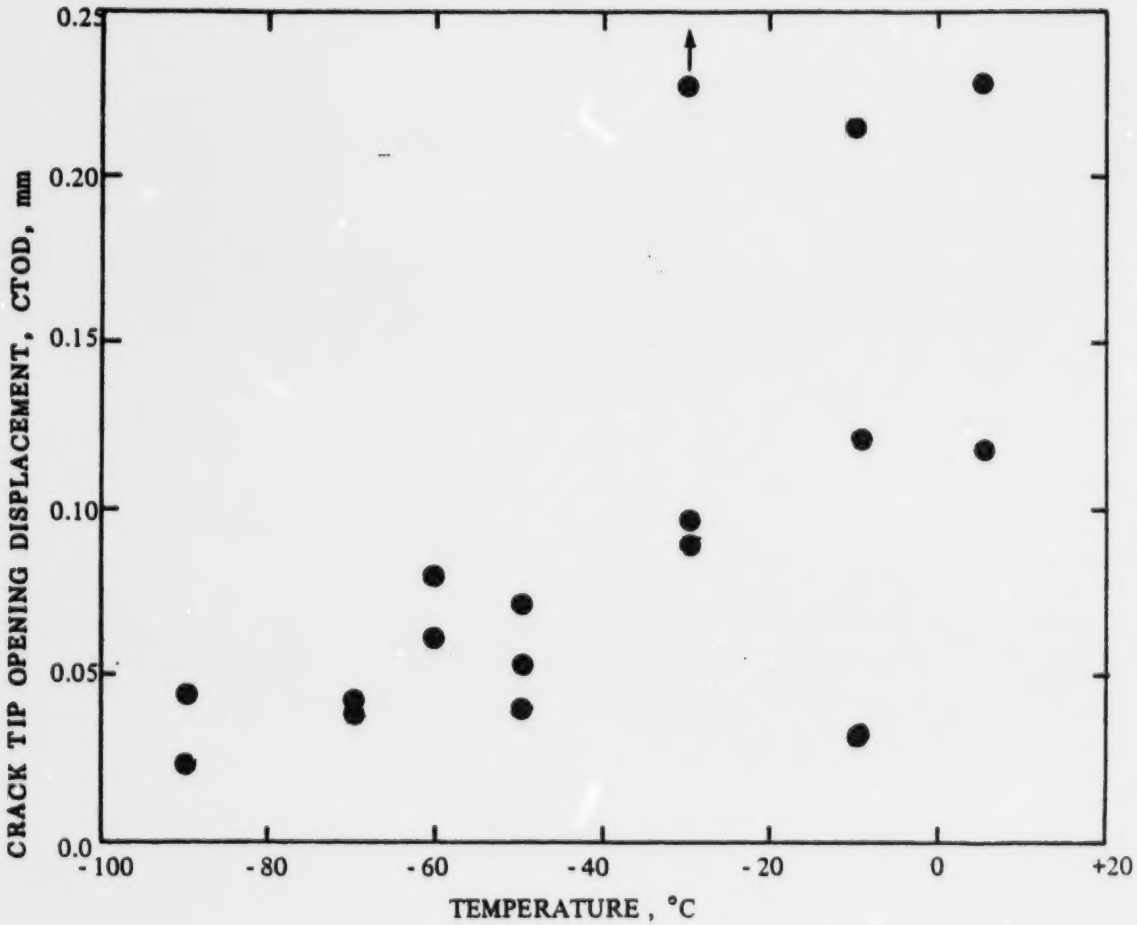

Figure 15. CTOD transition curve for weld 3A, bead-on-plate weld on 25 mm thick plate.

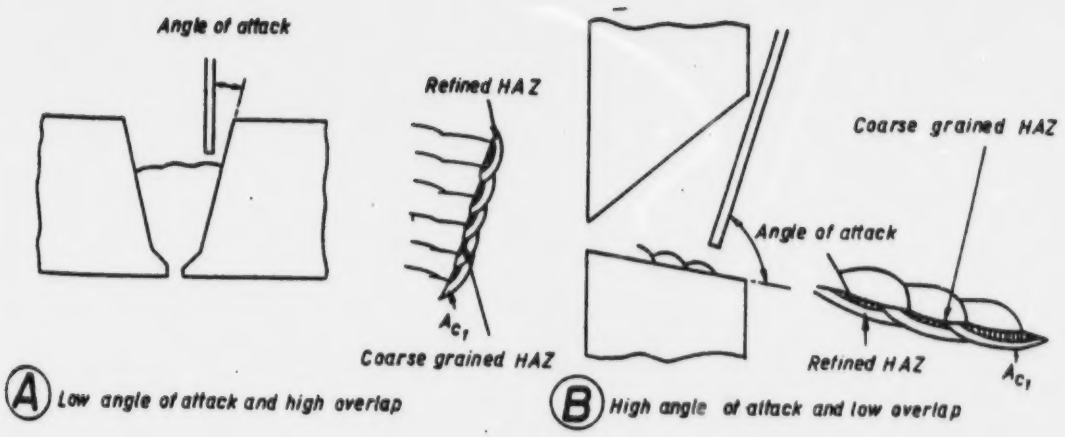
Angle of attack
Refined HAZ
Coarse grained HAZ
Angle of attack
Coarse grained HAZ
Refined HAZ
A Low angle of attack and high overlap
B High angle of attack and low overlap

Figure 16. A - Welding in the flat position, high degree of HAZ refinement: B- welding horizontal, vertical, low degree of HAZ refinement (62).

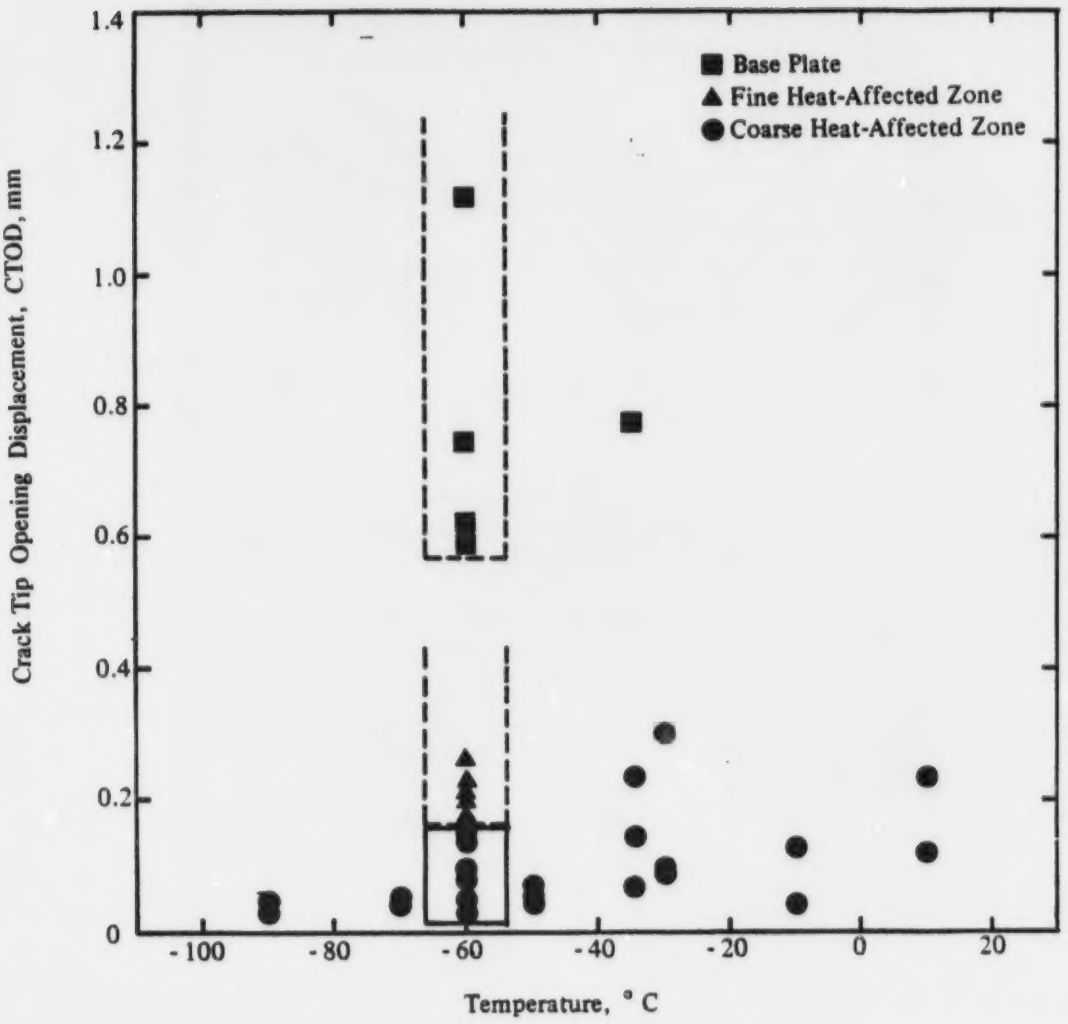

Figure 17. CTOD versus temperature for welds made using a heat input of 3 kJ/mm. Results include tests for bead-on-plate and K-prep welds.

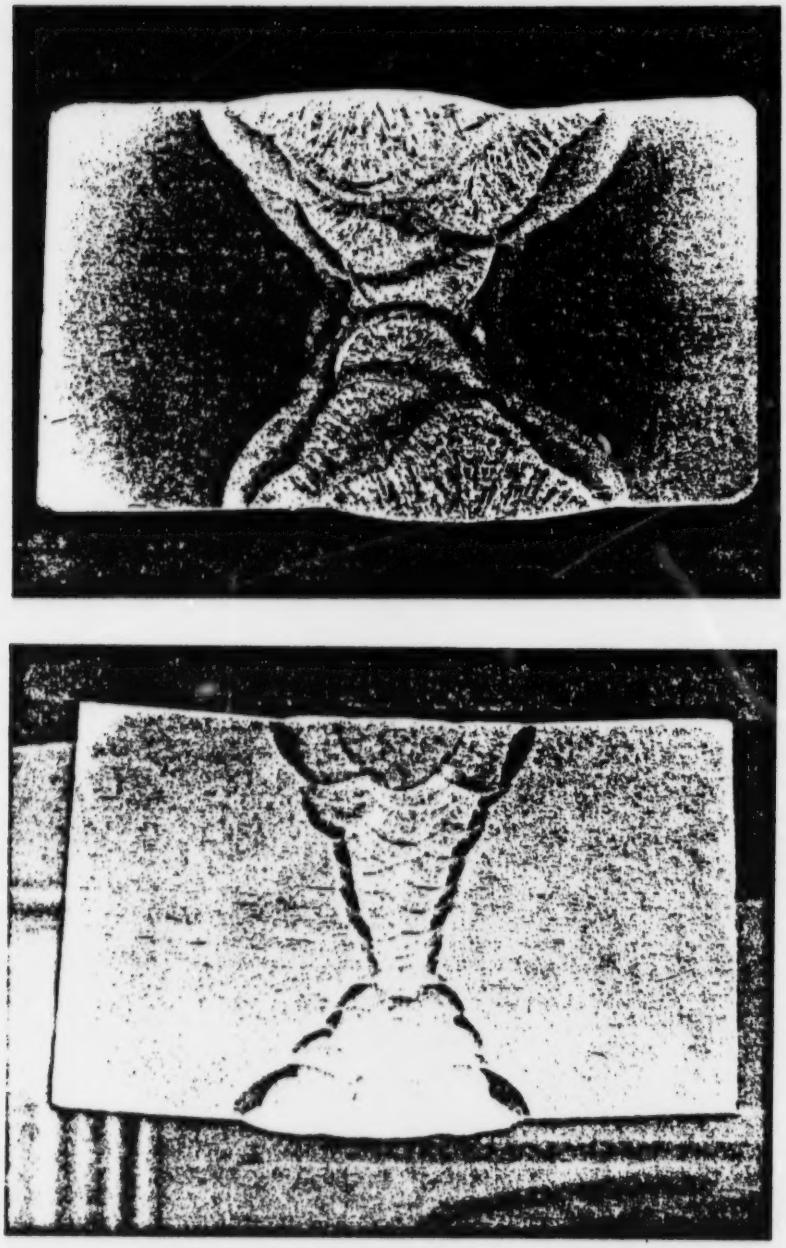

Figure 18. Completed butt weld sections from 25 (Neg 849B) and 75 mm (Neg 894B) plates.

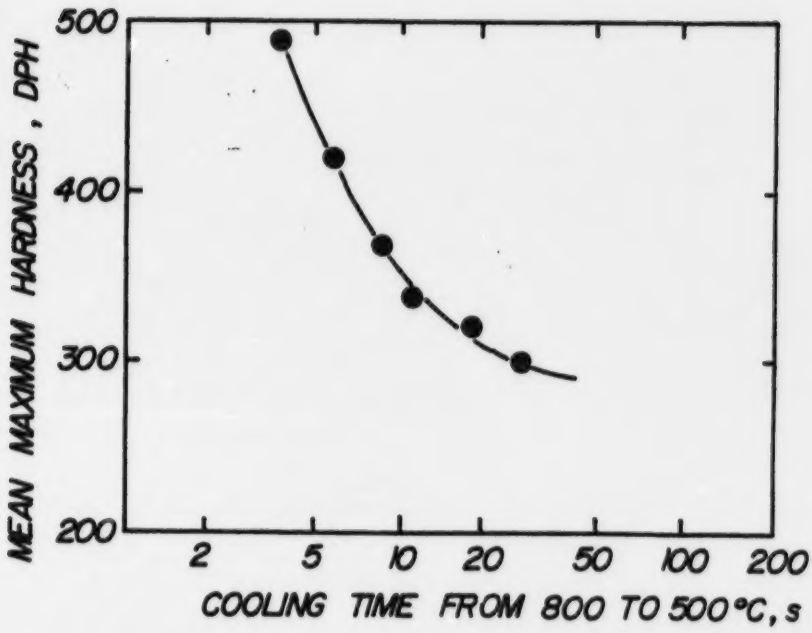

Figure 19. Typical hardening curve for a C-Mn steel.

	C	Mn	Si	Cr	Mo	V	Ni	Cu	Nb
A710	0·06	0·67	0·31	0·91	0·15	—	1·04	1·16	0·04
50E	0·16	1·42	0·30	0·02	—	—		0·03	0·04

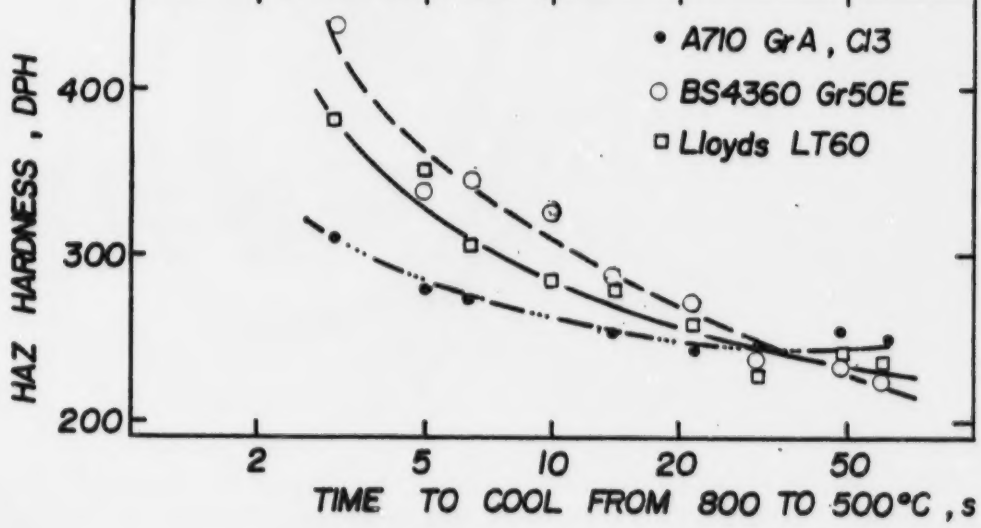

Figure 20. Hardening curve results for A710 Gr A C13, BS4360 Gr 50E, and Lloyds LT60 steels (94).

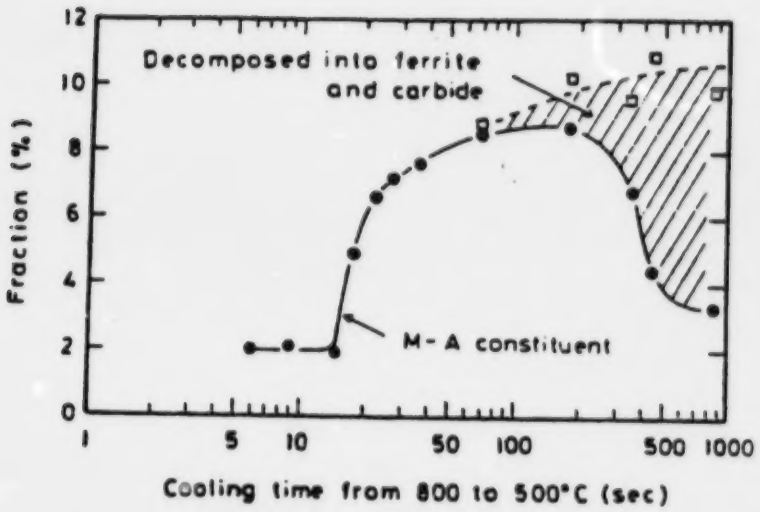

Figure 21. Relation between cooling time and the fraction of M-A constituent (96).

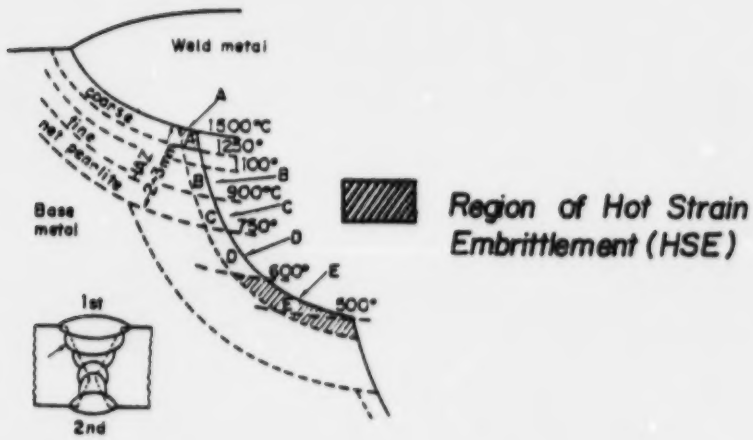

Figure 22. HSE area in multipass weld.

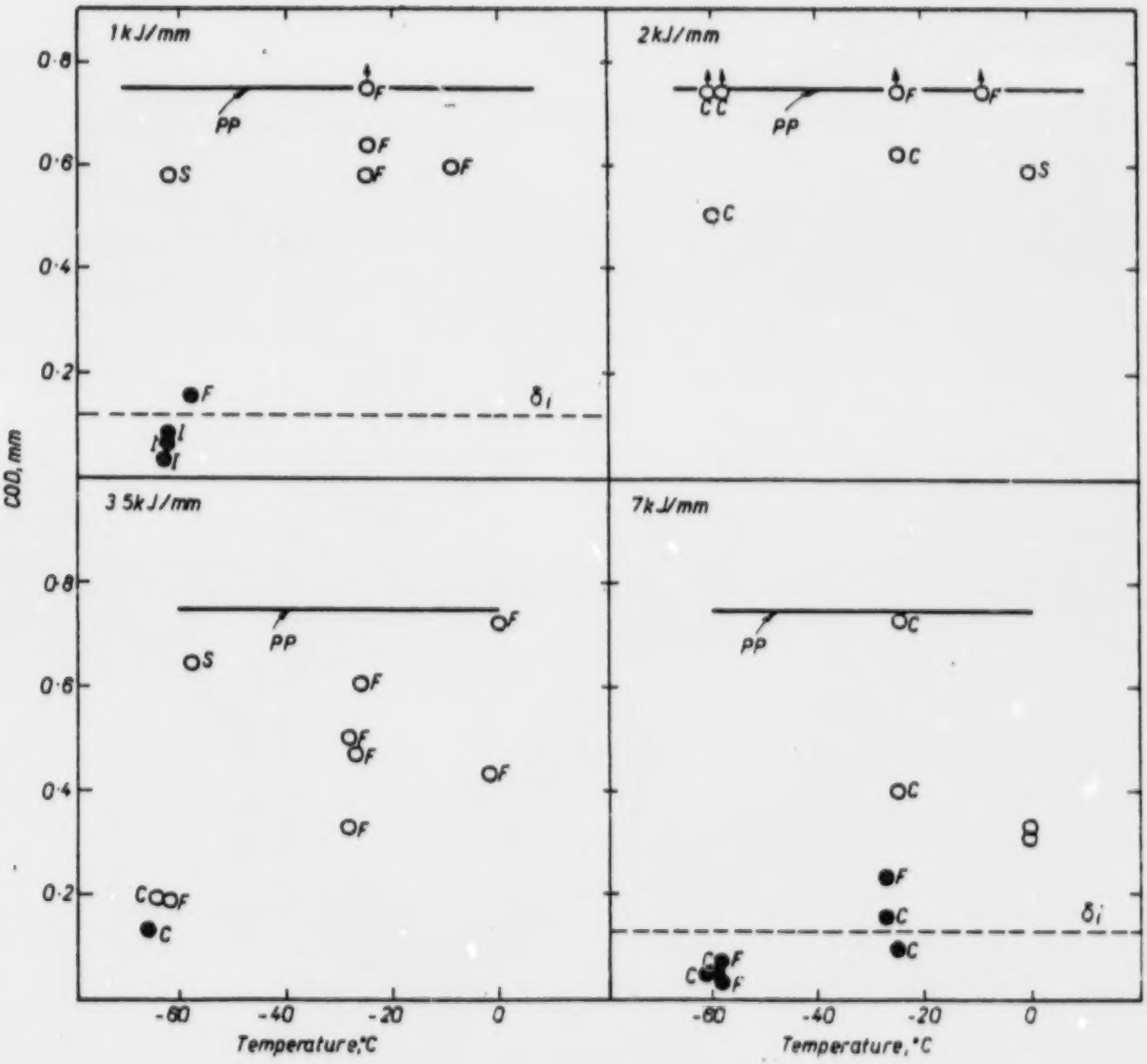

Figure 23. HAZ CTOD data for 0.15C-1.35 Mn-0.07 Nb steel, 25 x 25 mm section specimens. Positions of fatigue crack tip. C - grain coarsened HAZ, F - fine grained HAZ, I - intercritical HAZ, S - subcritical HAZ, PP - parent plate transition curve, ● - unstable fracture, ○ - stable tearing either to maximum load or clip gauge limit, as above but CTOD greater than 0.75 mm, δ_i - CTOD for fracture initiation by tearing.

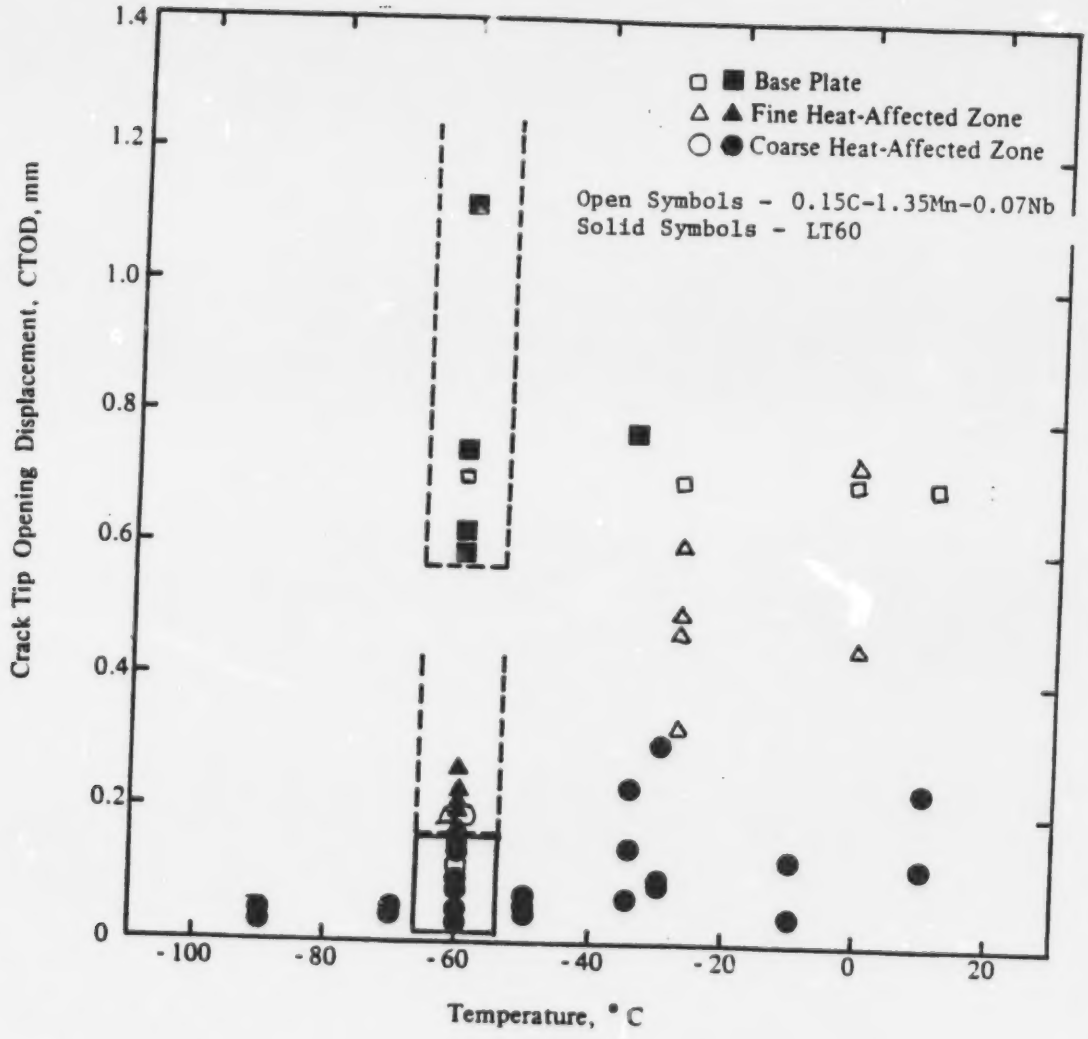

Figure 24. Comparison of CTOD results for LT60 steel and 0.15C - 1.35 Mn - 0.07 Nb steel, welded at 3 kJ/mm.

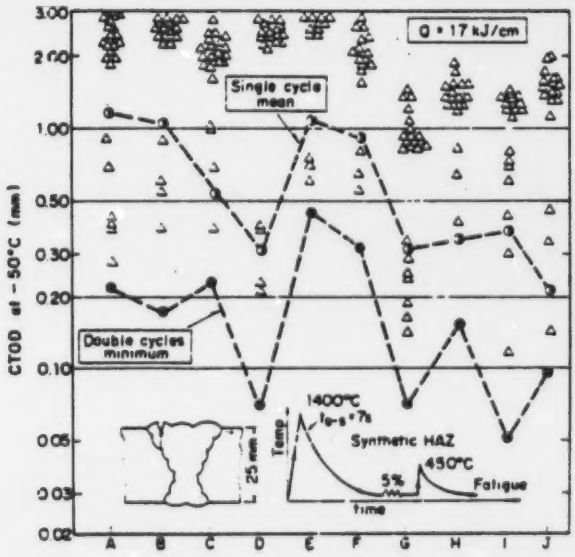

Figure 25. Comparison of critical CTOD values between synthetic HAZ and weld fusion line.

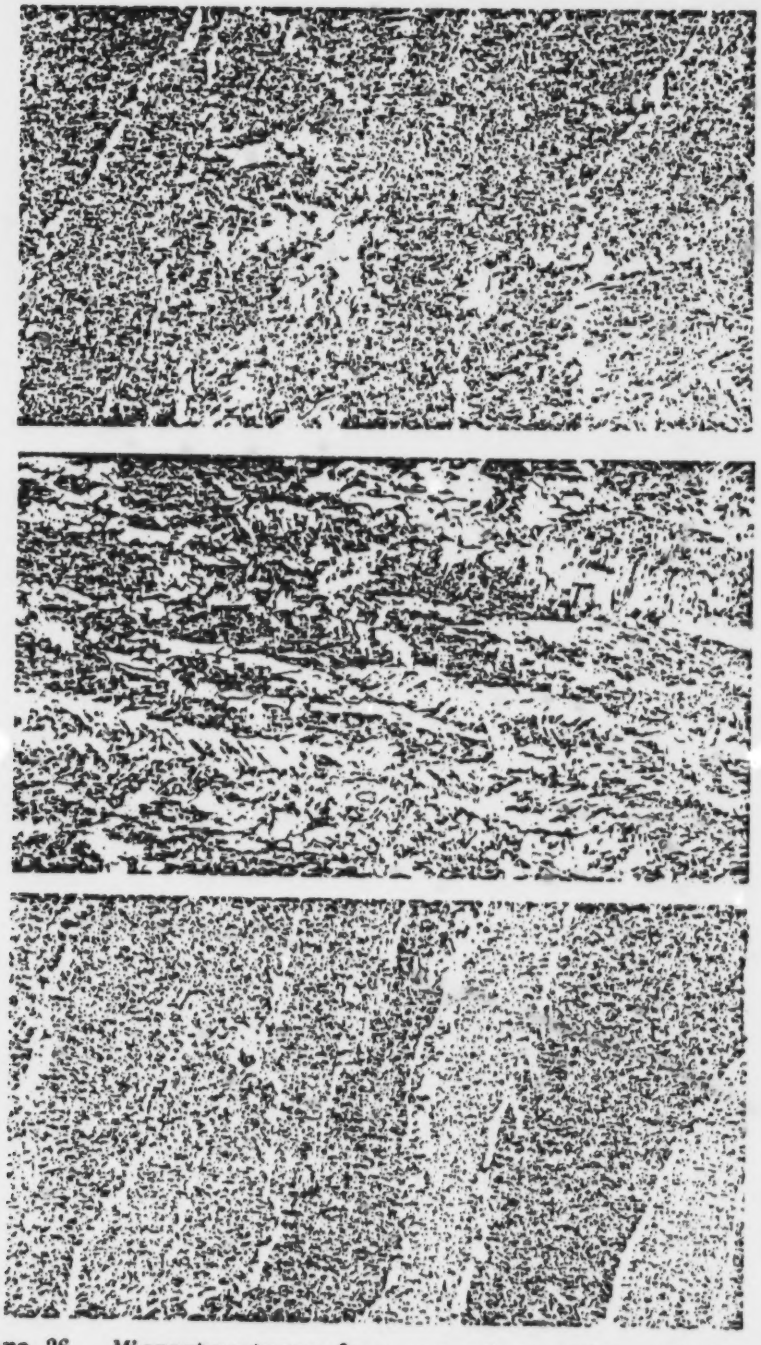

Figure 26. Microstructures from procedure welds, 200 X.
a) top, capping pass of 25 mm weld (Neg 907B).
b) middle, capping pass of 75 mm weld (Neg 908B).
c) bottom, root region of 75 mm weld (Neg 909B).

APPENDIX A

HARDNESS MEASUREMENTS OF HARDENING CURVE WELDS

5 kg Hardness Results - Bead on Plate Specimens

Calibration Test Block 317 VPN 6th July 1983
25 mm Plate

Specimen	1	2	3	4	5	AVG	AVG
1A2	358	338	310	310	341	331	
1A2	358	310	303	310	345	325	329
1A4	371	329	299	296	367	332	
1A4	345	317	304	313	353	326	
2A1	289	280	274	283	301	285	
2A1	296	283	265	276	306	285	
2A3	291	274	265	277	283	278	282
2A3	289	271	270	271	296	279	
3A2	245	260	249	262	260	255	
3A2	262	262	257	255	265	260	
3A4	262	257	257	268	275	264	260
3A4	274	265	260	244	268	262	
4A1	241	240	234	237	230	236	
4A1	239	239	245	246	239	242	
4A3	241	246	233	229	244	240	239
4A3	241	232	241	239	246	240	
5A1	228	225	221	221	226	224	
5A1	218	223	223	228	226	224	
5A3	221	229	229	225	232	224	224
5A3	229	218	225	227	227	225	

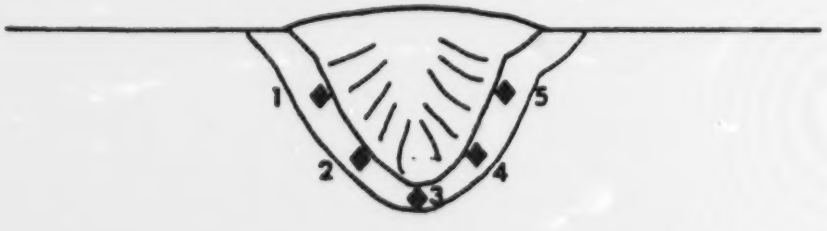

HAZ microspecimens 5A1 (finish side) Micro # H80 Photo 812B
1A4 (finish side) Micro # H81 Photo 810B
2A1 (finish side) Micro # H82 Photo 811B

APPENDIX A (cont'd)

HARDNESS MEASUREMENTS OF HARDENING CURVE WELDS

5 kg Hardness Results - Bead on Plate Specimens

50 mm Plate

Specimen	1	2	3	4	5	AVG	AVG
1B1	341	306	291	330	353	324	
1B1	327	321	299	332	332	322	
1B4	353	313	317	325	334	328	326
1B4	362	325	306	329	334	331	
2B1	296	296	280	283	289	289	
2B1	299	271	277	286	310	289	
2B4	303	283	277	283	293	297	293
2B4	303	281	286	303	313	297	
3B1	271	265	263	272	263	267	
3B1	270	265	252	260	257	261	
3B4	262	257	249	256	271	259	264
3B4	260	254	286	279	268	269	
4B1	254	252	252	249	257	253	
4B1	239	255	286	254	253	257	
4B4	249	249	241	252	252	249	254
4B4	255	255	261	252	268	258	
5B1	229	227	242	224	229	230	
5B1	230	232	232	234	238	231	231
5B4	229	232	237	225	234	231	
5B4	237	232	240	225	229	233	

HAZ Microspecimens 1B1 (start side) micro # H83
2B1 (start side) micro # H84
4B1 (start side) micro # H85

APPENDIX A (cont'd)

HARDNESS MEASUREMENTS OF HARDENING CURVE WELDS

5 kg Hardness Results - Bead on Plate Specimens

75 mm Plate

Specimen	1	2	3	4	5	AVG	AVG
1C2	353	313	310	310	329	323	
1C2	325	321	321	345	329	328	324
1C4	325	310	310	347	341	327	
1C4	325	323	306	313	325	318	
2C1	296	277	280	293	294	288	
2C1	303	287	280	286	283	288	287
2C3	303	268	277	283	293	285	
2C3	310	271	280	286	299	289	
3C2	265	262	265	262	265	264	
3C2	265	265	257	263	260	262	263
3C4	265	265	252	257	263	260	
3C4	263	252	262	268	268	263	
4C1	246	249	265	252	257	253	
4C1	260	257	254	252	252	255	251
4C3	249	254	240	245	265	251	
4C3	246	249	241	247	247	246	
5C1	239	233	232	229	234	233	
5C1	232	229	225	227	223	227	228
5C3	223	227	227	223	229	225	
5C3	218	229	227	227	227	225	

HAZ Microstructure 1C2 - Micro H89
2C1 - Micro H90
4C1 - Micro H91

APPENDIX B
CTOD ANALYSIS AND RESULTS

The various types of load-displacement diagrams obtained in CTOD testing are shown in Figure B1. The CTOD values are calculated for the critical events which are defined as:

1. First occurrence of pop-in or brittle fracture.
2. First attainment of maximum load.
3. Initiation of crack extension by ductile tearing.

The equation for calculating the CTOD given in BS5762:1979 is compatible with both elastic and elastic-plastic analysis. The analysis given by Pisarski and Dawes (103) is quoted below for analysis of the curves. The load is used to estimate a stress intensity factor, K, which in turn is used to estimate an elastic component of crack opening displacement. An additive plastic component of the CTOD is then calculated from the plastic component of clip gauge displacement. This calculation assumes that there is a point, 0.4 (W-a) ahead of the crack tip, which the hinge position approaches asymptotically at collapse of the specimen.

The crack tip CTOD in BS5762 is given by:

$$\delta_c,\ \delta_u,\ \delta_i,\ \delta_m = \frac{K^2(1-\nu 2)}{2\sigma_y E} + \frac{0.4(W-a)V_p}{0.4W + 0.6a + z}$$

where

δ_c = COD at unstable fracture or pop-in not preceded by tearing

δ_u = COD at unstable fracture or pop-in but preceded by tearing

δ_i = COD at the first attainment of a maximum load plateau not preceded by pop-in.

K = stress intensity factor calculated from the load P, relevant to the above events

$K = \frac{YP}{BW^{0.5}}$, where $Y = f(a/W)$

V_p is the plastic component of clip gauge opening displacement.

In the above equation 'a' is the average crack length measured at positions 25, 50 and 75% B along the crack front.

APPENDIX B
to Welding Institute of Canada Report RC142
RESULTS FROM CTOD TESTING OF BEAD-ON-PLATE WELDS

Sample	Test Temperature, °C	a, mm	W, mm	a/w	B, mm	CTOD, mm
1A1	-60	3.45	6.02	0.573	5.99	δ_u=0.041
1A3	-60	3.00	5.99	0.501	5.99	δ_u=0.104
2A2	-60	3.78	7.52	0.503	7.52	δ_m=0.203
2A4	-60	3.94	7.49	0.525	7.52	δ_u=0.048
3A(3)	5	3.69	7.49	0.493	7.47	δ_m=0.234
3A(13)	5	4.47	7.54	0.593	7.52	δ_m=0.119
3A(12)	-10	3.87	7.49	0.517	7.49	δ_u=0.041
3A(14)	-10	2.89	7.54	0.383	7.49	δ_u=0.218
3A(15)	-10	4.40	7.52	0.585	7.52	δ_u=0.124
3A(1)	-30	4.09	7.49	0.546	7.49	δ_u=0.091
3A(4)	-30	3.45	7.49	0.461	7.47	δ_m=0.300
3A(9)	-30	4.37	7.54	0.580	7.49	δ_m=0.097
3A(2)	-50	4.15	7.49	0.554	7.49	δ_u=0.0711
3A(5)	-50	4.03	7.49	0.538	7.47	δ_u=0.041
3A(7)	-50	4.07	7.49	0.543	7.49	δ_u=0.053
3A1	-60	4.09	7.47	0.548	7.49	δ_u=0.066
3A3	-60	3.76	7.49	0.502	7.49	δ_u=0.081
3A(6)	-70	3.78	7.49	0.505	7.47	δ_u=0.043
3A(8)	-70	3.66	7.49	0.489	7.49	δ_u=0.041
3A(10)	-90	3.57	7.49	0.477	7.49	δ_c=0.023
3A(11)	-90	3.64	7.49	0.486	7.49	δ_u=0.046
4A2	-60	3.81	7.49	0.509	7.49	δ_u=0.160
4A4	-60	3.89	7.49	0.519	7.52	δ_u=0.099
5A2	-60	2.57	7.49	0.343	7.49	δ_u=0.076
5A4	-60	3.91	7.49	0.522	7.47	$\delta_{u/c}$=0.026
1B2	-60	3.45	5.99	0.577	5.99	δ_u=0.052
1B3	-60	3.40	5.99	0.568	5.99	δ_u=0.025
2B2	-60	3.30	7.49	0.441	7.52	δ_u=0.071
2B3	-60	3.38	7.49	0.451	7.49	δ_u=0.074
3B2	-60	3.71	7.49	0.495	7.49	δ_u=0.150
3B3	-60	3.15	7.49	0.421	7.49	δ_u=0.104
4B2	-60	3.23	7.49	0.431	7.49	δ_u=0.069
4B3	-60	3.12	7.49	0.417	7.49	δ_u=0.086
5B2	-60	2.84	7.49	0.38-0	7.49	δ_u=0.091
5B3	-60	3.51	7.49	0.468	7.49	δ_u=0.028
1C1	-60	3.12	5.99	0.522	5.99	δ_u=0.048
1C3	-60	2.06	5.99	0.343	5.97	δ_u=0.175
2C2	-60	3.81	7.49	0.509	7.49	δ_u=0.064
2C4	-60	3.89	7.49	0.519	7.49	δ_m=0.094
3C3	-60	3.33	7.49	0.444	7.49	δ_c=0.091
4C2	-60	3.78	7.49	0.505	7.49	δ_u=0.137
4C4	-60	3.40	7.49	0.454	7.49	δ_u=0.074
5C2	-60	3.40	7.49	0.454	7.49	δ_u=0.064
5C4	-60	3.58	7.49	0.478	7.49	δ_u=0.058

Notes:
1. Sample numbers are as follows;
   heat inputs are identified first as nominally 1-5 kJ/mm plate thickness as letter designations - A, 25 mm; B, 50mm; C, 75 mm
   final number refers to section number
2. Brackets identify specimen numbers for 3 kJ/mm transition curve CTOD samples

APPENDIX B
to Welding Institute of Canada Report RC142
RESULTS FROM CTOD TESTING OF K-PREP WELDS

Sample	Specimen	Temp °C	a, mm	W, mm	a/w	B, mm	CTOD, mm
A7	t x 2t	-10	24.511	49.911	0.491	28.346	δ_m=0.716
A5	t x 2t	-35	24.790	49.911	0.497	28.169	δ_u=0.142
A11	t x 2t	-35	24.663	49.936	0.494	28.245	δ_u=0.234
A1	t x 2t	-60	24.359	50.013	0.487	28.042	δ_u=0.145
A3	t x 2t	-60	25.857	49.911	0.518	28.092	δ_u=0.066
A9	t x 2t	-60	25.298	49.911	0.507	28.372	δ_u=0.086
A2	t x t C	-60	12.624	28.169	0.448	24.994	δ_u=0.076
A8	t x t C	-35	12.090	28.397	0.426	24.968	δ_c=0.772
A4	t x t C	-60	12.116	28.067	0.432	24.943	δ_u=0.076
A6	t x t C	-60	11.989	27.94	0.429	24.968	δ_u=0.064
A10	t x t F	-60	11.786	28.245	0.417	24.968	δ_u=0.210
A12	t x t F	-60	10.566	28.067	0.376	24.968	δ_m=0.716
B1	t x t F	-60	21.438	51.994	0.412	50.013	$\delta_{u/c}$=0.036
B2	t x t F	-60	20.422	51.857	0.394	50.038	δ_c=0.008
B3	t x t F	-60	20.752	51.740	0.401	50.038	δ_c=0.005
B4	t x t C	-60	17.805	51.613	0.345	50.063	δ_u=0.066
B5	t x t C	-60	18.771	51.816	0.362	50.013	δ_u=0.201
B6	t x t C	-60	20.041	51.994	0.385	50.038	δ_c=0.013
C1	t x t F	-60	39.370	77.876	0.326	75.590	$\delta_{u/c}$=0.066
C3	t x t F	-60	37.338	78.384	0.476	70.155	δ_u=0.262
C5	t x t F	-60	37.346	78.054	0.485	72.263	δ_u=0.081
C2	t x t C	-60	37.338	78.232	0.477	71.069	$\delta_{u/c}$=0.076
C4	t x t C	-60	37.846	78.181	0.484	71.831	δ_c=0.033
C6	t x t C	-60	40.386	78.511	0.514	75.032	δ_c=0.028
25 mm plate 1	t x 2t	-60	28.931	57.531	0.503	28.092	δ_m=1.118
25 mm plate 2	t x 2t	-60	29.007	57.455	0.505	28.118	δ_u=0.620
75 mm plate 5	t x t	-60	39.370	78.740	0.500	78.029	δ_u=0.749
75 mm plate 6	t x t	-60	40.640	81.153	0.501	77.978	δ_c=0.595

Notes: 1 Letters refer to plate thickness: A, 25 mm; B, 50 mm; C, 75 mm, corresponding numbers identify specimen numbering
2 25 mm and 75 mm results listed above are for parent plate CTOD specimens.

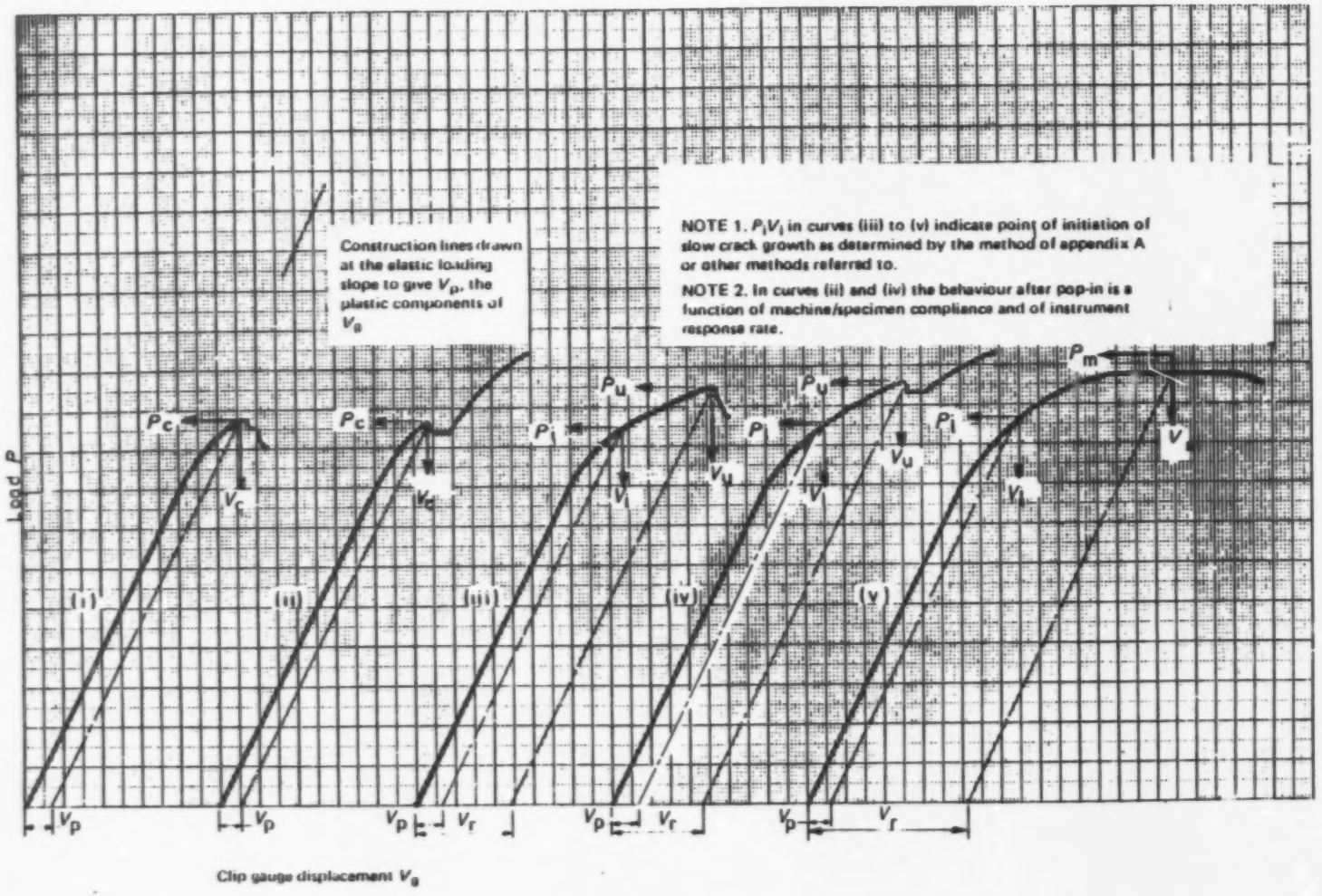
Construction lines drawn at the elastic loading slope to give V_p, the plastic components of V_g
NOTE 1. $P_i V_i$ in curves (iii) to (v) indicate point of initiation of slow crack growth as determined by the method of appendix A or other methods referred to.
NOTE 2. In curves (ii) and (iv) the behaviour after pop-in is a function of machine/specimen compliance and of instrument response rate.
Load P
P_c
P_u
P_i
P_m
V_c
V_u
V_i
V_m
(i)
(ii)
(iii)
(iv)
(v)
V_p
V_r
Clip gauge displacement V_g

Figure B1. Types of load clip gauge displacement graphs for calculation of CTOD.

Job # PC142

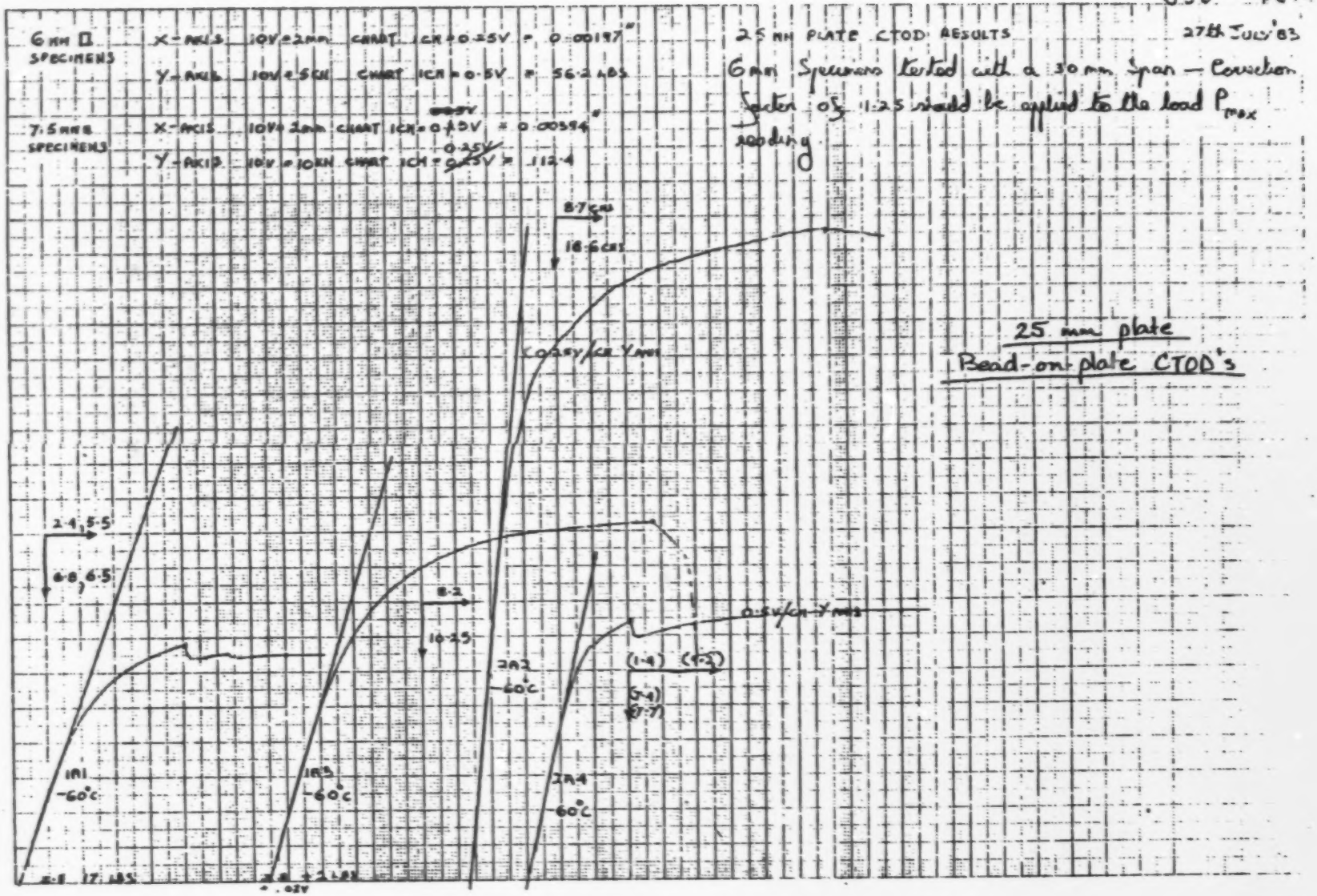
6 mm □ SPECIMENS
X-AXIS 10V = 2mm CHART 1CH = 0.5V = 0.0019"
Y-AXIS 10V = 5KN CHART 1CH = 0.5V = 56.2 LBS
7.5 mm □ SPECIMENS
X-AXIS 10V = 2mm CHART 1CH = 0.1DV = 0.00594"
Y-AXIS 10V = 10KN CHART 1CH = 0.25V = 112.4
25 mm PLATE CTOD RESULTS
27th JULY '83
6 mm Specimens tested with a 30 mm Span — Correction factor of 1.25 should be applied to the load P_{max}
Loading
8.7 cm
18.6 cms
0.5 v/cm Y axis
25 mm plate
Bead-on-plate CTOD's
2.1
5.5
6.8, 6.5
8.2
10.25
0.5 v/cm Y axis
(1.4) (1.2)
(5.4)
(7.7)
2A1
-60°C
2A2
-60°C
2A3
-60°C
2A4
-60°C
.02V

Job # PC 142

27th June '83

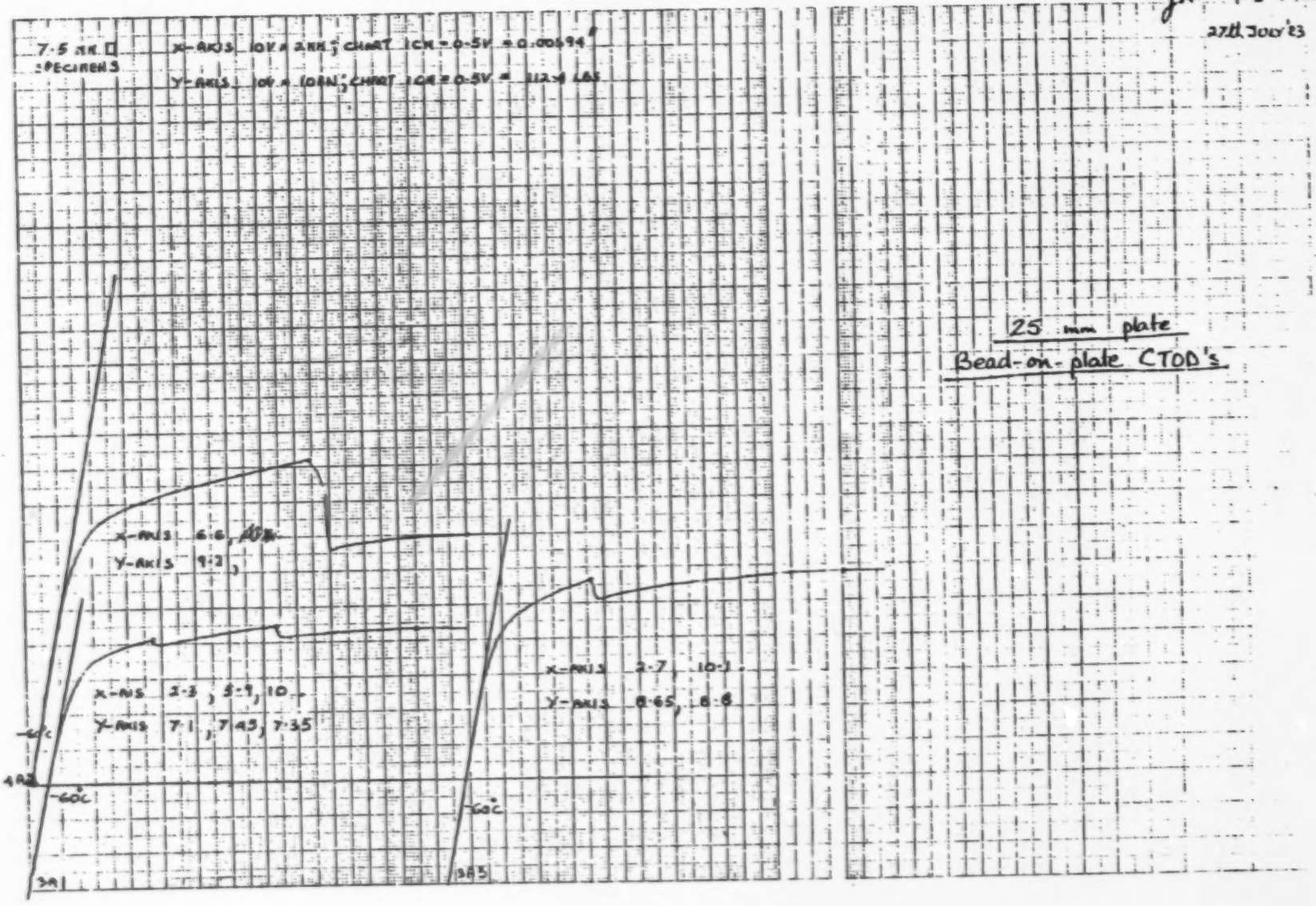

25 mm plate

Bead-on-plate CTOD's

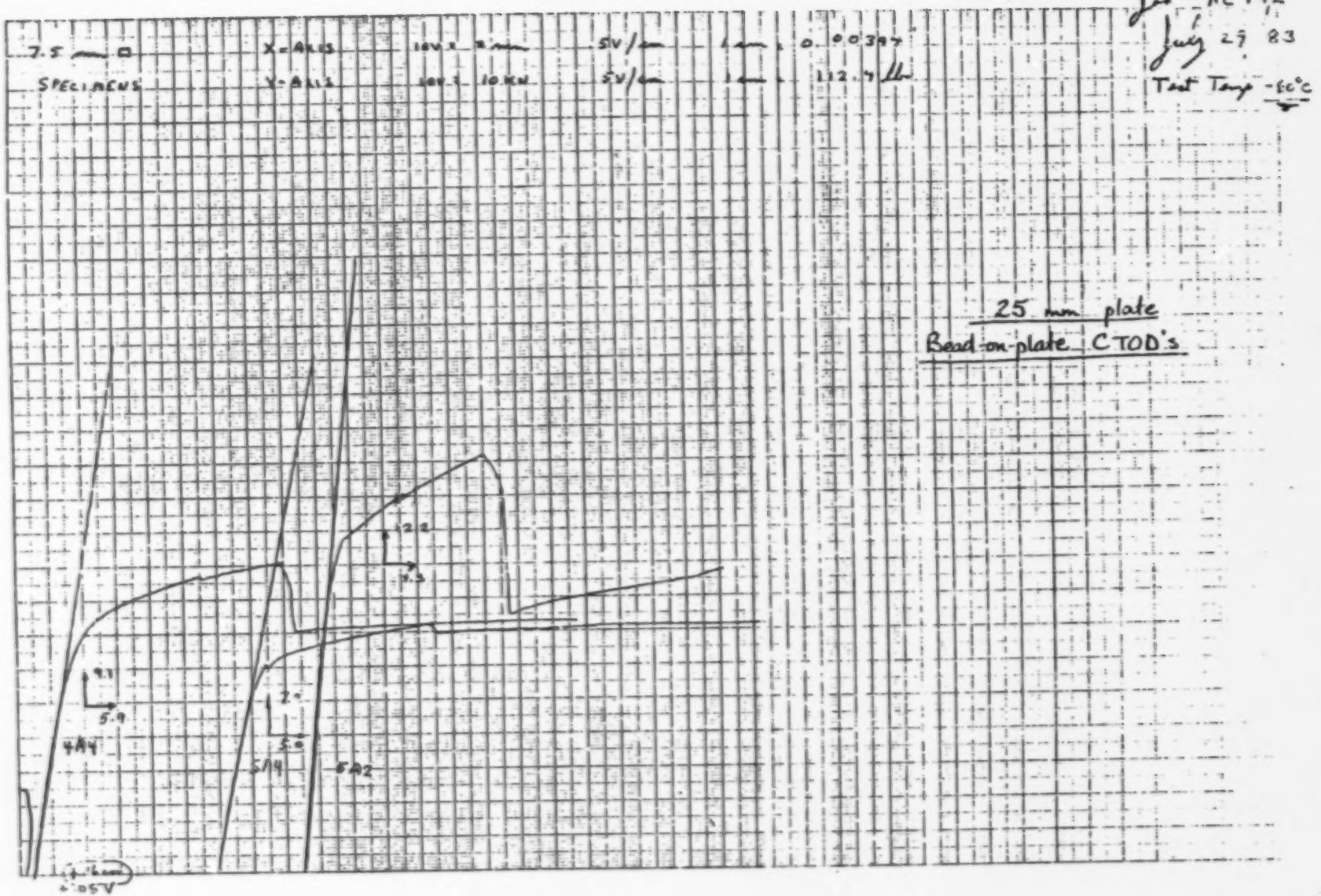
7.5 — □
SPECIMENS
X-AXIS
Y-AXIS
10V/cm
10V/cm
10 KN
5V/cm
5V/cm
0.00397
132.7 lbs
Test Temp -60°C
25 mm plate
Bead-on-plate CTOD's
12.2
7.3
9.1
5.9
4A4
5A4
5A2

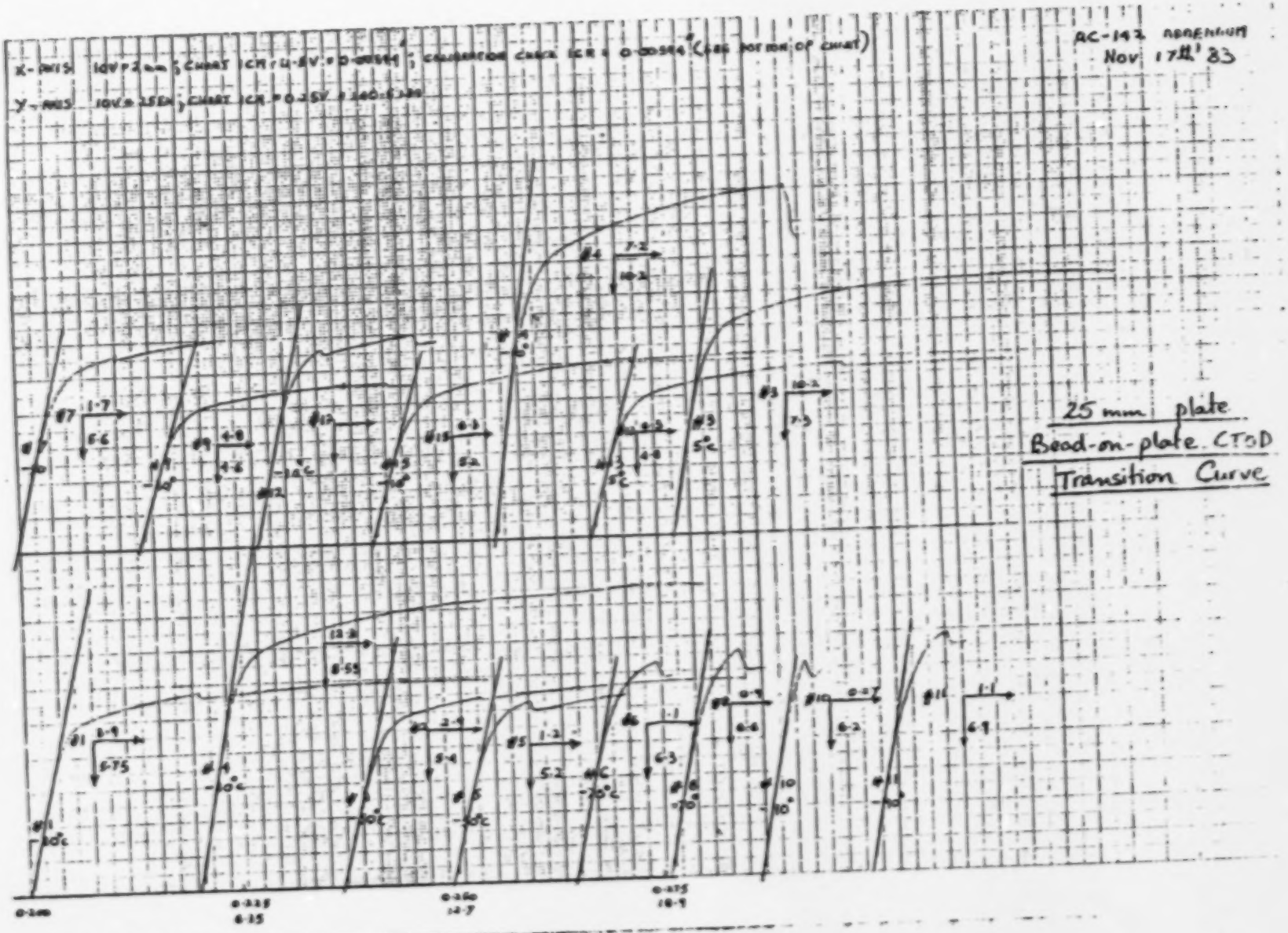
AC-143 ARGENTINIUM
Nov 17th '83
25 mm plate
Bead-on-plate CTOD
Transition Curve

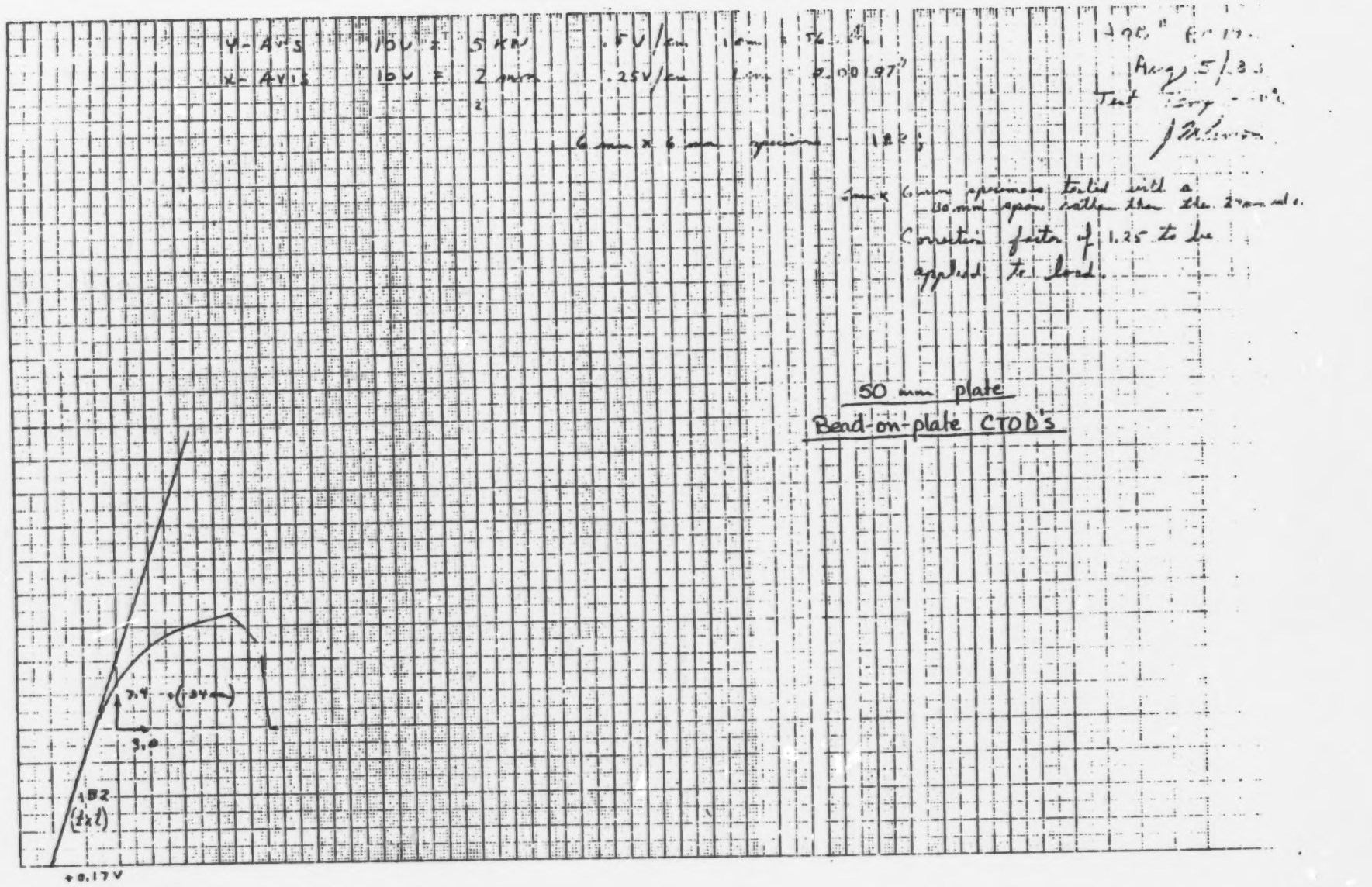
Y-Axis 10V = 5 KN .5V/cm 1 cm = 5%
X-Axis 10V = 2 mm .25V/cm 1 cm = 0.00 97"
6 mm x 6 mm specimen
5 mm x 6 mm specimen tested with a 150 mm span rather than the 24 mm std.
Correction factor of 1.25 to be applied to load.
50 mm plate
Bend-on-plate CTOD's
7.9
(.34")
3.0
1.82
(1x1)
+0.17V

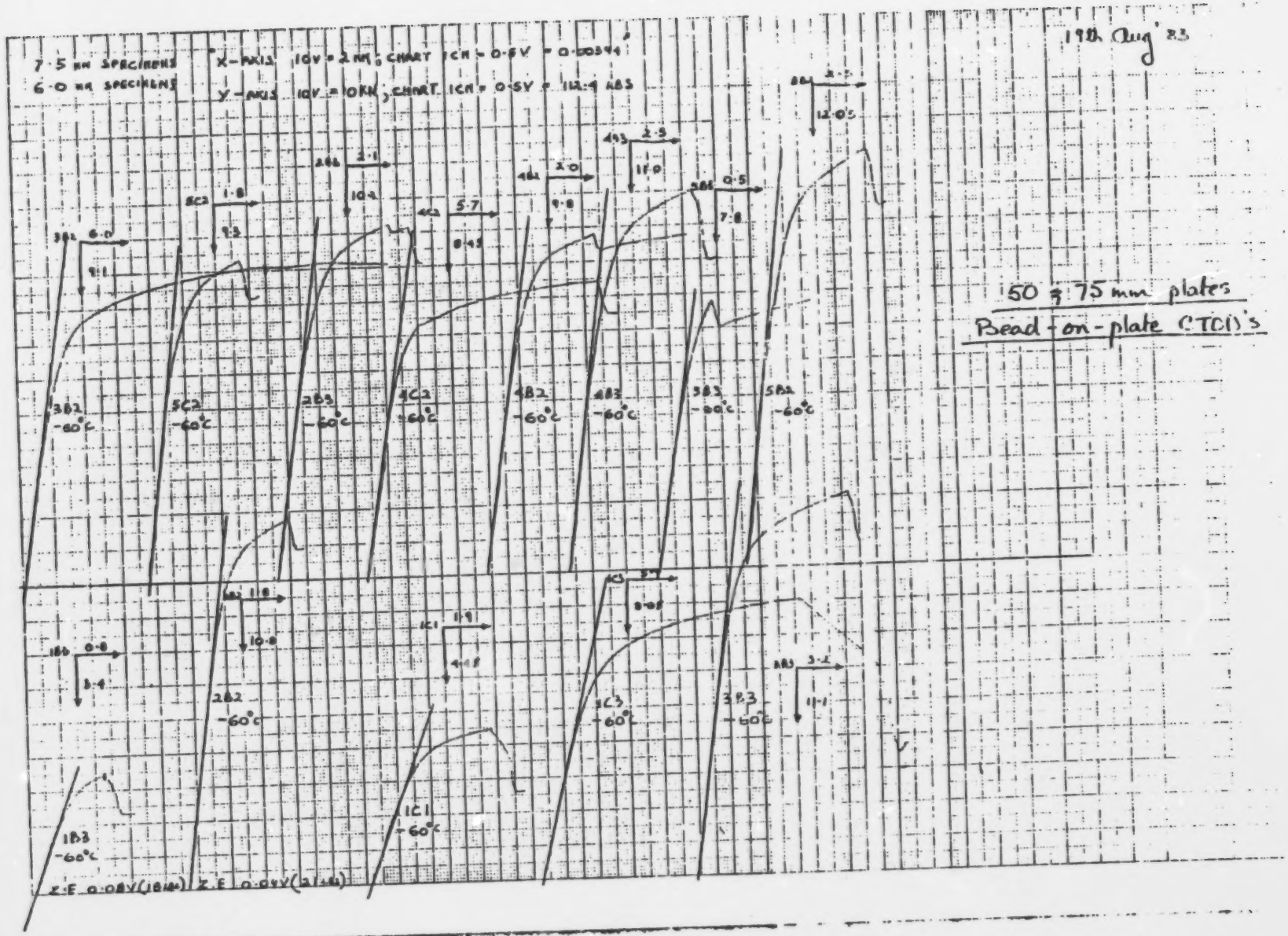
7·5 mm SPECIMENS
6·0 mm SPECIMENS
X-AXIS 10V = 2 mm; CHART 1CM = 0·5V = 0·0034"
Y-AXIS 10V = 10KN; CHART 1CM = 0·5V = 112·9 ABS
19th Aug' 83
50 & 75 mm plates
Bead-on-plate CTOD's
3B2 -60°C
5C2 -60°C
2B3 -60°C
4C2 -60°C
4B2 -60°C
4B3 -60°C
5B3 -60°C
5B2 -60°C
1B3 -60°C
2B2 -60°C
1C1 -60°C
3C3 -60°C
3B3 -60°C
Z.E 0·08V(18mm)
Z.E 0·04V(21·6)

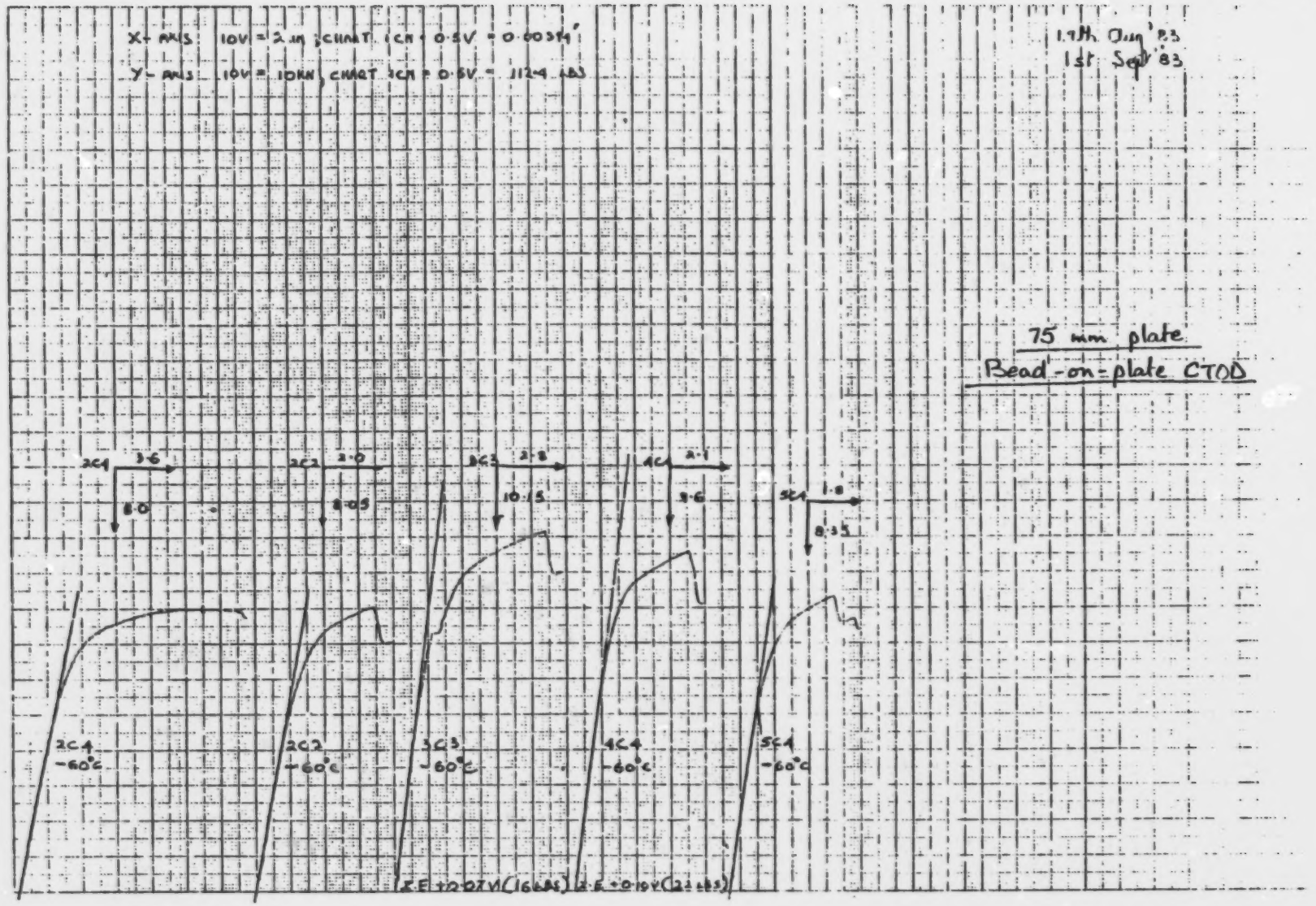
X+ AXIS: 10V = 2 in; CHART 1CM = 0·5V = 0·003"
Y- AXIS: 10V = 10KN; CHART 1CM = 0·5V = 112·4 LBS
17th Jan '83
1st Sept '83
75 mm plate
Bead-on-plate CTOD
2C1 3·6
8·0
2C2 2·0
8·05
3C3 2·8
10·15
4C4 2·1
3·6
5C4 1·8
8·35
2C1 -60°C
2C2 +60°C
3C3 -60°C
4C4 -60°C
5C4 -60°C
2·E +0·027V(16 LBS)
2·E +0·19V(22 LBS)

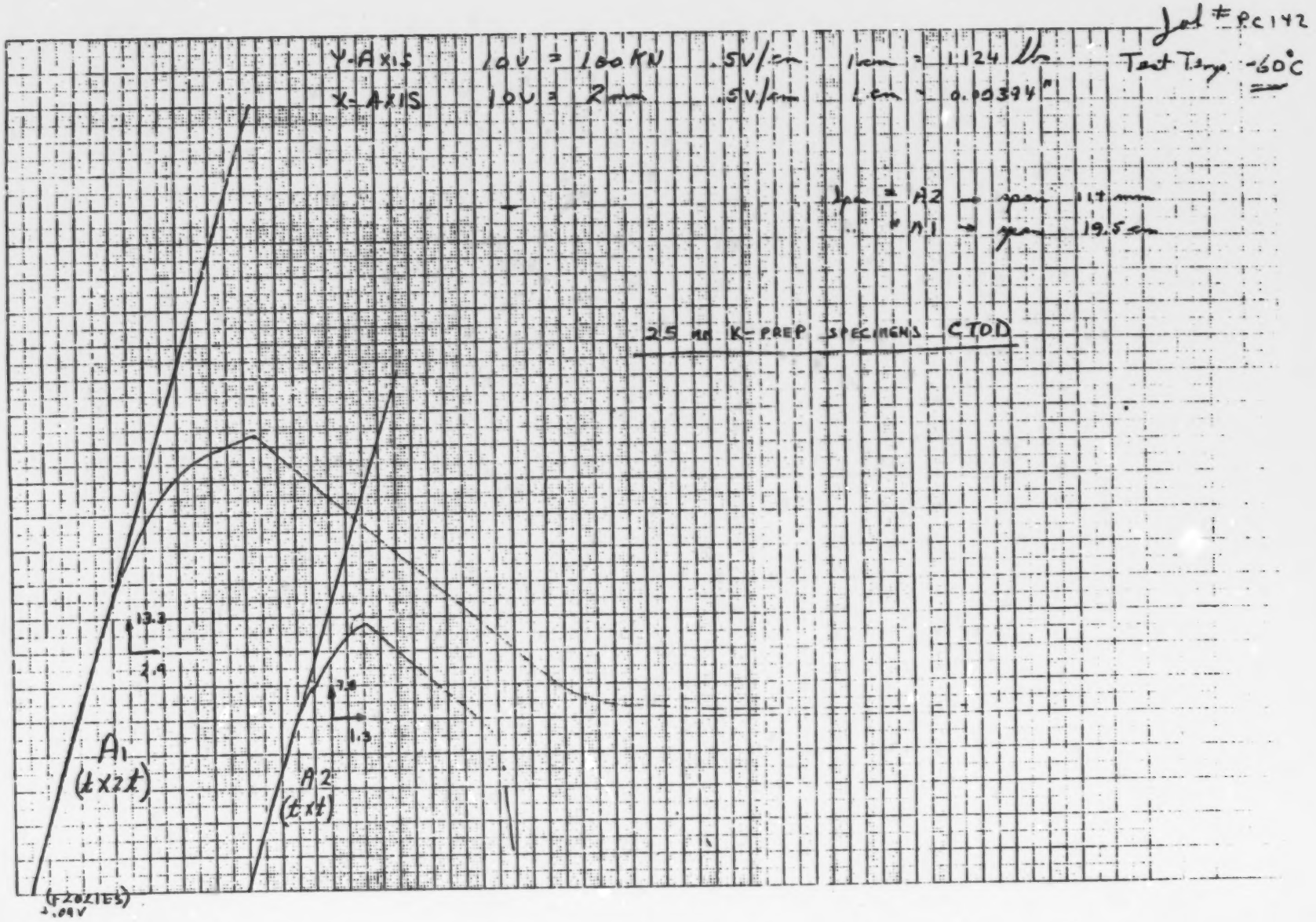
Y-AXIS 10V = 100 KN .5V/cm 1cm = 1.124 lbs
X-AXIS 10V = 2 mm .5V/cm 1 cm = 0.00394"
Test Temp -60°C
Span = A2 → span 11.7 mm
" A1 → span 19.5 mm
25 mm K-PREP SPECIMENS CTOD
13.2
2.9
7.8
1.3
A1 (t x 2t)
A2 (t x t)
(FROZEN)
2.09V

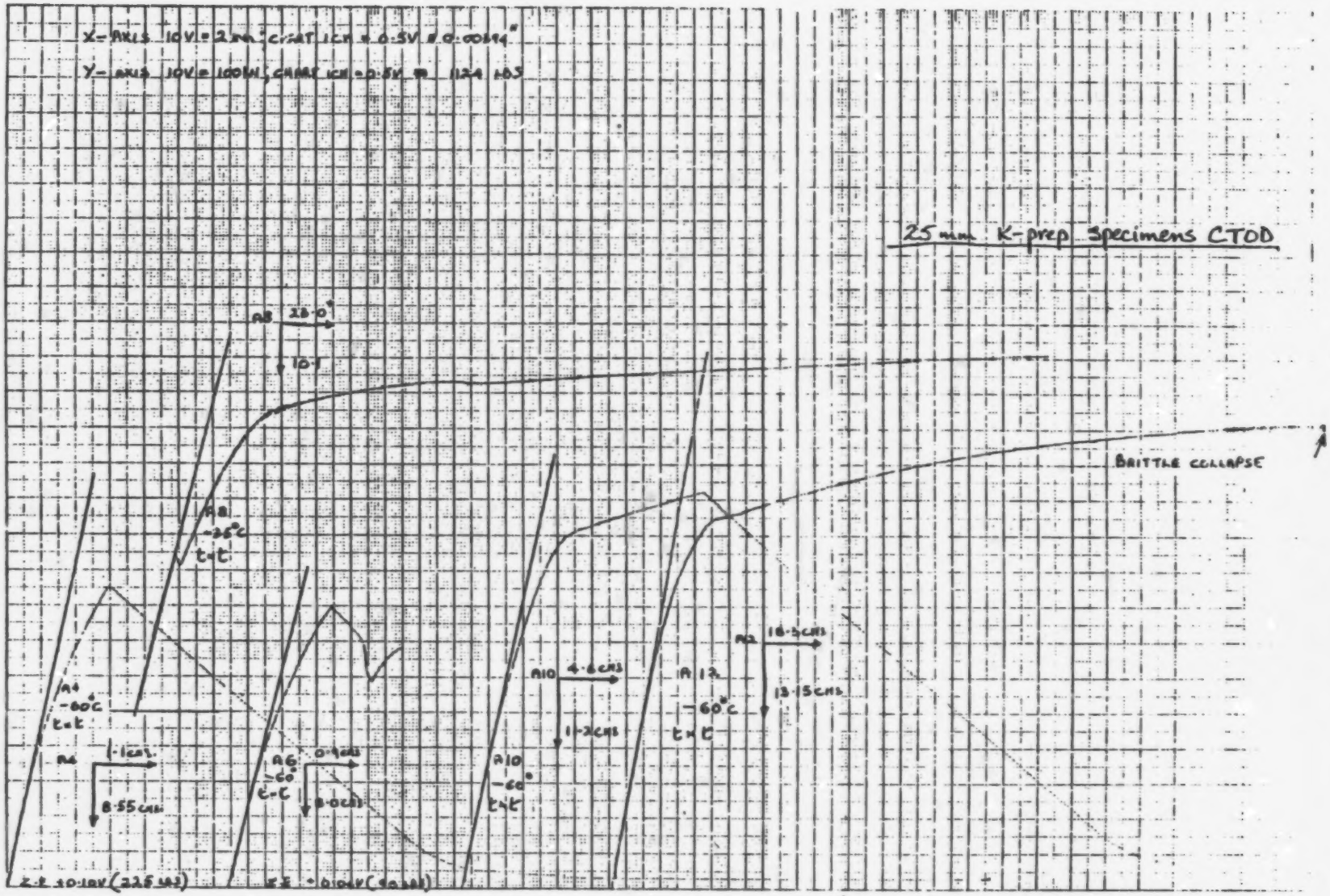
X-AXIS 10V = 2mm; CHART ICH = 0·5V = 0·0079"
Y-AXIS 10V = 100lbf; CHART ICH = 0·5V = 1124 lbf
25 mm K-prep Specimens CTOD
BRITTLE COLLAPSE
A8 28·0°
10T
A8 -35°C t+t
A4 -60°C t+t
A4 1·1CHS
8·55CHS
A6 -60° t-t
0·4CHS
8·0CHS
A10 -60° t+t
A10 4·6CHS
1·2CHS
A12 -60°C t+t
A12 18·5CHS
13·5CHS
Z-2 ±0·10V (225 Hz)
Y-2 ±0·10V (90 Hz)

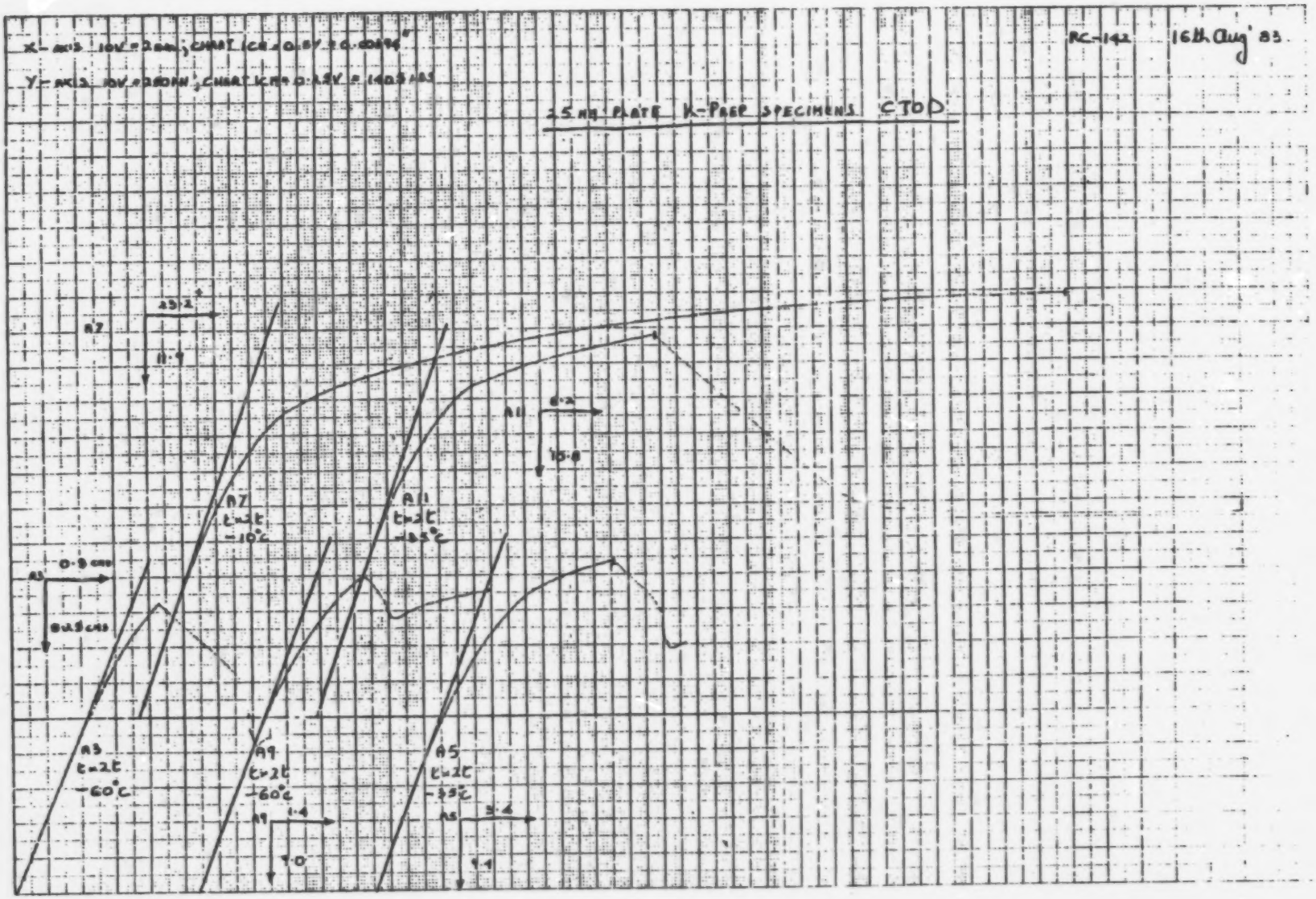
X-axis 10V = 2 cm; CHART ICR = 0.5V = 0.004"
Y-axis 10V = 2 cm; CHART ICR = 0.5V = 1403 MS
RC-142 16th Aug' 83
25 mm PLATE K-PREP SPECIMENS CTOD
A7
25·2
11·9
A11
6·2
15·8
A7 t=2t -10°C
A11 t=2t -35°C
A3
0·9 cm
0·45 cm
A3 t=2t -60°C
A9 t=2t -60°C
A5 t=2t -35°C
A9
1·4
1·0
A5
3·4
1·1

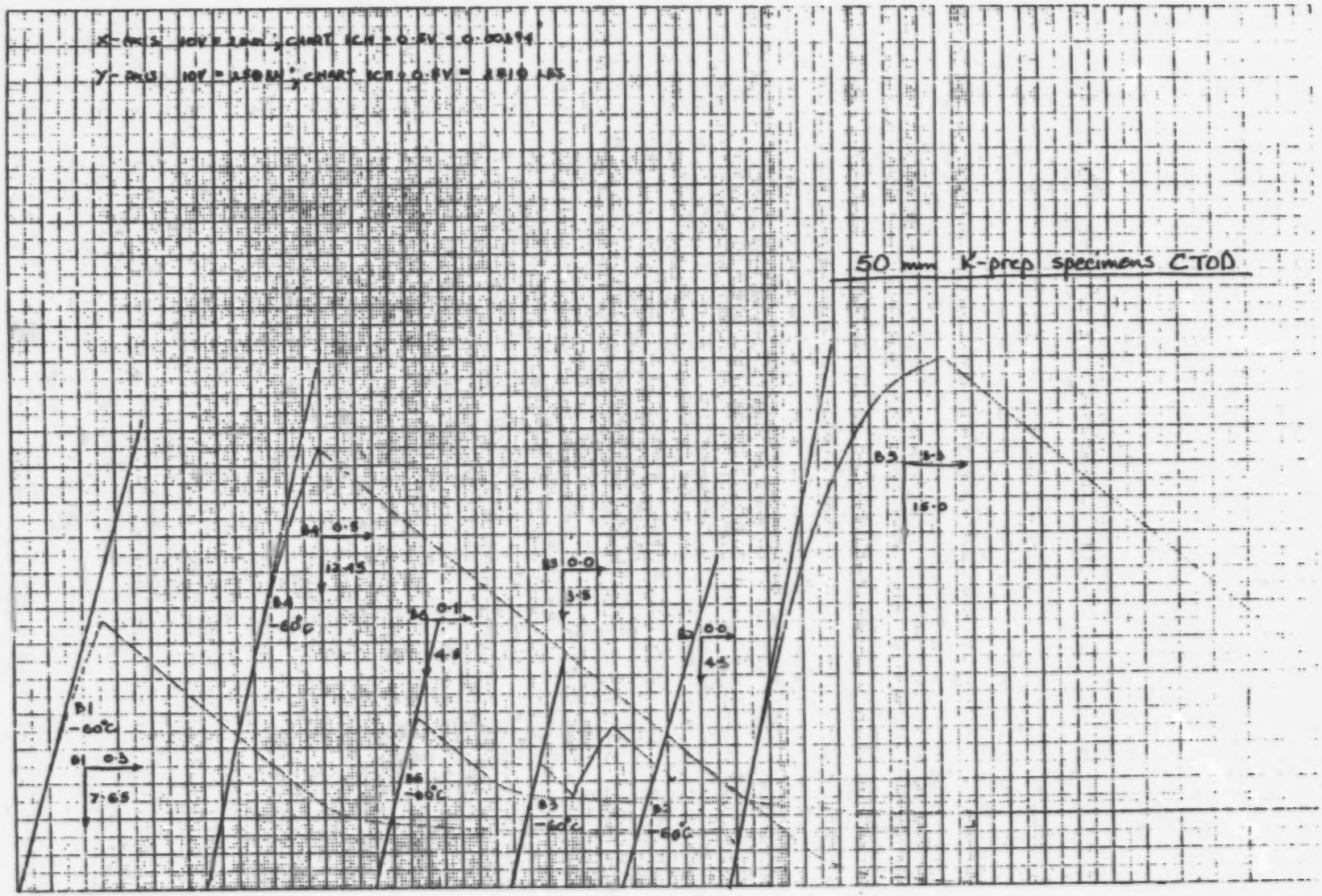
50 mm K-prep specimens CTOD
B1 -60°C
B1 0·3
7·65
B4 0·5
12·45
B4 -60°C
B6 0·1
4·6
B6 -60°C
B5 0·0
3·5
B3 -60°C
B2 0·0
4·5
B2 -60°C
B3 1·1
15·0

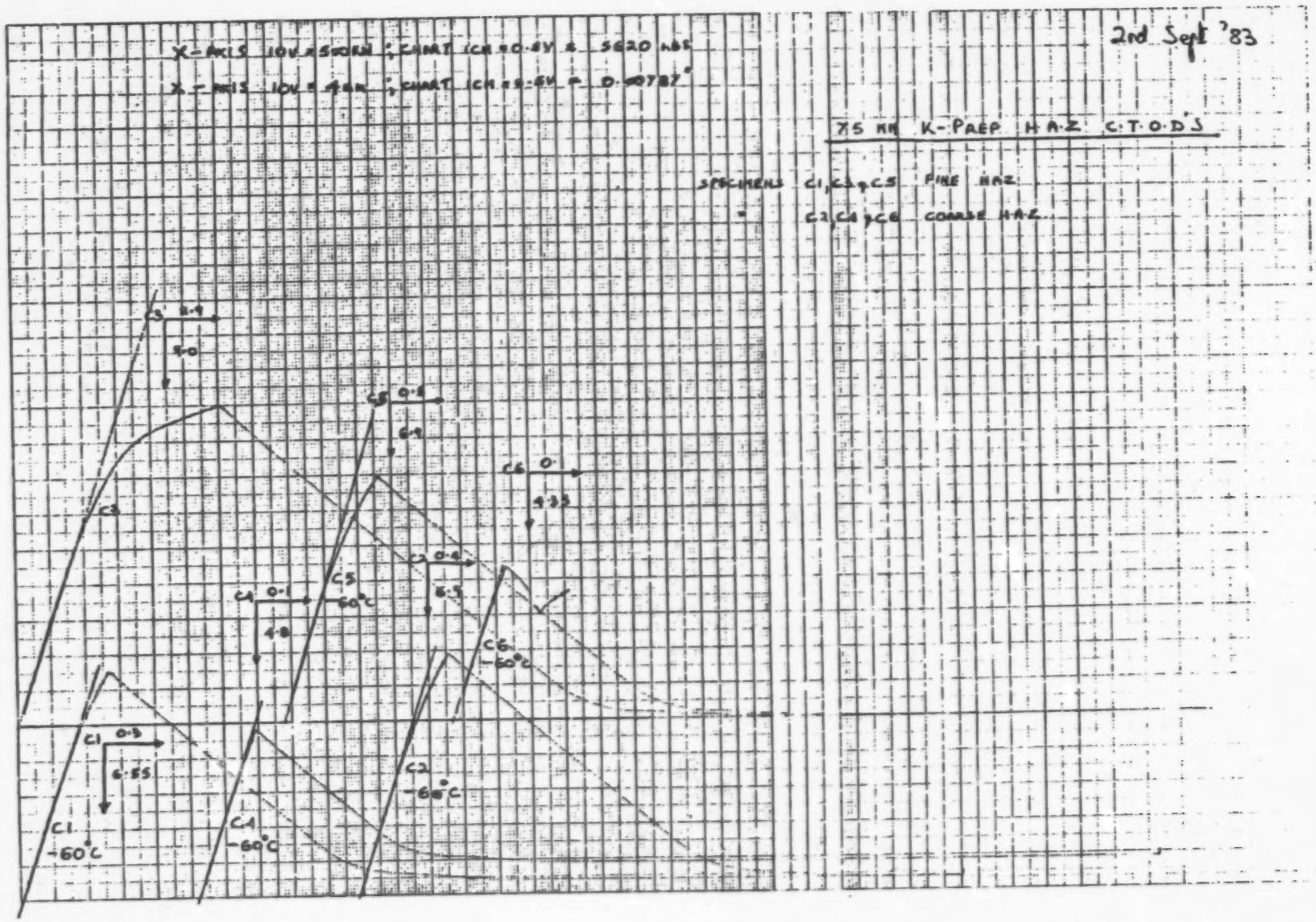
X-AXIS 10V = 500KN ; CHART (CH 1) 0·5V = 5020 MBS
X-AXIS 10V = 4KN ; CHART (CH 1) 0·5V = 0·00787"
2nd Sept '83
75 KN K-PREP HAZ C.T.O.D.S
SPECIMENS C1, C3, C5 FINE HAZ
" C2, C4, C6 COARSE HAZ.
C3 2·9
5·0
C5 0·2
6·9
C6 0·
9·33
C4 0·1
4·8
C5 -60°C
0·9
6·5
C6 -60°C
C1 0·3
6·55
C1 -60°C
C4 -60°C
C2 -60°C

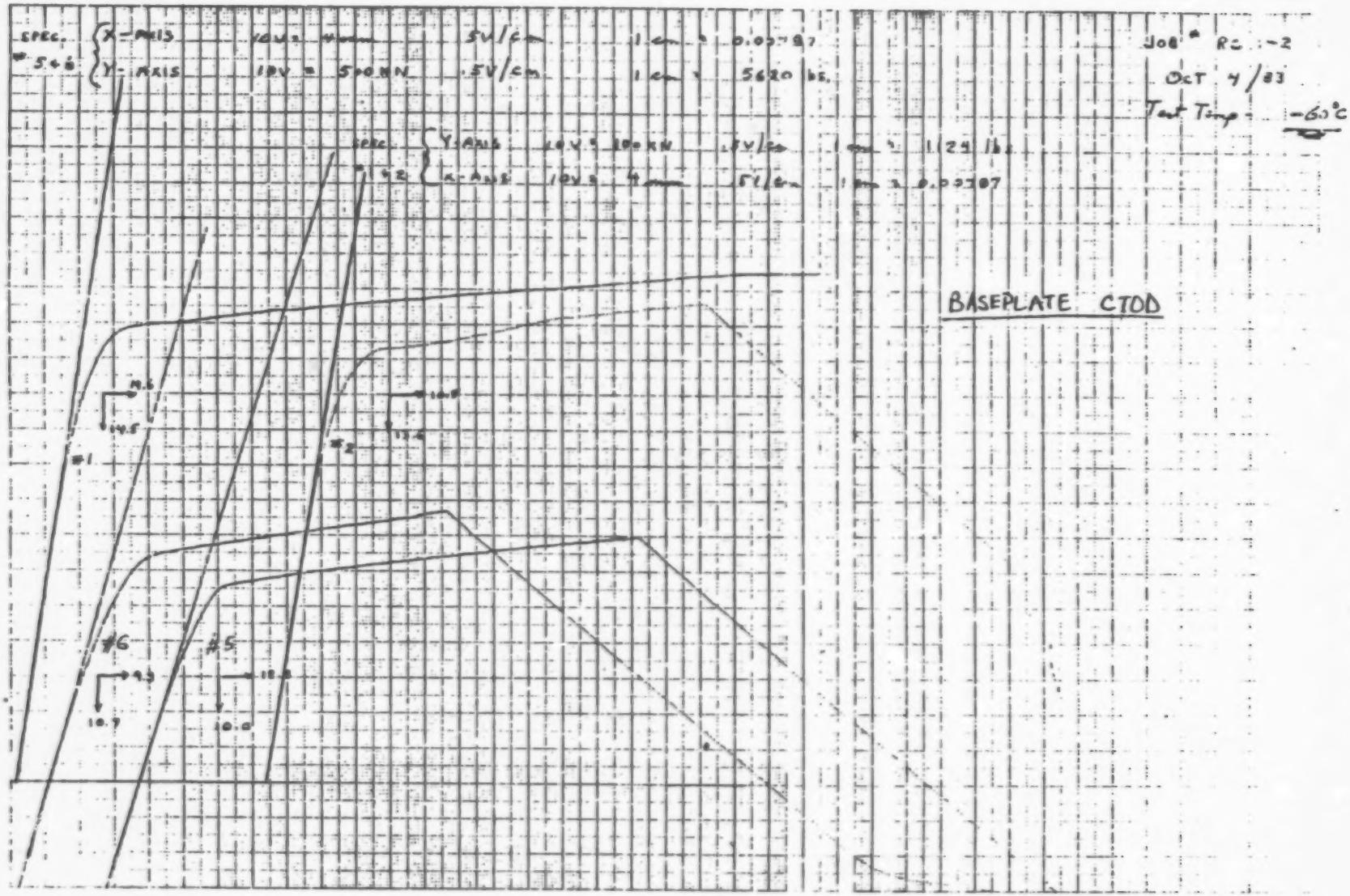
SPEC. #548
X-AXIS
Y-AXIS
1DV = 500 KN
5V/cm
.5V/cm
1 cm = 0.05787
1 cm = 5620 lbs.
JOB # RC-2
OCT 4/83
Test Temp. -60°C
SPEC. #42
Y-AXIS
X-AXIS
1DV = 100 KN
1DV = 4 mm
1V/cm
5V/cm
1 cm = 1124 lbs.
1 cm = 0.02307
BASEPLATE CTOD
#1
#2
#5
#6
14.5
11.6
10.0
10.7

APPENDIX C
WELDING PROCEDURE DATA SHEETS

WELDING PROCEDURE INFORMATION SHEET
Welding Institute of Canada - Technical Division

Project Title INVESTIGATION OF ALGOMA LT-60 STEEL(S) (HAZ) Project Number RC-142

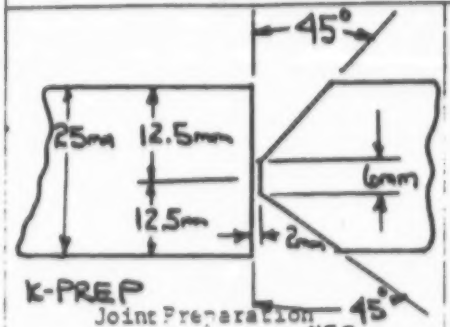

K-PREP
Joint Preparation

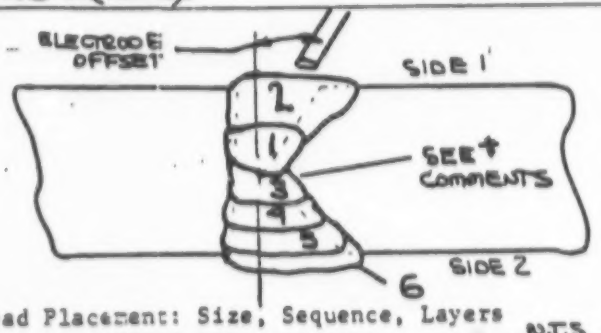

Bead Placement: Size, Sequence, Layers

N.T.S

Weld Layer	Process	Filler Metal Class	Filler Metal Dia. (mm)	Current Type	Current Amps	Voltage	Travel Speed (mm/s)	Preheat / Interpass Other Temp (max)
1	SAW	TI-BOR 22	4.0	DC+	550	34	7.0	35°C
2	"	"	"	"	"	"	"	110°C
3	"	"	"	"	"	"	"	105°C
4	"	"	"	"	"	"	"	105°C
5	"	"	"	"	"	"	"	112°C
6	"	"	"	"	"	"	"	110°C

Base Metal
Specification Type & Grade ALGOMA LT-60
Thickness 25mm Diameter N.A.
Other

Filler Metals
Electrode Class N.A. Size 4.0mmϕ
Electrode Trade Name TI-BOR 22
Flux: Class N.A. Trade Name OP121T
Other FLUX AND ELECTRODE FROM OERLIKON

Position
Position of Groove FLAT (1G)
Weld Progression (Uphill, Downhill) N.A.

Preheat SEE ABOVE
Preheat Temp 35°C Interpass Temp 112°C (MAX)
Other

Postweld Heat Treatment
Temperature Time
Other

Technique
String or Weave Bead
Oscillation
Multipass or Single Pass (perside) MULTI
Single or Multiple Electrodes SINGLE
Other ELECTRICAL STICK-OUT 1/8 INCHES
ELECTRODE OFFSET 10 TO 15°

Comments: ① BACK GOUGE TO SOUND METAL PRIOR TO DEPOSITION OF BEADS 3 TO 6
TI-BOR ELECTRODE CAST NO. OV641D

Relevant Code(s)
Date OCT 3/83 Operator
Witnessed by

WELDING PROCEDURE INFORMATION SHEET
Welding Institute of Canada - Technical Division

Project Title: INVESTIGATION OF ALGOMA LT-60 STEEL(S) (HAZ)
Project Number: RC-142

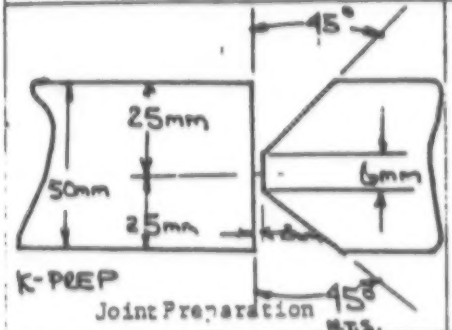

Joint Preparation

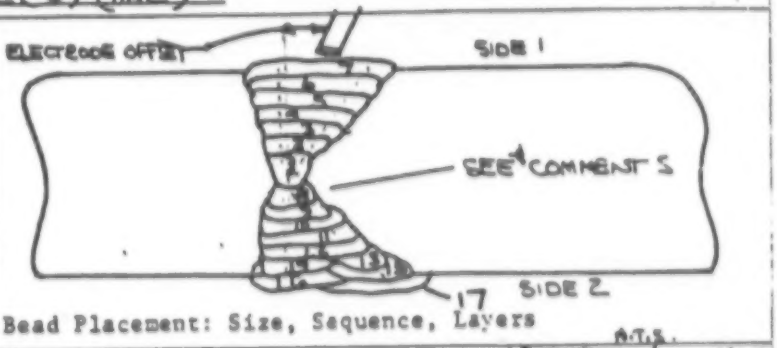

Bead Placement: Size, Sequence, Layers

Weld Layer	Process	Filler Metal Class	Filler Metal Dia. (mm)	Current Type	Current Amps	Voltage	Travel Speed (mm/s)	PREHEAT / INTERPASS Other TEMP (max) N.T.S.
1	S.A.W	Ti-Bor 22	4.0	DC+	500	34	6.5	26°C
2 to 7	S.A.W.	"	"	"	600	34	7.2	90°C TO 110°C (max)
8	"	"	"	"	500	34	6.5	90°C
9 to 17	"	"	"	"	600	34	7.2	90°C TO 110°C (max)

Base Metal
Specification Type & Grade: ALGOMA LT-60
Thickness: 50mm Diameter: N.A.
Other:

Preheat
Preheat Temp. 26°C Interpass Temp. 110°C (max)
Other: SEE ABOVE

Filler Metals
Electrode Class: N.A. Size: 4.0mm ϕ
Electrode Trade Name: TI-BOR-22
Flux: Class: N.A. Trade Name: ODIZIT
Other: FLUX AND ELECTRODE FOR DEPOSITION

Postweld Heat Treatment
Temperature: Time:
Other:

Position
Position of Groove: FLAT (1G)
Weld Progression (Uphill, Downhill): N.A

Technique
String or Weave Bead:
Oscillation:
Multipass or Single Pass (perside): MULTI
Single or Multiple Electrodes: SINGLE
Other: ELECTRICAL STICK OUT 1/8 INCHES ELECTRODE OFFSET 10° TO 15°

Comments: 4 BACK GOUGE TO SOUND METAL PRIOR TO DEPOSITION OF BEADS 8 TO 17
TI-BOR CAST NO. OV6419

Relevant Code(s)
Date: OCT 3/83 Operator:
Witnessed by:

WELDING PROCEDURE INFORMATION SHEET
Welding Institute of Canada - Technical Division

Project Title: INVESTIGATION OF ALGOMA LT-60 STEEL (S) (HAZ)

Project Number: RC-147

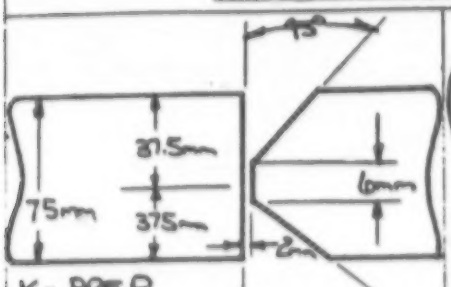

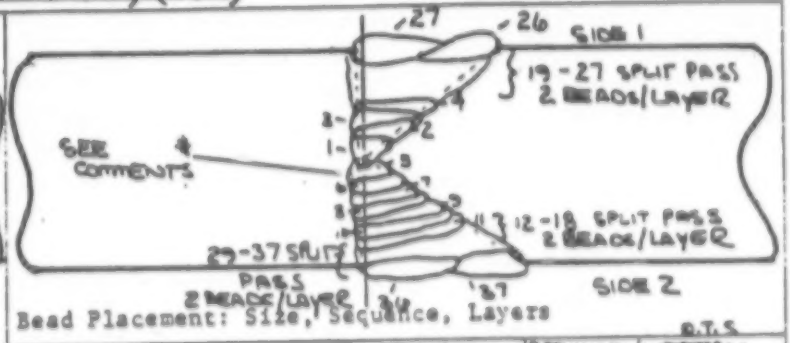

Weld Layer	Process	Filler Metal Class	Filler Metal Dia. (mm)	Current Type	Current Amps	Voltage	Travel Speed (mm/s)	Preheat / Interpass Other Temp °C (min)
1	S.A.W.	Ti-Bor-22	4.0	DC+	500	34	6.5	23°C
2-4	"	"	"	"	650	34	7.2	58°C TO 98°C (MAX)
5-18	"	"	"	"	650	34	7.2	79°C TO 140°C (MAX)
19-27	"	"	"	"	650	34	7.2	100°C TO 130°C (MAX)
28-37	"	"	"	"	650	34	7.2	80°C TO 125°C (MAX)

Base Metal
Specification Type & Grade: ALGOMA LT-60
Thickness: 75mm Diameter: N.A.
Other:

Filler Metals
Electrode Class: N.A. Size: 4.0mm ϕ
Electrode Trade Name: Ti-Bor-22
Flux: Class: N.A Trade Name: OP121T
Other: FLUX AND ELECTRODE FROM HERLIKON

Position
Position of Groove: FLAT (1G.)
Weld Progression (Uphill, Downhill): N.A.

Preheat
Preheat Temp: 23°C Interpass Temp: 140°C MAX
Other: SEE ABOVE

Postweld Heat Treatment
Temperature: Time:
Other:

Technique
String or Weave Bead:
Oscillation:
Multipass or Single Pass (perside): MULTI
Single or Multiple Electrodes: SINGLE
Other: ELECTRICAL STICKOUT 1" DIAGRAM ELECTRODE OFFSET 10° TO 15°

Comments: # BACK GOUGE TO SOUND METAL PRIOR TO DEPOSITION OF BEADS 5-18
Ti-Bor CAST NO. OV6419

Relevant Code(s)
Date: Oct 3 83 Operator:
Witnessed by:

WELDING PROCEDURE INFORMATION SHEET
Welding Institute of Canada - Technical Division

Project Title INVESTIGATION OF ALGOMA LT-60 STEEL(S) (WELDABILITY) Project Number RC-142

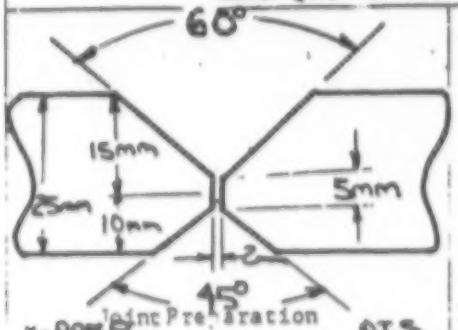

X-Prep Joint Preparation N.T.S

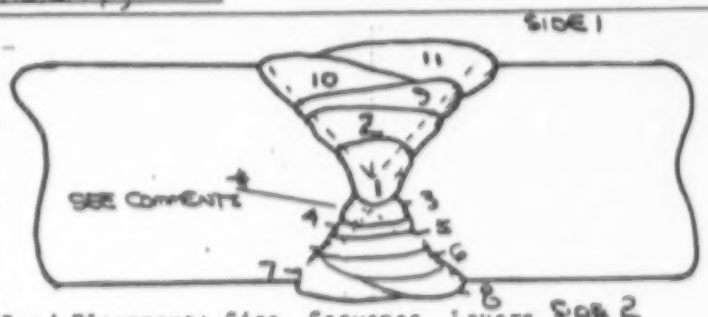

Bead Placement: Size, Sequence, Layers N.T.S

Weld Layer	Process	Filler Metal Class	Filler Metal Dia. (mm)	Current Type	Current Amps	Voltage	Travel Speed (mm/s)	Preheat Temp	Preheat Other	Interpass (max)
1	S.A.W	TIBOR-22	4.0	DC+	500	34	6.5	28°C		
2-5	SAW	" "	" "	" "	" "	"	7.2	70°C TO 80°C (MAX)		
6-11	SAW	SD2N12	4.0	DC+	500	34	7.2	28°C TO 110°C (MAX)		

Base Metal
Specification Type & Grade ALGOMA LT-60
Thickness 25mm Diameter N.A.
Other

Filler Metals
Electrode Class N.A. Size 4.0mm
Electrode Trade Name TIBOR-22 AND SD2N12
Flux: Class N.A. Trade Name OP21T
Other FLUX AND BOTH ELECTRODES FROM OERLIKON

Position
Position of Groove FLAT (1G)
Weld Progression (Uphill, Downhill) N.A.

Preheat
Preheat Temp 28°C Interpass Temp 110°C (MAX)
Other SEE ABOVE.

Postweld Heat Treatment
Temperature Time
Other

Technique
String or Weave Bead
Oscillation
Multipass or Single Pass (per side) MULTI
Single or Multiple Electrodes SINGLE
Other ELECTRICAL STICKOUT 1" USING ELECTRODE OFF SET OF C

Comments: BACK GOUGE TO SOUND METAL PRIOR TO DEPOSITION OF BEADS 3-5
TIBOR-22 CAST NO: DV6419: SD2N12 CAST NO. 5246

Relevant Code(s)
Date Dec 3/1985 Operator
Witnessed by

WELDING PROCEDURE INFORMATION SHEET
Welding Institute of Canada - Technical Division

Project Title INVESTIGATION OF ALGOMA LT-60 STEEL(S) (WELDABILITY) Project Number RC-142

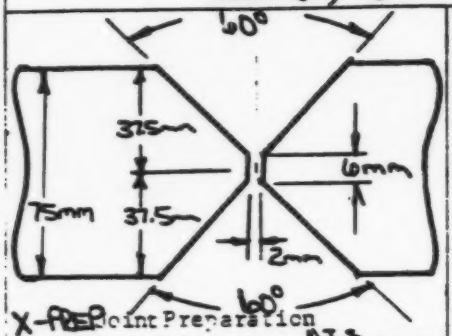

X-PREP Joint Preparation

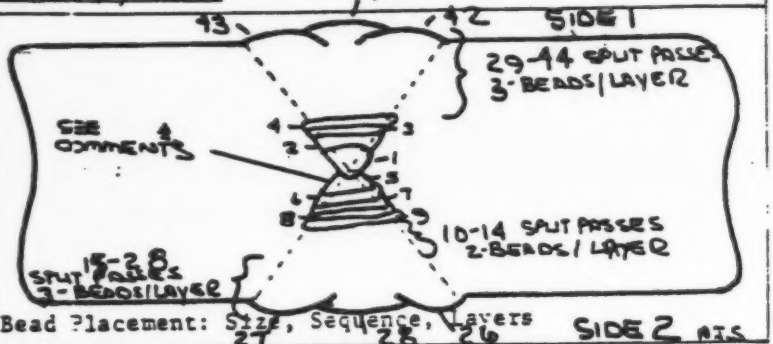

Bead Placement: Size, Sequence, Layers

Weld Layer	Process	Filler Metal Class	Filler Metal Dia. (mm)	Current Type	Current Amps	Voltage	Travel Speed (mm/s)	Preheat / Interpass Temp Other (MAX)
1	SAW	TI-BOR-22	4.0	DC+	500	34	6.5	25°C
2	"	"	"	"	600	34	7.2	40°C
3-4	"	"	"	"	700	34	7.2	60°C TO 90°C (MAX)
5	"	"	"	"	500	34	6.5	31°C
6	"	"	"	"	600	34	7.2	40°C
7-14	"	"	"	"	700	34	7.2	70°C TO 110°C (MAX)
15-44	SAW	SD2N12	4.0	DC+	700	34	7.2	100°C TO 120°C (MAX)

Base Metal
Specification Type & Grade ALGOMA LT60
Thickness 75mm Diameter N.A.
Other

Preheat
Preheat Temp 25°C Interpass Temp 120MAX
Other SEE ABOVE

Filler Metals
Electrode Class N.A. Size 4.0mm ϕ
Electrode Trade Name TIBOR-22 AND SD2N12
Flux: Class N.A. Trade Name OP121T
Other FLUX AND BOTH ELECTRODES FROM OERLIKON

Postweld Heat Treatment
Temperature Time
Other

Position
Position of Groove FLAT (1G)
Weld Progression (Uphill, Downhill) N.A

Technique
String or Weave Bead
Oscillation
Multipass or Single Pass (perside) MULTI
Single or Multiple Electrodes SINGLE
Other ELECTRICAL STICKOUT 1 1/8" ELECTRODE OFFSET 0°

Comments: 4 BACK GOUGE TO SOUND METAL PRIOR TO DEPOSITION OF BEADS 5-14
TIBOR-22 CAST NO DV6419; SD2N12 CAST NO. 52416

Relevant Code(s)
Date OCT 3/1983 Operator
Witnessed by

APPENDIX D

ULTRASONIC AND RADIOGRAPHIC TEST REPORTS

Ultrasonic Testing

Weld sections of 75 mm thick plate were ultrasonically tested using both longitudinal tranducer (90°) and angle bead transducers (60°)
Frequency med 2 MHZ
Couplant - oil and grease
Calibration IIW block for probe exit point and angle.
IIW block for sweep calibration
DAC constructed from 1/16" side drilled hole over 200 mm metal path.

Scanning DAC sensitivity plus 18dB

Evaluation of reflectors: - DAC sensitivity level

Recording all reflectors indicated at DAC sensitivity will be recorded
Scanning: Base material carrying the angle beam was scanned 100%.
Scan paths were overlapped a minimum of 15%.

The weld zone was scanned 100% from each side of the weld, and on each side of the plate. Scan paths were overlapped a minimum of 15%.

Test Results

No reflectors were apparent at DAC sensitivity settings.

ATLAS
TESTING
LABS
AND
SERVICES (OAKVILLE) LTD.

August 25, 1983

REPORT TO

Welding Institute Of Canada Ltd.
391 Burnhamthorpe Road, East
Oakville, Ontario
L6J 6C9

Attention: Mr. Price

Type of Inspection: Radiographic Inspection - IR192

Work Location: Our Oakville Lab, Oakville, Ontario

Inspection Date: August 24, 1983
Part: RC142
P.O. No.: T3368
Atlas Job No.: 08308-57-4-1

Job Description:

Radiographic Inspection on test plate RC142.

Results: As per attached

Technique No.: As per attached
Specifications: ASME Section IX
Atlas Inspector: P. Brady
Certifications: CGSB 48-GP-4 Level III
SNT TC-1A Level III

ATLAS TESTING LABS AND SERVICES (OAKVILLE) LTD.
Report Submitted by:

P. Brady
Technical Co-Ordinator

389 DAVIS ROAD, OAKVILLE, ONTARIO L6J 2X2
TELEPHONE: (416) 845-9542

ATLAS TESTING LABS AND SERVICES (OAKVILLE) LTD.

RADIOGRAPHIC INSPECTION REPORT

DATE: AUGUST 24, 1983

CLIENT: WELDING INSTITUTE OF CAN. LTD. JOB NO.: 08308-57-4-1

LOCATION: OUR LAB, OAKVILLE, ONTARIO CLIENT SPEC.: ASME SECTION IX

NO. OF EXPOSURES	FILM TYPE & SIZE	SCREEN TYPE & THICKNESS	TYPE OF ENERGY	PHYSICAL SIZE	STRENGTH	S.F.D. OR F.F.D.	ANGLE	MAT'L THICKNESS	PENETRAMETER SIZE	EXP. TIME (CI/MINS) OR (MA. SEC)	DENSITY
2	7X17KM	.010F Pb .010B	IR192	2X3mm	50Ci.	25"	90°	25mm	20	150	2.0-4.0

ABBREVIATIONS:
*-Welder's Number
IP-Incomplete Penetration
S-Slag
BT-Burn Through
LC-Low Cover
UC-Under Cut
W-Windows
HL-High-Low
C-Crater
P-Porosity
I-Icicles
NF-Non Fusion
1-Slight
2-Medium
3-Severe

FILM I.D.	LOCATION	*	IP	S	BT	LC	UC	W	HL	C	P	I	NF	Crack	REMARKS	MEETS SPEC.	DOES NOT MEET SPEC.
RC142	0-12															X	
	12-19														WATER MARKS	X	

ATLAS INSPECTOR(S) P. BRADY CGSB 48-GP-4 LEVEL III CLIENT REPRESENTATIVE

389 DAVIS ROAD, OAKVILLE, ONTARIO L6J 2X2
TELEPHONE: (416) 845-9642

APPENDIX E

ACCEPTANCE CRITERIA FOR BUTT WELDS

Mechanical Property Requirements of Welded Assemblies as Specified by Lloyds

Thickness mm	Transverse Test N/mm2	Charpy V-Notch Weld Metal Test Temp °C	Charpy V-Notch Weld Metal Average Energy, J, min(2)	Fusion Lines HAZ Test °C	Fusion Lines HAZ Average Energy J, min
≤ 35 mm	490	-60	27	-60	31
> 35 < 55	490	-80	27	-60	31

* No individual result to be lower than 18J

APPENDIX 2

28th November, 1983.

Dr. J. D. Ray
Senior Research Metallurgist
The Algoma Steel Corporation, Ltd
Sault Ste. Marie, Ontario
P6A 5P2

Dear Dr. Ray,

REPORT No. CSP-83/07
Re: NIL DUCTILITY TESTS ON LT.60 PLATE

Nil Ductility tests (ASTM E208) were carried out on the following LT.60 plate samples provided by The Algoma Steel Corporation, Limited with resulting nil-ductility temperatures as shown.

	Nil-Ductility Temp. (^{o}F)
- 3" plate - Longitudinal -	-45
- 3" " - Transverse -	-45
- 2" " - Longitudinal -	-65
- 2" " - Transverse -	-55
- 1" " - Longitudinal -	-65
- 1" " - Transverse -	-65

Samples were final machined and prepared with the welded notch as outlined in the ASTM E208 - P-1 specification. The final thickness of each sample was 1" and welded notches were applied on the original surfaces. All nil ductility tests were carried out using a drop hammer energy of 800 ft.lbf. Detailed results of each test are shown in Table I.

The relationship of Nil-Ductility Temperature, CVN Transition Temperature are not well established. However, a schematic representation, shown in Figure 1, indicates some results obtained during our previous work on pipeline steel.

I have returned one "break" and one "no break" sample from each of the materials tested for your evaluation. We will retain the remaining samples until the New Year in case further work is required.

W.F. Fossen, P.Eng.
Associate Research Engineer,
Materials Division.

:jr
Enclos.

Figure 1: Data on Pipeline Steels

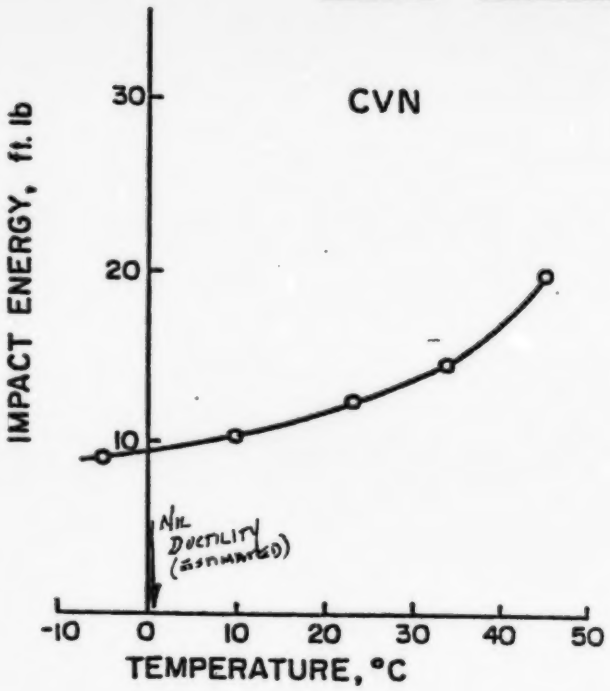

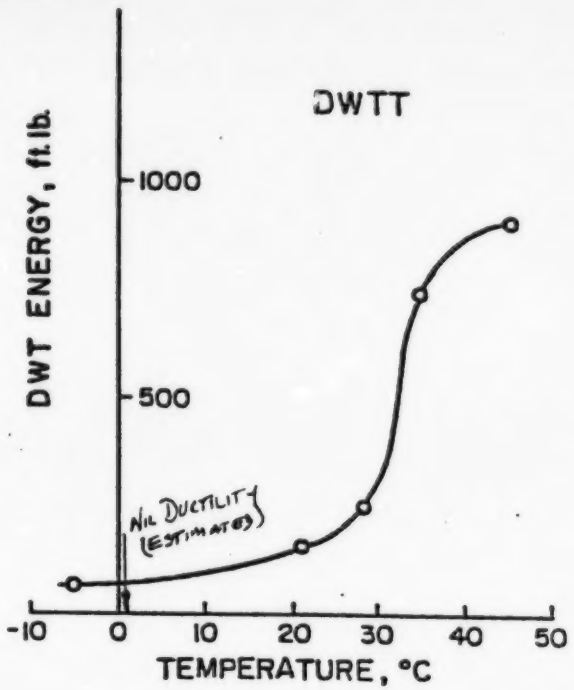

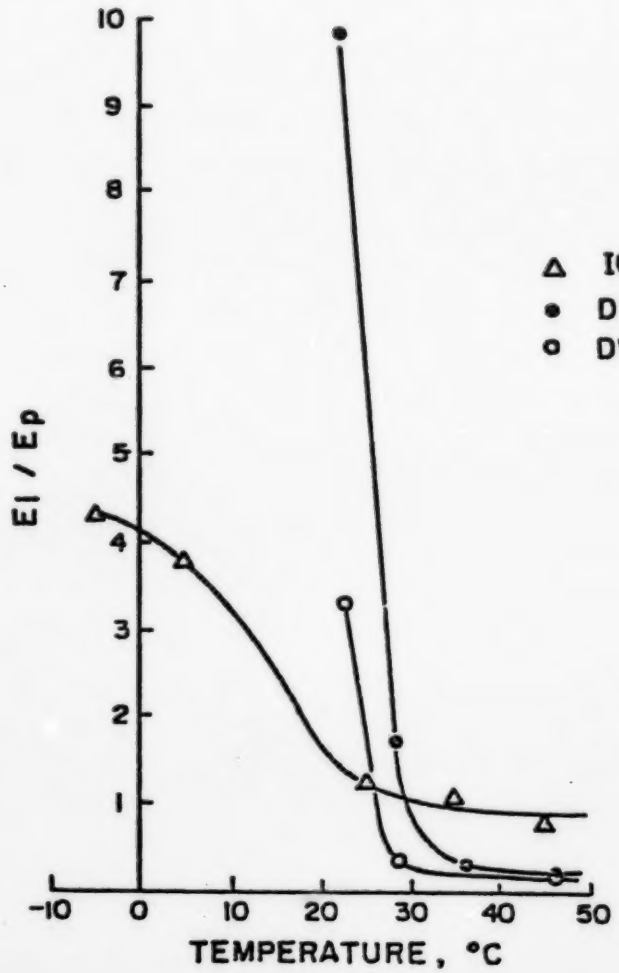

Report No. CSP-83/07

TABLE I.

Material 3"	Temp. °F	Results	
L	-100	Break	
L	-80	Break	L-45
L	-60	Break	
L	-45	Break	
L	-35	N. Break	
T	-65	Break	T-45
T	-45	Break	
T	-40	N. Break	
T	-33	N. Break	
Material 2"			
L	-65	Break	L-65
L	-65	Break	
L	-55	N. Break	
L	-55	N. Break	
T	-66	Break	
T	-60	Break	T-55
T	-55	Break	
T	-55	N. Break	
T	-45	N. Break	
Material 1"			
L	-65	Break	
L	-65	N. Break	L-65
L	-65	Break	
L	-55	N. Break	
L	-55	N. Break	
T	-75	Break	
T	-65	N. Break	T-65
T	-65	Break	
T	-55	N. Break	
T	-55	N. Break	

POOR

QUALITY

ORIGINAL